UNIVERSITÀ
DEGLI STUDI
FIRENZE

DOTTORATO DI RICERCA IN
Medicina Clinica e Sperimentale

CICLO XXXI
COORDINATORE Prof. Marco Matucci Cerinic

Ruolo della tirosin-chinasi Mer nella progressione delle malattie epatiche croniche e nello sviluppo del carcinoma epatocellulare

Role of Mer tyrosin-kinase in the progression of chronic hepatic diseases and in the development of hepatocellular carcinoma

Settore Scientifico Disciplinare MED/09

Dottoranda
Dott.ssa Mirella Pastore

Tutore
Prof. Fabio Marra

Coordinatore
Prof. Marco Matucci Cerinic

2015/2018

INDEX

ABSTRACT

Liver fibrosis is the consequence of chronic liver diseases caused by distinct etiologies, which can ultimately lead to cirrhosis and hepatocellular carcinoma (HCC). Among the main events initiating the fibrogenic process is the recruitment of inflammatory cells, such as monocytes and macrophages, besides the activation of resident macrophages (Kupffer cells). These cells release several soluble mediators which induce the activation of various cells including hepatic stellate cells (HSCs).
MerTK (Myeloid-epithelial-reproductive Tyrosine Kinase) is a receptor tyrosine kinase belonging to the TAM (Tyro3, Axl, Mer) subfamily of receptors and it is mainly expressed in macrophages.
A recent study has shown the involvement of MerTK in the NAFLD (Non-alcoholic fatty liver disease) pathogenesis. This kinase is overexpressed in murine models of hepatic fibrogenesis and by activated human HSCs. Furthermore, a low expression of MerTK was associated with a reduced prevalence of severe fibrosis in NAFLD patients.
In neoplastic diseases, MerTK is overexpressed in hematologic and epithelial malignant cells besides in non-neoplastic cells present in the tumor microenvironment; in this context, MerTK activates a network of pro-oncogenic downstream signaling pathways.
In our study we evaluated the role of MerTK in the pathogenesis of hepatic fibrosis and development of HCC.
A potential involvement of MerTK in the cross-talk between HSCs and macrophages was studied on primary human HSCs and THP1-derived macrophages or peripheral monocytes-derived macrophages. Inhibition of MerTK expression or activity was performed by knockdown with specific siRNAs or by the UNC569 inhibitor. HSCs were exposed to Conditioned Medium of Gas-6-stimulated macrophages. HSC migration of was assessed by modified Boyden chamber, viability was measured by MTT assay, proliferation was evaluated by BrdU incorporation assay and gene expression by Real Time PCR.
To investigate the possible role of MerTK in the HCC pathogenesis, two HCC cell lines (HuH7 and HepG2) were employed. MerTK expression and activation were evaluated by western blotting analysis and cell migration assay was performed by modified Boyden chamber.
MerTK activation in macrophages promoted HSC profibrogenic features, by inducing a significant increase in cell migration, viability and proliferation. Furthermore, the expression of profibrogenic genes was augmented. These effects were specifically related to MerTK expression and activity, as indicated by knockdown experiments and by pharmacologic inhibition.
Moreover, MerTK was expressed in HCC cell lines and its activation induced an increase in cell migration that was reverted by pretreatment with UNC569.

Altogether, these data suggest the potential role of MerTK pathway both in liver fibrosis and in the HCC pathogenesis.

RIASSUNTO

La fibrosi epatica è la conseguenza di malattie epatiche croniche causate da distinte eziologie, che possono progredire in cirrosi e carcinoma epatocellulare (HCC). Uno dei primi eventi che caratterizzano il processo di fibrogenesi epatica è il reclutamento di cellule infiammatorie, come monociti e macrofagi, oltre all'attivazione di macrofagi residenti (cellule di Kupffer). Tali cellule rilasciano numerosi fattori solubili che determinano l'attivazione di vari tipi cellulari quali le cellule stellate epatiche (HSC).
MerTK (Myeloid-epithelial-reproductive Tyrosine Kinase) è una tirosina chinasi recettoriale appartenente alla sottofamiglia dei recettori TAM (Tyro3, Axl, Mer) prevalentemente espressa nei macrofagi. Uno studio recente ha dimostrato il coinvolgimento di questa proteina nella patogenesi della NAFLD (Steatosi epatica non alcolica) osservando che MerTK risulta over-espressa in modelli murini di fibrogenesi epatica e in HSC umane attivate. Inoltre, una ridotta espressione di MerTK è stata associata a una minore prevalenza di fibrosi severa in pazienti con NAFLD.
MerTK è over-espressa in cellule maligne ematologiche ed epiteliali, oltre che in cellule non neoplastiche presenti nel microambiente tumorale, dove attiva pathway prooncogeniche.
Nel presente progetto è stato valutato il ruolo di MerTK nella patogenesi della fibrosi epatica e nello sviluppo dell'epatocarcinoma.
HSC primarie umane e macrofagi derivati da cellule THP1 o da monociti circolanti sono stati impiegati per studiare il potenziale coinvolgimento di MerTK nel cross-talk tra HSC e macrofagi. L'inibizione dell'espressione o dell'attività di MerTK è stata eseguita mediante knockdown con siRNA specifici o con l'inibitore, UNC569. Le HSC sono state trattate con il Medium Condizionato dei macrofagi stimolati con Gas-6. La migrazione delle HSC è stata valutata in camere di Boyden modificate, la vitalità cellulare mediante test MTT, la proliferazione mediante test di incorporazione di BrdU e l'espressione di geni profibrogenici mediante Real Time PCR.
Il ruolo di MerTK nel carcinoma epatocellulare è stato studiato in cellule HuH7 e HepG2, due linee umane di epatocarcinoma, in cui è stata valutata l'espressione e l'attivazione di questa proteina mediante western blotting e la migrazione cellulare mediante camere Boyden modificate.
L'attivazione di MerTK nei macrofagi influenzava in senso profibrogenico le attività biologiche delle HSC, determinando un aumento della migrazione, vitalità e proliferazione cellulare, oltre ad un aumento nell'espressione di fattori profibrogenici. Questi effetti erano specificatamente correlati all'espressione ed attività di MerTK, come dimostrato dagli esperimenti di knockdown o inibizione farmacologica.
Inoltre, MerTK risultava essere espressa nelle due linee di epatocarcinoma studiate e la sua attivazione determinava un aumento della migrazione

cellulare, che veniva significativamente ridotta dal pretrattamento con l'inibitore UNC569.
Complessivamente, questi dati suggeriscono un potenziale ruolo della via di segnalazione di MerTK sia nella fibrosi epatica che nella patogenesi del carcinoma epatocellulare.

1. INTRODUCTION

1.1 CHRONIC LIVER DISEASE

Liver diseases are becoming one of the most serious public health problems. The etiology of liver diseases can be of different origin (Del Campo et al. 2018); the main causes of hepatic disorders in industrialized countries include chronic HCV infection, alcohol abuse, bile duct damage, non-alcoholic fatty liver disease (NAFLD) and non-alcoholic steatohepatitis (NASH) (Caligiuri, Gentilini, and Marra 2016).

NAFLD, that was firstly described in 1980 (Ludwig et al. 1980), is currently the most common liver disorder in Western countries (Ofosu, Ramai, and Reddy 2018) and the most frequent cause of chronic liver disease worldwide (Li, Zhang, and Zhan 2018). The global incidence of NAFLD is estimated to be about 25%, with the highest rates in Middle East (32%) and South America (31%), followed by Asia (27%), USA (24%), Europe (23%) and Africa (14%), where NAFLD is less common (Younossi et al. 2016).

NAFLD can be considered as the hepatic manifestation of the metabolic syndrome and is closely associated with obesity, insulin resistance or type 2 diabetes and other metabolic abnormalities, such as dyslipidemia and hypertension (Gentilini et al. 2016). NAFLD includes a spectrum of conditions ranging from simple steatosis, defined as hepatic lipid accumulation without

inflammation to non-alcoholic steatohepatitis (NASH), characterized by hepatic fat deposition with hepatocellular damage, inflammation and fibrosis, which in a small proportion can lead to a series of complications including cirrhosis, liver failure and hepatocellular carcinoma (HCC)(Marra et al. 2008) (Ofosu, Ramai, and Reddy 2018).

The underlying mechanism for the development and progression of NAFLD is complex and multifactorial. According to the "two hits hypothesis", an excess of lipid accumulation in the hepatocytes, due to a high intake of saturated fats and obesity, represents the 'first hit', sensitizing the liver to further insults acting as a 'second hit' (Del Campo et al. 2018, Buzzetti, Pinzani, and Tsochatzis 2016). The 'second hit' gives rise to a lipotoxic microenvironment which further damages the hepatic tissue promoting inflammation and fibrogenesis (Figure 1.1).

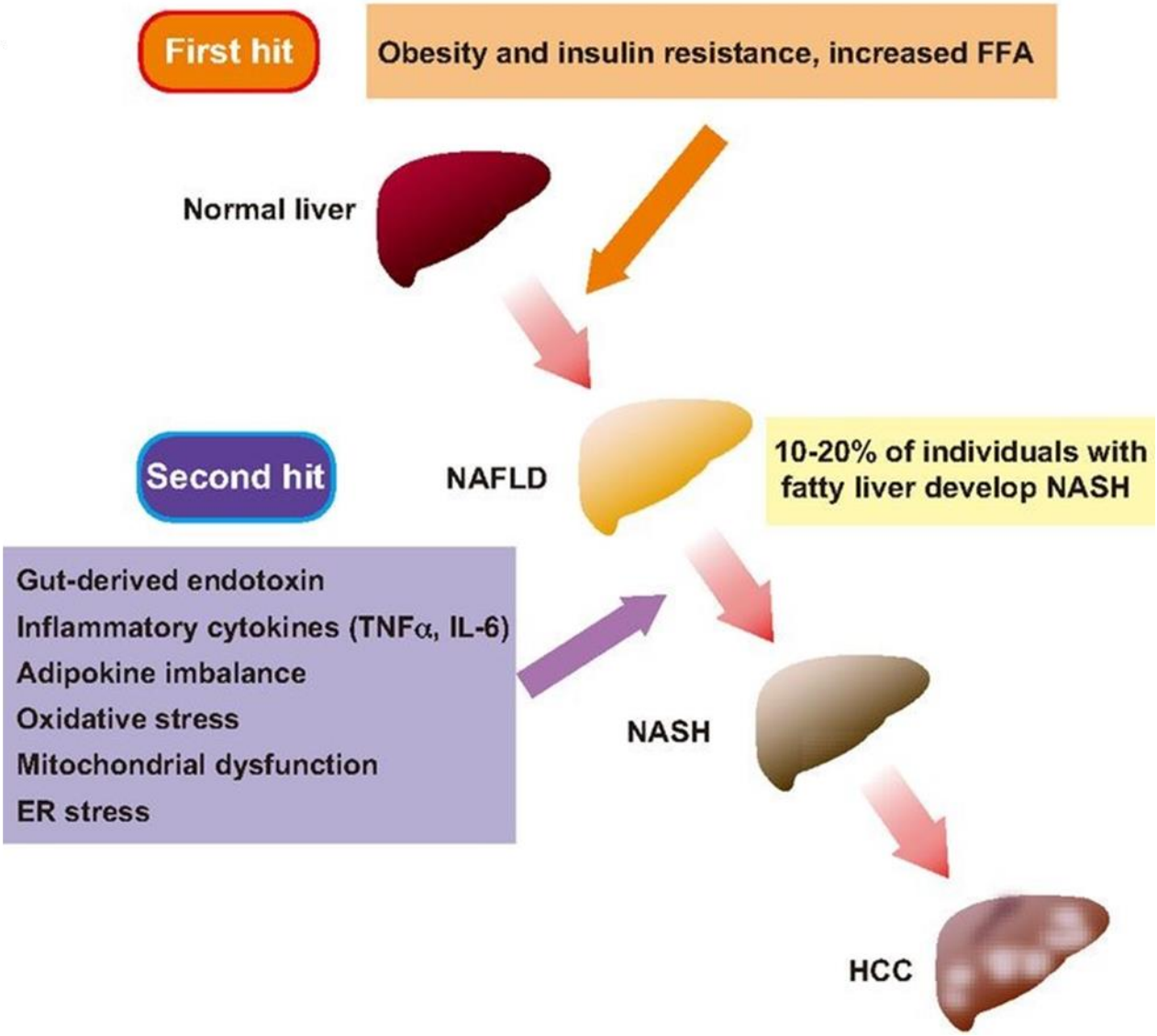

(Asaoka et al. 2013)

Figure 1.1. Mechanisms of NAFLD: the two-hit model.

In the "two-hit hypothesis" steatosis represents the 'first hit' that sensitizes the liver to further injury induced by 'second hit'.

Liver fibrosis represents an early step in the progression of cirrhosis, that is a significant health problem worldwide, due to the lack of effective

treatments. Indeed, liver cirrhosis is a major cause for liver-related morbidity and mortality in patients with NAFLD (Angulo 2010).

Cirrhosis may develop after about 15–20 years of chronic hepatocellular damage and it is mainly featured by an altered deposition of extracellular matrix (ECM) components, that in cirrhotic liver can be up to six times higher than in normal liver (Parola and Pinzani 2018) (Bataller and Brenner 2005). Moreover, the inflammatory response aggravates the fibrotic process, contributing to portal hypertension, hepatic encephalopathy, liver failure and increased risk of HCC, which can ultimately cause organ failure and death (Tacke and Trautwein 2015).

1.2 HEPATOCELLULAR CARCINOMA

Hepatocellular carcinoma (HCC) is currently the sixth most common neoplasia worldwide and it is considered the second deadliest cancer for men and the sixth for women (Jemal et al. 2011).

HCC, in most cases, arises in the setting of underlying end-stage liver disease, as cirrhosis, secondary to either viral hepatitis, specifically hepatitis B (HBV) or hepatitis C (HCV), or other non-viral chronic liver diseases (Singal and El-Serag 2015).

Due to the asymptomatic nature of the early-staged disease, the greater part of HCC cases is detected in advanced stages, resulting in incurable disease. Currently, Sorafenib is the only approved systemic medication for the

treatment of advanced HCC. Hence, it is extremely necessary to develop effective and focused therapies for this pathological condition (Finn 2013). Persistent changes in the liver microenvironment, including neoangiogenesis and development of a fibro-inflammatory stroma, contribute to HCC progression. In particular, the HCC pathogenesis has been associated with hepatocyte death, inflammatory cell infiltration and compensatory liver regeneration, sustained by hepatic mitogenic cytokines, that induce a protumoral M2 phenotype in tumor associated macrophages (TAMs) (He and Karin 2011) (Figure 1.2). The acquisition of protumoral M2 features by TAMs is mediated by a wide variety of stimuli expressed within the tumor microenvironment, that can be released both by cancer and stromal cells. As in most human tumors (Mantovani et al. 2008), TAM infiltration in HCC is generally associated with poor prognosis (Li et al. 2009).

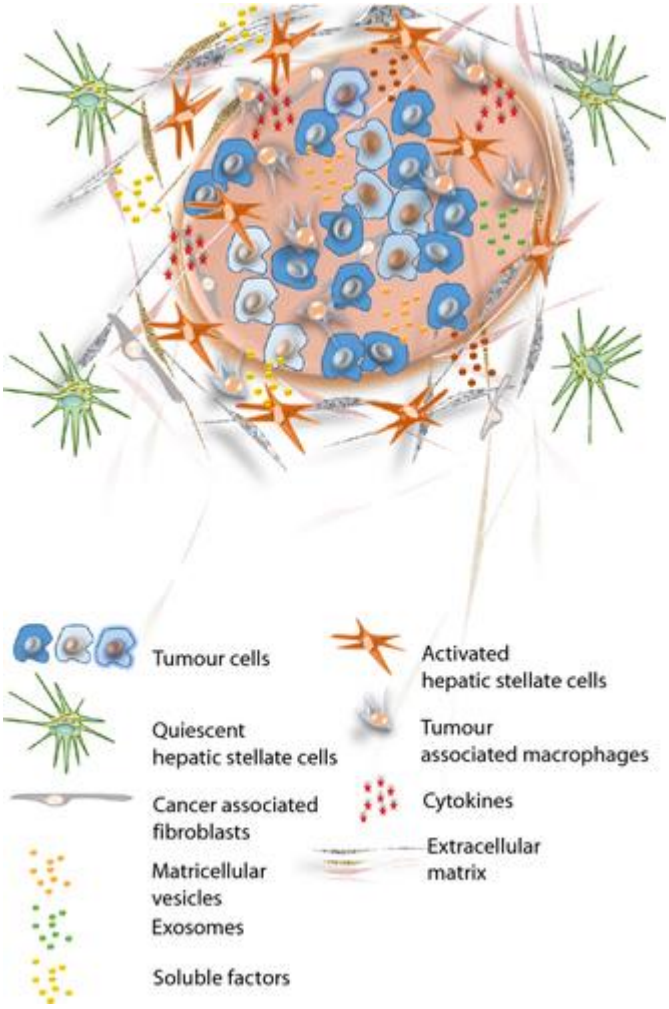

(Carloni, Luong, and Rombouts 2014)

Figure 1.2. HCC and tumor microenvironment.

HCC development is influenced by many cell types through intercellular transport of soluble mediators and cytokines.

1.3 PATHOGENESIS OF FIBROSIS

Fibrogenic response is a reparative mechanism mainly characterised by deposition of excessive fibrous tissue, resulting in a progressive architectural remodelling in nearly all tissues and organs (Weiskirchen, Weiskirchen, and

Tacke 2018a) (Figure 1.3). In most cases, the fibrogenic process initiates following parenchymal cell destruction, mediated by the action of various injurious agents and mechanisms, that cause cell death (necrosis, apoptosis, necroptosis, pyroptosis, ferroptosis and others). The resulting tissue damage is associated with an inflammatory response, in which local immune cells (mainly tissue macrophages) become activated and several type of blood cells are recruited to the site of injury. Local and recruited immune cells produce a wide variety of soluble mediators including cytokines and chemokines that lead to the activation of mesenchymal cells, which produce ECM components, proinflammatory cytokines, chemokines and angiogenic factors (Weiskirchen, Weiskirchen, and Tacke 2018a). In addition, the complement system becomes activated, attracting phagocytes that are stimulated to clear harmful or damaged material (Danobeitia, Djamali, and Fernandez 2014). Moreover, the coagulation cascade and the fibrinolytic system allow the reabsorption of blood clots. When all these biological activities are sufficient for injurious agent removal and wound healing, the soluble mediators are removed and tissue homeostasis is restored.

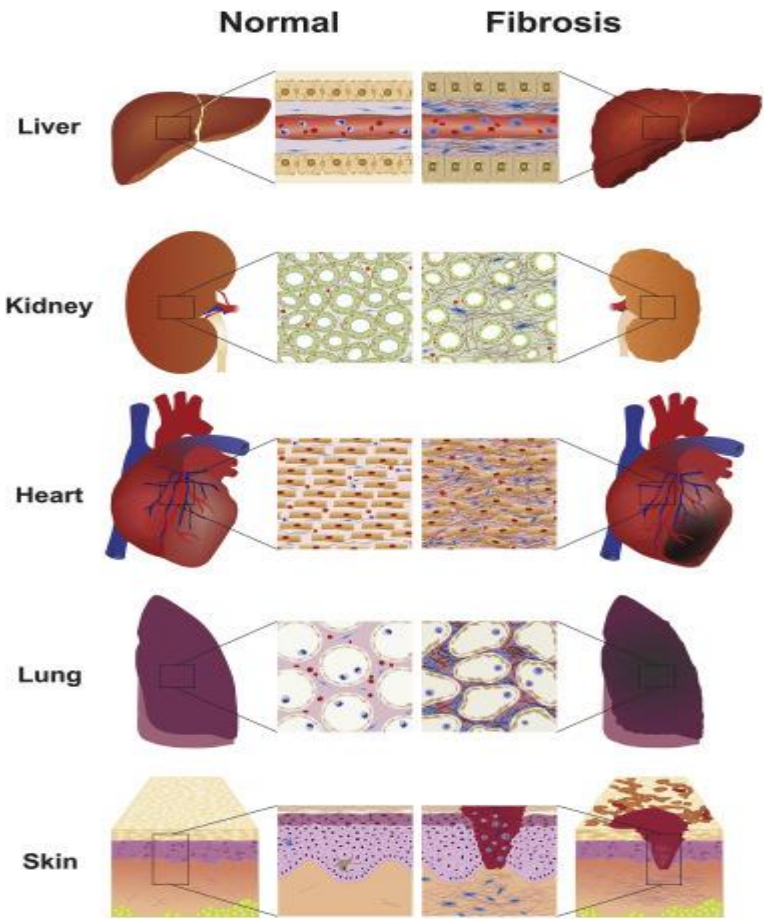

(Weiskirchen, Weiskirchen, and Tacke 2018a)

Figure 1.3. Common characteristics of organ fibrosis.

Injurious events lead to organ damage, inflammation and fibrosis in liver, kidney, lung, heart and skin.

Nevertheless, if these initial responses are insufficient to eliminate damaging stimuli, the inflammation persists and immune cells (e.g., macrophages and T lymphocytes) are induced to produce cytokines and enzymes that cause long lasting damage (Weiskirchen, Weiskirchen, and Tacke 2018a). These processes induce parenchymal cell death, resulting in loss of cell membrane integrity and release of cell death-related products and profibrogenic

mediators in the milieu, that in turn stimulate the activation of profibrogenic cells. In this scenario, cells producing ECM components increase in number or become excessively activated, leading to an excess of ECM with consequent scar formation and destruction of the normal organ architecture (Pakshir and Hinz 2018).

1.4 LIVER FIBROSIS

The liver is certainly the organ that retains among the most complex functions in the human body, responsible for protein, carbohydrate and lipid metabolism, elimination of drugs and toxins from blood and regulation of immune response (Protzer, Maini, and Knolle 2012). The hepatic parenchyma is organized in lobules, which are functional units consisting of hepatocytes, endothelial cells, Kupffer cells, hepatic stellate cells (HSCs) and bile duct cells (Hernandez-Gea and Friedman 2011). Hepatocytes, that represent about 80% of total liver weight and about 70% of all liver cells, play an important role in the metabolic functions of this organ (Si-Tayeb, Lemaigre, and Duncan 2010). All hepatic cells are susceptible to numerous insults and participate to various pathological mechanisms following liver damage (Malhi, Guicciardi, and Gores 2010). On the other hand, the liver has a considerable regenerative potential, as shown by the ability to regulate its growth and mass after hepatectomy and recover after acute liver injury (Mao, Glorioso, and Nyberg 2014). Chronic damage leads to the development of liver fibrosis with

accumulation of ECM components, mostly fibrillar collagens, fibronectin and proteoglycans, which are major players in the alteration of the hepatic architecture (Böttcher and Pinzani 2017). The mechanisms underlying liver fibrosis are complex and involve the interplay of multiple factors; among these, a key role is played by the cross-talk between various liver-resident and infiltrating cellular subsets, that produce and secrete different soluble mediators (cytokines and chemokines) and is further modulated by the chemical and biological properties of the causative agent (Weiskirchen, Weiskirchen, and Tacke 2018b). In most cases, tissue injury induces an inflammatory response involving the local vascular system, immune cells and release of endocrine and neurological mediators. In this context, non-parenchymal cells (endothelial and HSCs) and resident or recruited immune cells (macrophages, dendritic cells and mast cells) possessing specialized surface receptors, which recognize pathogen-associated molecular patterns (PAMPs) and damage-associated molecular patterns (DAMPs) secrete a variety of inflammatory and profibrogenic mediators. These factors, especially cytokines and chemokines, as tumor necrosis factor α (TNFα) and interleukin-1β (IL1β), as well as reactive oxygen species (Tilg and Diehl 2000), lead to the activation of matrix producing cells including HSCs, transdifferentiating to myofibroblasts (Weiskirchen, Weiskirchen, and Tacke 2018b) (Figure 1.4).

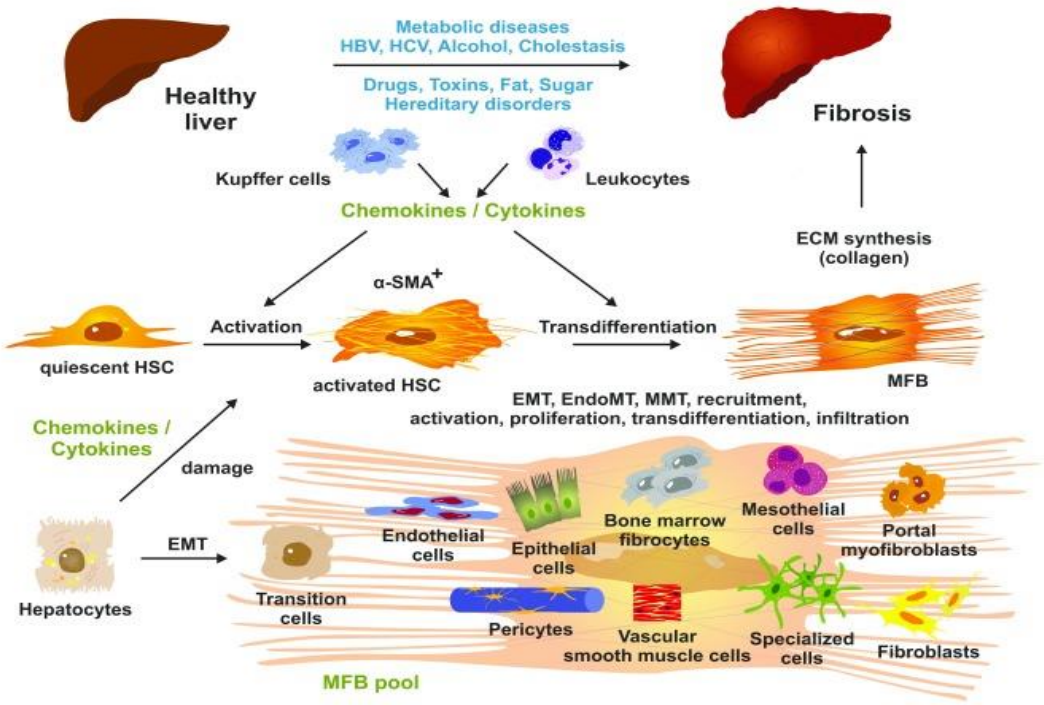

(Weiskirchen, Weiskirchen, and Tacke 2018b)

Figure 1.4. Pathological characteristics of liver fibrosis.

Extended liver damage results in changes in hepatic architecture and advanced fibrosis. The relevant molecular and cellular mechanisms including epithelial-to-mesenchymal transition (EMT), endothelial-to-mesenchymal transition (EndoMT), mesothelial-to-mesenchymal transition (MMT) and activation of quiescent hepatic stellate cells (HSCs) by soluble mediators (chemokines and cytokines) released by liver-resident macrophages (Kupffer cells), infiltrating leukocytes and other cell types including damaged hepatocytes. Activated HSCs are the predominant source of extracellular matrix (ECM).

1.5 HEPATIC STELLATE CELLS

Hepatic Stellate Cells (HSCs) were described for the first time by Carl von Kupffer in 1876, as "sternzellen" ("star cells" in German) (Aterman 1986).

These were renamed as fat-storing cells by Toshiro Ito (Friedman 2008), Bronfenmajer, Schaffner and Popper (Bronfenmajer, Schaffner, and Popper 1966) proposed the name "lipocytes" to reflect their role in fat (vitamin A) uptake. Finally, Wake (Wake 1971) firmly established the HSCs as cell type capable to store vitamin A lipid droplets.

HSCs comprise about 15% of resident cells in normal liver (Giampieri, Jezequel, and Orlandi 1981) and approximately one-third of the non-parenchymal cells (Friedman 2008). These cells located in the perisinusoidal space of Disse between the basolateral surface of hepatocytes and the anti-luminal side of sinusoidal endothelial cells. Structurally, they have a moderately developed rough endoplasmic reticulum (rER), juxtanuclear small Golgi complex, protuberant dendritic cytoplasmic processes and subendothelial processes extending around sinusoids between endothelial cells and hepatocytes (Wake 1999). On the surface of these processes there are numerous microprojections that detect chemotactic signals and transmit them to the cell's mechanical apparatus to generate a contractile force (Melton and Yee 2007).

Due to their anatomical position, HSCs are optimally located to interact with many cell types in the liver, through mediators and cytokines (Wake 1989).

The main feature of HSCs in normal liver is the storage of vitamin A (retinoid) (Wake 1971). Indeed, under physiological conditions, 50–80% of total retinoid in the body is stored in the liver (Blomhoff et al. 1990), 80–90% of which in HSCs. Vitamin A has pleiotropic functions in liver homeostasis and in controls innate immunity by regulating the action of neutrophils, monocytes,

macrophages, natural killer (NK) cells and lymphocytes and modulating myeloid cells differentiation (Weiskirchen and Tacke 2014).

Following liver injury, HSCs undergo to substantial changes, lose vitamin A and acquire the "activated" phenotype, characterized by the appearance beneath the cell membrane of numerous smooth muscle actin-α (α-SMA) containing microfilaments (Gabbiani et al. 1981), an enlarged rough endoplasmic reticulum and a well-developed Golgi apparatus, indicating an active protein synthesis (Minato, Hasumura, and Takeuchi 1983). Activated HSCs are also characterized by increased proliferation and ECM production (Bachem et al. 1992). HSC activation can be schematically divided into two major phases: ***Initiation*** and ***Perpetuation***, followed by resolution of fibrosis if injury recedes (Figure 1.5).

1. Initiation phase, also defined as pre-inflammatory, refers to the first events that make quiescent HSCs responsive to a series of growth factors, cytokines and other local stimuli. During this phase new transcriptional events and the induction of early genes occur.

Among the most characterized target genes of transcription factors described in HSCs, there are type I collagen, α-SMA, transforming growth factor beta 1 (TGF-β1), TGFβ receptors, matrix metalloproteinases (MMPs) and tissue inhibitors of metalloproteinases (TIMPs).

Stimuli that initiate HSC activation derive from damaged hepatocytes, endothelial cells, inflammatory cells, Kupffer cells and platelets. Hepatocytes are a robust source of lipid peroxides (Novo et al. 2006); moreover damaged hepatocytes promote HSC activation through a process mediated by Fas,

involving the TNF-related apoptosis-inducing ligand (TRAIL) (Canbay, Friedman, and Gores 2004).

Infiltration and activation of inflammatory cells and Kupffer cells also contribute to HSC activation. Kupffer cells stimulate matrix synthesis, cell proliferation and release of retinoids by HSCs through cytokines in particular TGF-β1 and reactive oxygen intermediates/lipid peroxides (Bilzer, Roggel, and Gerbes 2006). Furthermore, rapid activation of β-Platelet derived Growth Factor Receptor (β-PDGFR) and modulation of growth factor signaling are fundamental features of this early response.

2. Perpetuation phase, is characterized by cellular events that determine the achievement and maintenance of an activated phenotype. Perpetuation involves autocrine and paracrine secretion. It is composed by several changes in HSC behavior, including: ***proliferation, contractility, chemotaxis, fibrogenesis, matrix degradation*** *and* ***inflammatory signaling activation.***

Proliferation – Platelet Derived Growth Factor (PDGF) signaling was the first autocrine loop found to be involved in HSC activation and remains among the most important (Borkham-Kamphorst et al. 2007). Early induction of PDGFR during HSC activation increases their responsiveness to this potent mitogen (Wong et al. 1994). Downstream pathways of PDGF signaling are well known and include PI3kinase and ERK1/2 (Lechuga et al. 2006) (Pinzani and Marra 2001). Other compounds with mitogenic activity and a potential role in fibrogenesis include Vascular Endothelial Growth Factor (VEGF) (Yoshiji et al.

2003), thrombin and its receptor (Marra et al. 1998) and b Fibroblast Growth Factor (bFGF) (Yu et al. 2003).

Contractility - Contractility is one of the specific changes that characterizes the activated phenotype of HSCs. Specifically, their contractile ability is associated with increased expression of the cytoskeletal protein α-SMA (Rockey et al. 1992) and Ca^{2+} dependent and Ca^{2+} independent mechanisms (Laleman et al. 2007). The contractility of HSCs has a multitude of effects in injured liver, including perisinusoidal constriction and portal hypertension, leading to an increase in portal resistance during hepatic fibrosis (Xu et al. 2012).

Chemotaxis - Activated HSCs acquire the ability to migrate towards the sites of injury, driven by chemoattractants. The best studied chemotactic molecules include PDGF (Kinnman et al. 2000), monocyte chemoattractant protein-1 (MCP-1) (Marra et al. 1999) and CXCR3 (Bonacchi et al. 2001).

Fibrogenesis - HSCs mediate the fibrogenic process by increasing matrix production. The main component of hepatic scar is type I collagen (Anania et al. 2001). The most potent stimulus for production of type I collagen and other matrix constituents, as cellular fibronectin and proteoglycans, by HSCs is TGF-β1, which is derived from both paracrine and autocrine sources (Inagaki and Okazaki 2007). Moreover, lipid peroxidation derivatives are also important stimuli for extracellular matrix production (Svegliati Baroni et al. 1998).

Matrix Degradation - Liver fibrosis implies a balance between ECM production and degradation. Early disruption of the normal liver matrix by

proteolytic enzymes, mainly by MMPs, accelerates its replacement by scar matrix, which has deleterious effects on cell function. Matrix degradation is considered to be "pathological", but resorption of excessive matrix in patients with chronic liver disease provides the opportunity to reverse hepatic dysfunction and portal hypertension. HSCs are the principal source of MMP2 (Milani et al. 1994), MMP9 (Han et al. 2007) and MMP3 (Vyas et al. 1995). Activation of latent MMP2 may require interaction with hepatocytes (Théret et al. 1997). HSCs also produce functional tissue inhibitors of metalloproteinases: TIMP1 and TIMP2 (Arthur 2000). These proteins inhibit the activity of metalloproteinases leading to reduced degradation of the accumulating matrix (Iredale 2007).

Inflammatory signaling - Activated HSCs acquire high-impact features on the immune system, not just as passive targets of inflammatory cytokines, but these cells can act as antigen presenting cells (APC), are able to mediate autophagy, control phagocytosis of apoptotic bodies of hepatocytes and modulate the activity of dendritic cells, macrophages and NK cells (Weiskirchen and Tacke 2014).

Resolution

Two possible mechanisms may determine the reduction in activated HSC number: reversion to a quiescent phenotype or clearance through apoptosis (Gaça et al. 2003) (Issa et al. 2001).

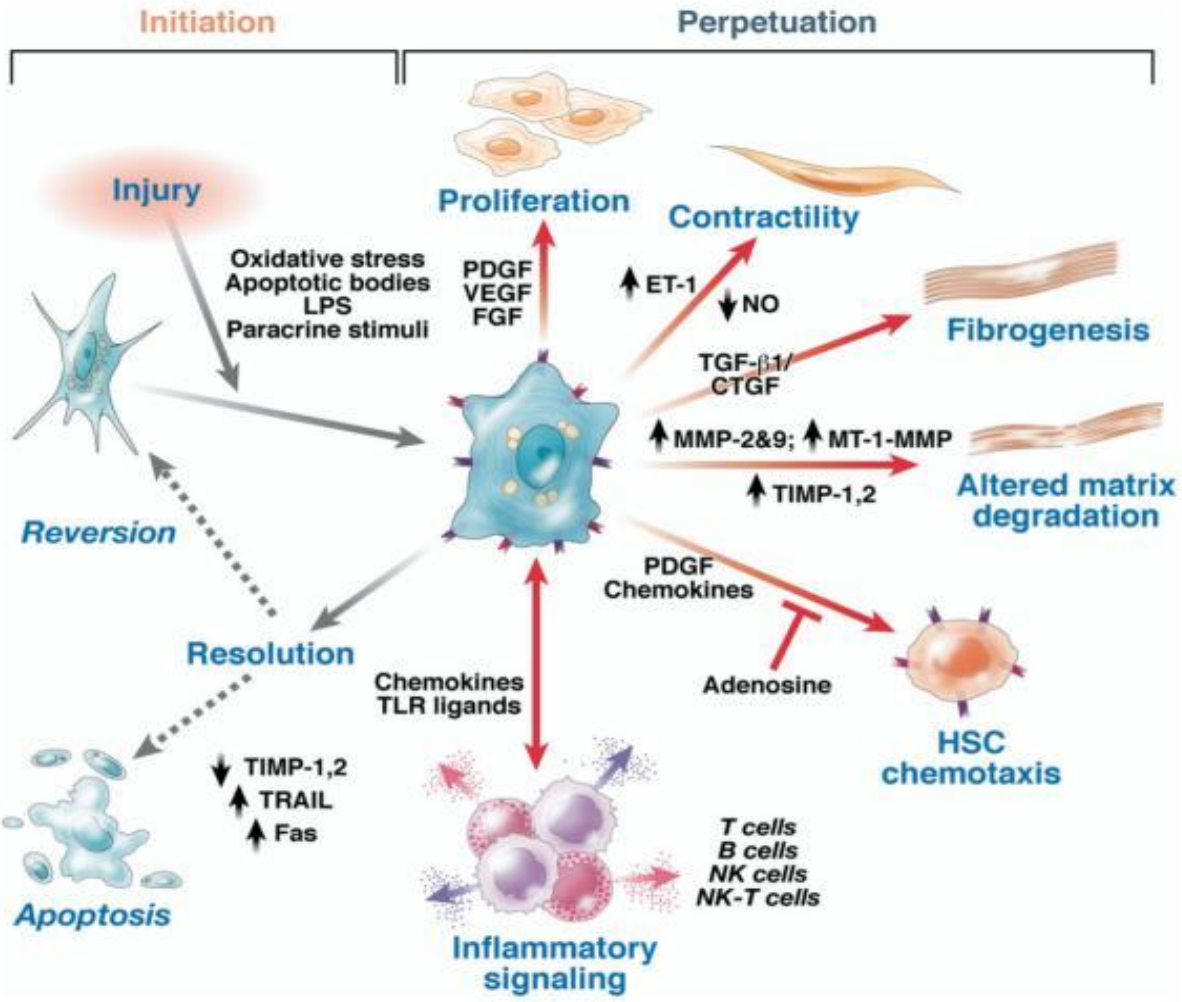

(Friedman 2008)

Figure 1.5. Molecular mechanisms underlying HSC activation.

Features of HSC activation can be distinguished between those that stimulate initiation and those that contribute to perpetuation. Initiation is caused by soluble stimuli that include oxidant stress signals (reactive oxygen intermediates), apoptotic bodies, lipopolysaccharide and paracrine stimuli from neighboring cell types including hepatic macrophages (Kupffer cells), sinusoidal endothelium and hepatocytes. Perpetuation is characterized by specific phenotypic changes including proliferation, contractility, fibrogenesis, altered matrix degradation, chemotaxis and inflammatory signaling.

1.6 MACROPHAGES

Macrophages play an essential role in the pathogenesis of chronic liver injury (Murray and Wynn 2011). Whereas in healthy liver the number of intrahepatic macrophages remains constant, following liver damage the intrahepatic macrophages are massively expanded, due to the influx of peripheral monocytes (Zimmermann, Trautwein, and Tacke 2012). Moreover, both clinical and experimental findings have demonstrated that the activation of Kupffer cells (KCs) plays a crucial role in the initiation of liver response to an insult (Wan et al. 2014). Indeed, hepatic macrophages contribute to the progression of liver fibrosis by several mechanisms, including the release of MMP, mainly MMP9, as well as chemokines, cytokines and growth factors like TGF-β1, VEGF and angiotensin II that accelerate the activation of hepatic resident cells. Moreover, Kupffer cells together with other liver cells (HSCs and hepatocytes) secrete chemokines, such as MCP-1, promoting a massive infiltration of monocytes in the injured liver (Dal-Secco et al. 2015). In this context, monocytes rapidly differentiate to macrophages.

As macrophages have been recently shown to display some degree of plasticity and heterogeneity, macrophage polarization is becoming a topic of great interest (Gordon and Taylor 2005). Activated macrophages differentiate in two main subsets, generated in different inflammatory conditions: M1 (classically activated) and M2 (alternatively activated). M1 macrophages produce pro-inflammatory cytokines, whereas M2 macrophages regulate inflammatory reactions and tissue repair. M2 macrophages can be further

distinguished in diverse subtypes, each induced by different molecules and eliciting different signals. In particular, M2a macrophages are stimulated by IL-4 and IL-13, and mainly induce a Th2 response, M2b macrophages are stimulated by immune complexes or LTR ligands and are involved in Th2 activation and immune regulation, M2c macrophages are stimulated by IL-10 or TGF-β and are involved in immune suppression, tissue repair and matrix remodeling (Spiller et al. 2016) (Figure 1.6).

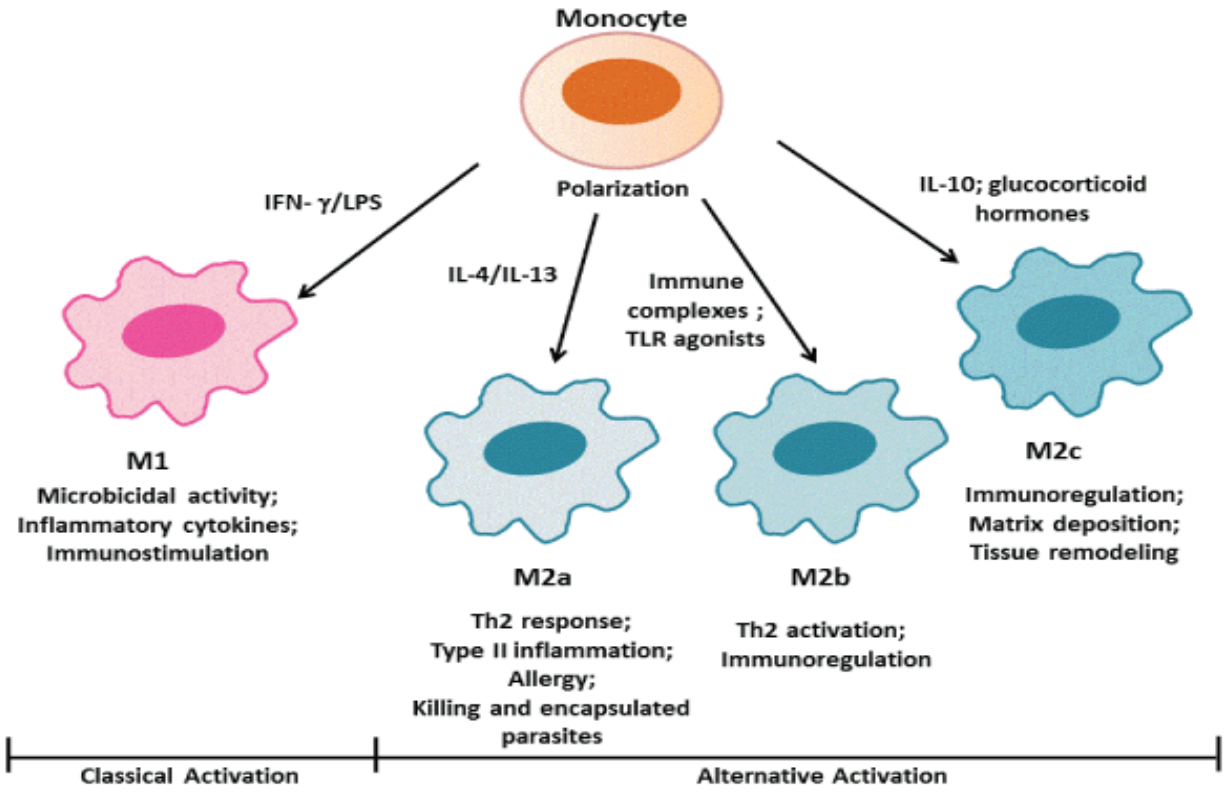

(Zanluqui et al. 2015)

Figure 1.6. Macrophages polarization spectrum.

Macrophage microenvironment stimuli define differential macrophage polarization via classical activation (M1) or alternative activation (M2).

The balance between M1 and M2 macrophages mediates the progression or resolution of liver fibrosis. During the early stages of liver injury, bone marrow-derived monocytes are intensively recruited to the liver and differentiate into inflammatory macrophages (mostly M1) to produce pro-inflammatory (such as IL-1β, IL-6, IL-8, IL-12 and TNF-α) and profibrotic cytokines, promoting inflammatory responses and HSC activation. Subsequently, recruited macrophages switch to M2 phenotype, which secrete a wide variety of MMPs (MMP2, MMP9, MMP12, MMP13 and MMP14) and anti-inflammatory cytokines (such as IL-4, IL-13 and IL-10) aimed to facilitate fibrosis resolution (Pradere et al. 2013) (Figure 1.7).

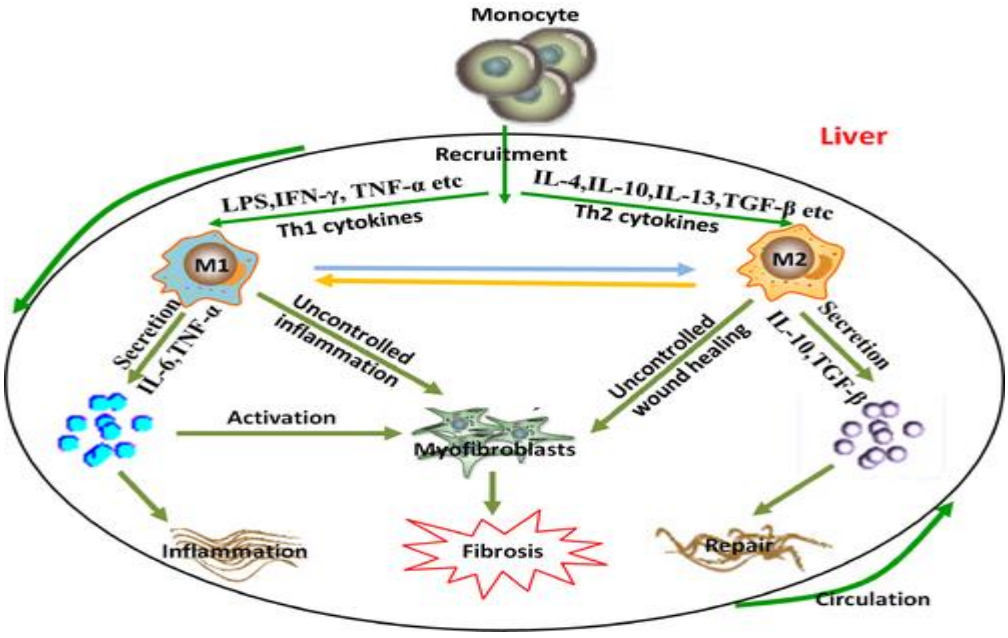

(Sun et al. 2017)

Figure 1.7. Macrophage phenotypes in liver injury and repair.

During liver inflammation, circulating monocytes can be recruited to the injured liver and then differentiate into macrophages via growth factors and chemokine signals.

Macrophage polarization is mainly regulated by signaling pathways, transcription factors, post-transcriptional regulators and epigenetic regulation. Classic regulatory pathways including JNK, PI3K/AKT, Notch, JAK/STAT, NF-kB, play a critical role in the macrophages polarization (Yang et al. 2014). In particular, PI3K pathway can regulate many aspects of cellular activity as metabolism, motility and proliferation (Hartmann et al. 2012). AKT is known to be an important effector of PI3K which plays a crucial role in macrophages polarization.

1.7 RECEPTOR TYROSINE KINASES (RTKs)

Receptor tyrosine kinases (RTK) are a family of integral membrane receptors. To date, 58 human RTKs are known, which are divided into 20 subfamilies (Figure 1.8).

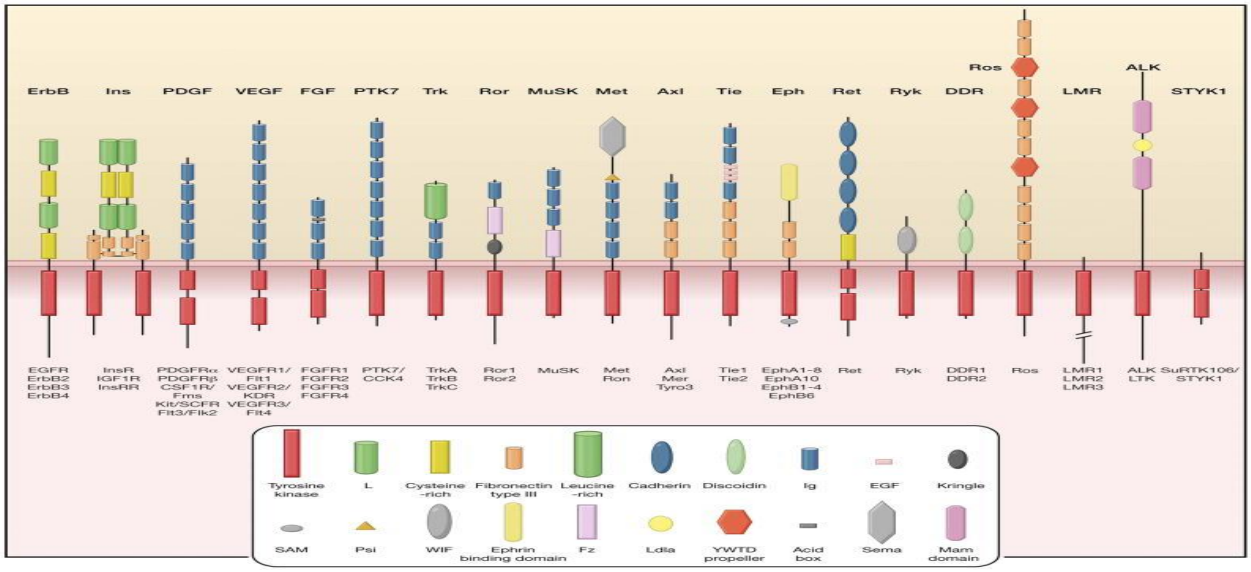

(Lemmon and Schlessinger 2010)

Figure 1.8. Receptor Tyrosine Kinase Families.

All RTKs have a similar structure, with a ligand binding domain in the extracellular region (about 50-80 kDa), a single transmembrane helix and a cytoplasmic region (150 to 350 kDa) that contains the protein tyrosine kinase (TK) residues plus additional carboxy (C-) terminal and juxtamembrane regulatory regions (Lemmon and Schlessinger 2010).

Early studies on RTKs have suggested that a ligand-induced dimerization mechanism is required to induce receptor activation: a bivalent ligand concurrently interacts with two receptor isoforms by forming a dimeric complex (Hunter 1998). Ligand-induced dimerization of the extracellular region leads to autophosphorylation and activation of the intracellular tyrosine kinase domain (TKD), with the consequent recruitment and activation of downstream molecules (Lemmon and Schlessinger 2010), containing SH2 or PTB domains (Pawson 2004). This interaction can be direct or indirect, mediated by docking protein (Schlessinger 2000). RTKs play a central role in various signaling networks involving multiple proteins that regulate important processes, including survival, growth, differentiation and motility. Dysregulation of these networks has been implicated in cancer, diabetes, inflammation, severe bone disorders, arteriosclerosis, angiogenesis and other diseases. The elevated complexity of RTK-mediated signaling have driven the development of pathway-biased synthetic peptide or small molecule ligands that can selectively modulate or block RTK activity (Lemmon and Schlessinger 2010).

1.7.1 TAM Receptor Tyrosine Kinases

The name of TAM family is derived from the first letter of the three components: Tyro3, Axl and Mer.

As all RTKs, these receptors contain an extracellular region, a transmembrane region and a conserved intracellular kinase domain (Lemke 2013).

The TAM family is characterized by adhesion molecule-like domains in the extracellular region and a conserved sequence, KW (I/L)A(I/L)ES, within the kinase domain (Linger et al. 2008). More specifically, the amino-terminal residue of the extracellular region carries two immunoglobulin-like (Ig) domains that mediate ligand binding (Sasaki et al. 2006), which are followed by two fibronectin type III (FNIII) (Lemke and Rothlin 2008) (Figure 1.9). The modules of extracellular region may be important in cell–cell contacts and mimic the structure of neural cell adhesion molecule (NCAM), which contains five Ig domains and two FNIII domains (Yamagata, Sanes, and Weiner 2003). The TAM RTKs genes share similar genomic structure, encoding transcripts that vary in size from 3 to 5 kb (Linger et al. 2008). Tyro-3 and Axl have the most similar structure, sharing the same number (20) and size of exons (Lewis et al. 1996).

The amino acids sequence of human TAM RTKs present 31–36% of identity within the extracellular region and 54–59% within the intracellular region, with higher homology in the tyrosine kinase domain (Linger et al. 2008). TAM RTKs single, double and even triple knockout have not defects at birth (Linger et al. 2008), suggesting that they are nonessential for embryogenesis and

early development (Lemke and Lu 2003). Contrariwise, adult TAM RTKs knockout mice develop different phenotypes in a wide range of tissues (Lu et al. 1999) as splenomegaly and enlarged lymph nodes, a common manifestation of chronic and lymphoid activation (Lu and Lemke 2001).

Immune regulation is the most important function of TAM RTKs. Indeed these receptors regulate innate immune responses by modulating cytokine production, promoting wound healing and resolution of inflammation (Rothlin et al. 2007). Combined loss of MerTK, AXL, and TYRO3 results in a highly active autoimmune state, with massive lymphocyte proliferation and lupus-like autoimmunity (Lu et al. 1999).

Furthermore, TAM RTKs are overexpressed in numerous cancers, including myeloid and lymphoblastic leukemias, melanoma, lung, breast, kidney, liver, gastric, colon, ovarian, uterine and brain cancers (Graham et al. 2006) (Linger et al. 2008).

1.7.2 TAM Ligands

The best-studied ligands for TAM RTKs are the Vit-K modified-carboxylated proteins: Gas-6 and Pros-1 (Mark et al. 1996) (Anderson et al. 2003). These glycoproteins share ~44% of homology and have analogous domain structure, consisting of a N-terminal-carboxyl-glutamic acid (Gla) domain, 4 tandem Epidermal Growth Factor (EGF)-like repeats and a C-terminal Sex Hormone-Binding Globulin-like region (SHBG) containing 2 Laminin G (LG) repeats (Mark et al. 1996) (Figure 1.9).

Gla-domain need to be carboxylated in a vitamin K-dependent reaction to make Gas-6 and Protein-S biologically active (Stenhoff, Dahlbäck, and Hafizi 2004). This domain mediates the $Ca2^{+}$-dependent binding to negatively charged membrane phospholipids, such as phosphatidylserine (PtdSer) exposed on the surface of apoptotic cells (Huang et al. 2003).

LG domains are involved in the ligand-receptor interaction by forming a V-shaped structure, stabilized by a calcium-binding site (Sasaki et al. 2002).

In human plasma, Pros-1 is highly concentrated (0.30 μM/L) (Rezende, Simmonds, and Lane 2004) (approximately 1000 times higher), compared to Gas-6 (0.16 to 0.28 nM/L) (Balogh et al. 2005), conceivably due to the involvement of Pros-1 in the coagulation pathways, where it functions as a co-factor for Protein C during Factors Va and VIIIa inactivation (Heeb 2008). Gas-6 is instead expressed mainly in vascular smooth muscle and endothelial cells and it is frequently upregulated after tissue damage (Ekman et al. 2010).

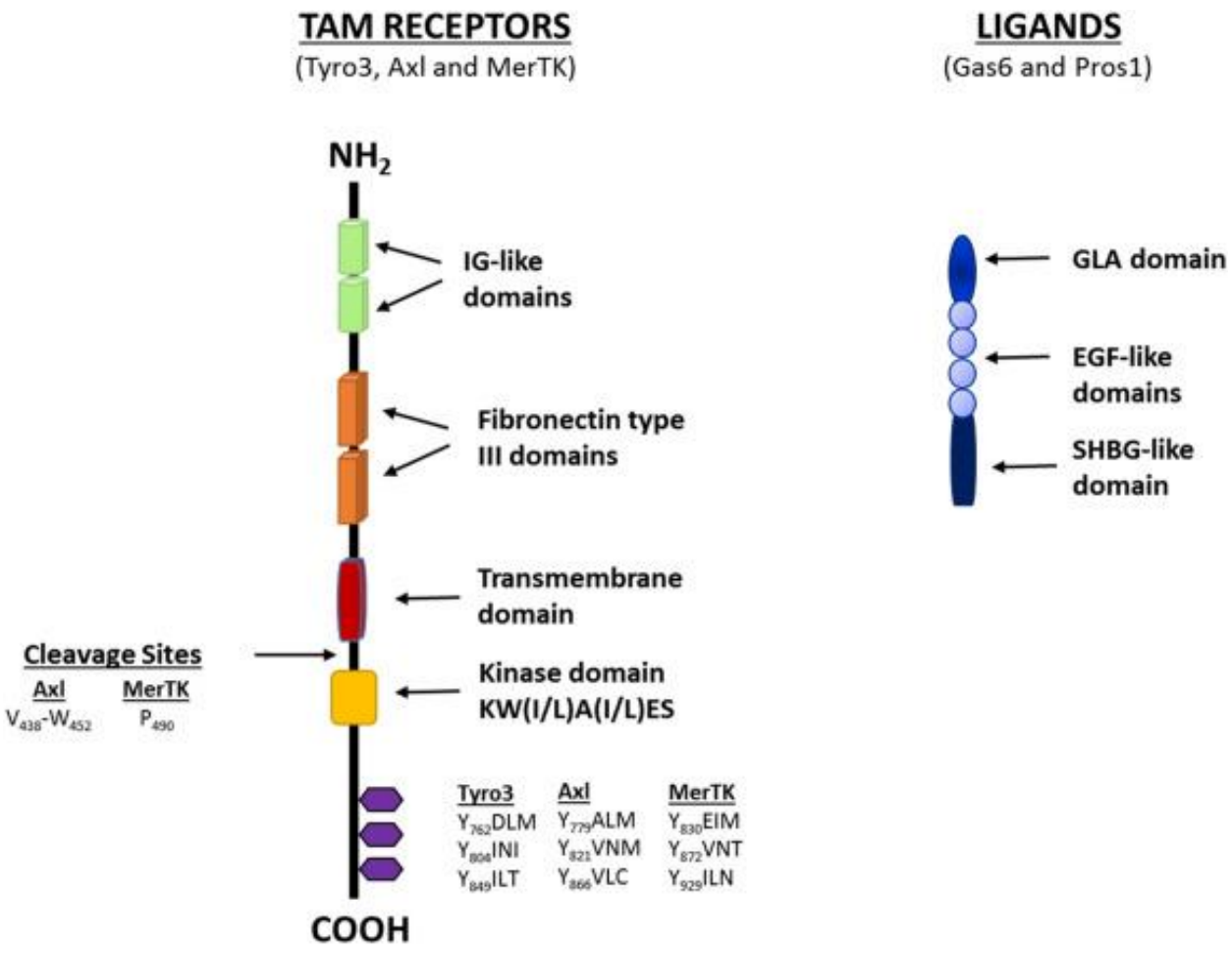

(Shafit-Zagardo, Gruber, and DuBois 2018)

Figure 1.9. Structural characterization of the TAM RTKs and their ligands.

1.7.3 MerTK

Myeloid-epithelial-reproductive Tyrosine Kinase (MerTK) was the second member of TAM Receptor Tyrosine Kinase (RTK) family to be described.

The full-length Mer protein contains 999 amino acids; though the predicted protein size is 110 kDa, the actual molecular weight ranges from 165 to 205 kDa due to post-translational modifications, including glycosylation, phosphorylation and ubiquitination (Linger et al. 2008).

This receptor is normally expressed in monocytes/macrophages, dendritic cells, NK cells, NKT cells, HSCs, megakaryocytes, platelets, epithelial tissue and reproductive tissue (Behrens et al. 2003, Petta et al. 2016).

1.7.3.1 Biological role of MerTK

MerTK is expressed at high levels in macrophages displaying the M2c phenotype capable of clearing ACs (Zizzo et al. 2012).

MerTK signaling plays a central role in dampening the innate immune response, as demonstrated in experimental endotoxemia models, in which MerTK knockout mice exhibit extreme activation of inflammatory responses and ineffective resolution of inflammation, mediated by elevated levels of TNF-α and IL-1 (Lee et al. 2012).

MerTK acts in maintaining both central and peripheral tolerance, through different mechanisms, including efferocytosis, a physiological process aimed to maintain immune homeostasis, by which apoptotic cells are engulfed by phagocyte (Sather et al. 2007). MerTK ligands, as Gas-6, simultaneously bind MerTK expressed on phagocytes and PtdSer residues present on the outer plasma membrane leaflets of apoptotic cells. Gas-6, linked to the externalized PtdSer, activates MerTK, initiating phagocytic process and inducing transcriptional events that lead to a decrease of proinflammatory cytokines, such as IL-12 and increase in inflammatory repressors, as IL-10 and TGF-β, thus generating an antiinflammatory milieu (Tibrewal et al. 2008).

Efferocytosis plays important roles in the regeneration and repair of damaged tissues by inducing growth factors such as VEGF and hepatocyte growth factor (HGF) (Morimoto et al. 2001) (Golpon et al. 2004). MerTK is not required for this process during embryogenesis, whereas it is essential for the phagocytosis that continually occurs in adult organs as part of normal tissue homeostasis.

Furthermore, MerTK also impacts in homeostasis by promoting platelet aggregation and survival of endothelial cells (Angelillo-Scherrer et al. 2001).

MerTK is also involved in the progression of NAFLD. In human NAFLD specimens MerTK was found to be mostly expressed in macrophages and HSCs loosely aggregated within inflammatory foci (Petta et al. 2016).

In a recent genome-wide association study, a single nucleotide MERTK polymorphism (SNP), the rs4374383 G>A SNP, has been associated with a reduced prevalence of severe liver fibrosis in patients with NAFLD and correlates with decreased hepatic expression of MerTK.

MerTK is also overexpressed in murine models of fibrogenesis and in patients with NASH and severe fibrosis (Petta et al. 2016).

Overexpression of MerTK has been observed in several human cancers where it promotes tumour growth, metastasis and chemoresistance stimulating cell survival, migration and invasion (Graham et al. 2014) (Lee-Sherick et al. 2015). This receptor activates several pathways involved in tumor progression including MAPK/ERK and PI3K/AKT pathways (Figure 1.10).

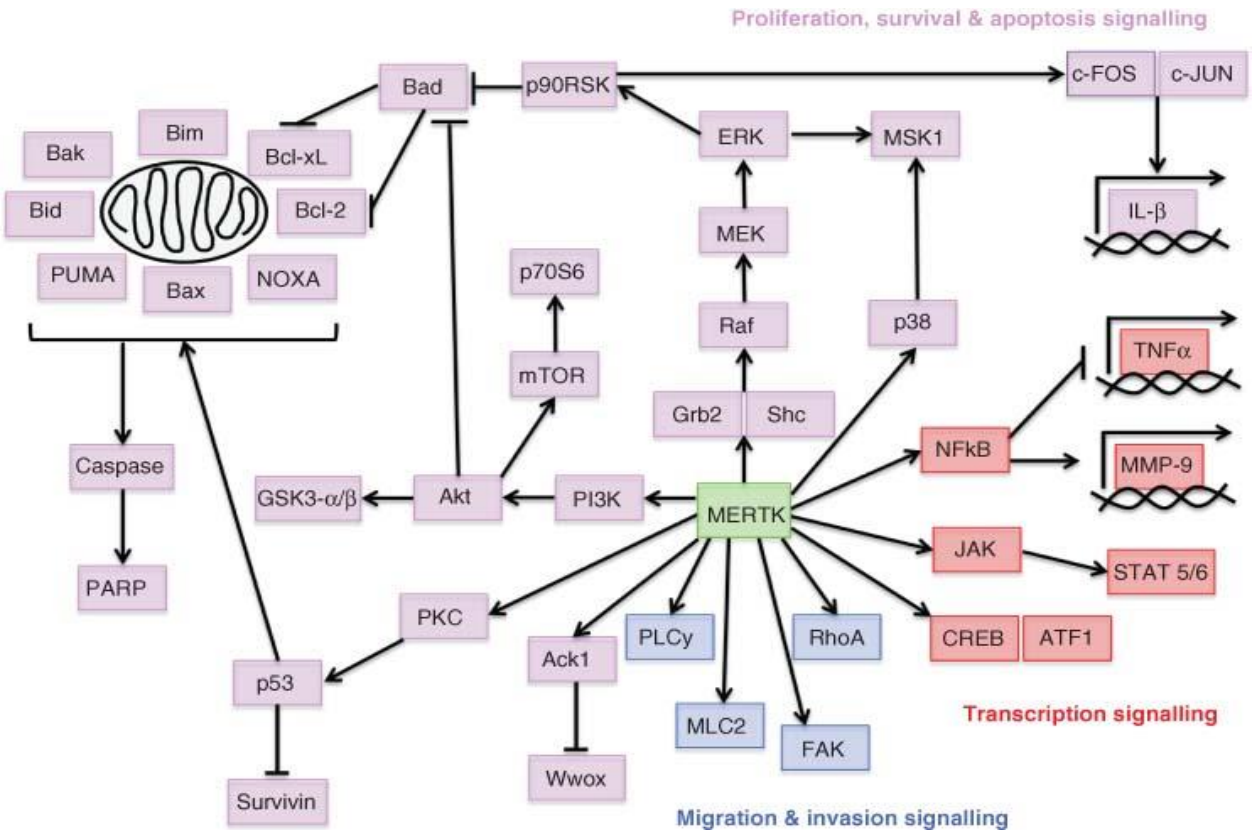

(Hill et al. 2015)

Figure 1.10. MerTK signaling pathways.

MerTK alters gene transcription via the JAK/STAT pathway or other transcription factors, such as STAT-5 and STAT-6 (Brandao et al. 2013) (Linger et al. 2013).

An important transcriptional effector of MerTK is NF-κB which contributes to oncogenesis by regulating genes related to proliferation, migration and apoptosis (Cui et al. 2014). MerTK signaling also plays a role in the migratory and invasive potential of solid tumours, promoting increase in both RhoA and activated FAK, which play important roles in cell motility (Rogers et al. 2012).

1.7.3.2 Therapeutic Targeting MerTK

Various therapies targeting MerTK are currently developing (Figure 1.11). Small molecule tyrosine kinase Inhibitor have been recently described, including UNC569 (Christoph et al. 2013), UNC1062 (Schlegel et al. 2013) and UNC1666 (Lee-Sherick et al. 2015). These compounds competitively bind MerTK in its catalytic site, impeding phosphorylation and activation of the kinase domain. Treatment with these inhibitors causes a decrease in MerTK signaling downstream. Next-generation inhibitors have also been reported, including UNC2025, a potent, orally bioavailable inhibitor (Zhang et al. 2014). Other agents include Mer590, a monoclonal antibody that directly binds to the extracellular domain and induces internalization and degradation of MerTK. (Cummings et al. 2014).

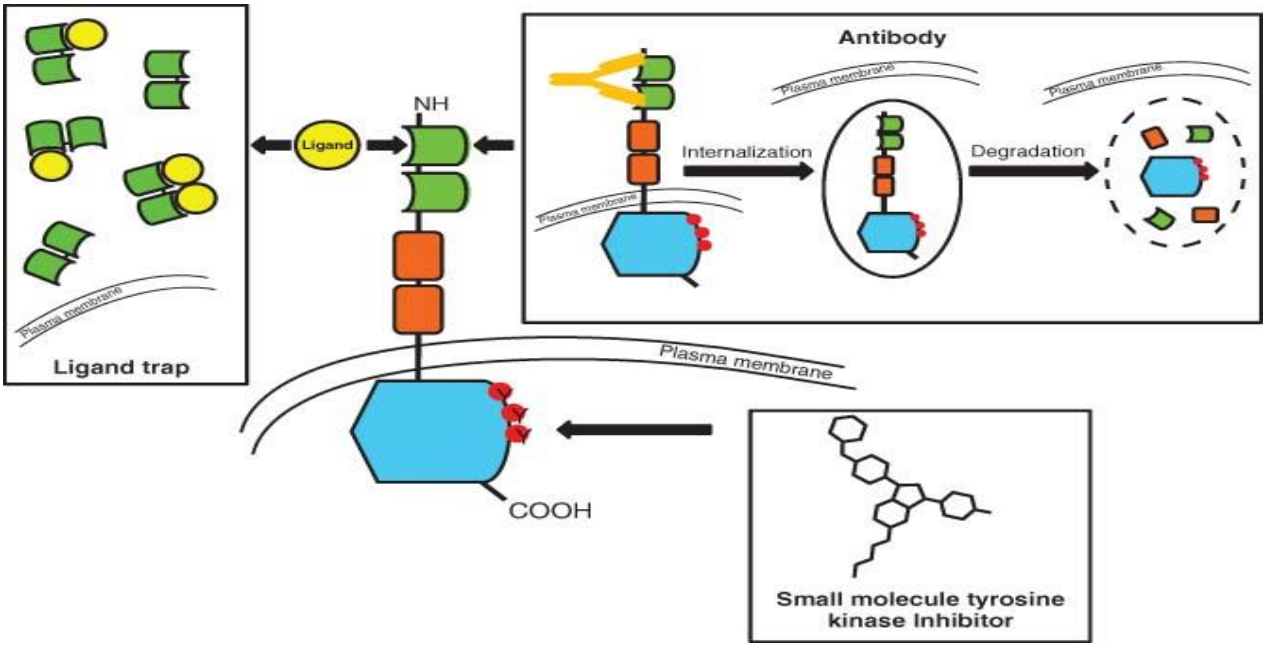

(Hill et al. 2015)

Figure 1.11. MerTK therapeutic targeting

2. AIM

Recent findings have described the involvement of MerTK in the progression of NAFLD. Considering that advanced fibrosis and cirrhosis are major risk factors for the development of HCC, there is a strong rationale for the involvement of MerTK in the progression of liver fibrosis and HCC development.

Based on the above background, the first aim of this project was to investigate the potential effects of MerTK activation in macrophages on profibrogenic phenotype of HSCs. To accomplish this, THP1-derived macrophages and peripheral monocytes-derived M2c macrophages were employed to examine the interaction between macrophages and HSCs.

A second part of our study was aimed to investigate the potential role of MerTK in the biology of HCC, by using human HCC cell lines (HuH7 and HepG2).

3. MATERIALS AND METHODS

3.1 CELL CULTURES

THP1 human monocytic leukemic cell line kindly gifted by Dr. Elisabetta Rovida, was maintained in RPMI 1640 supplemented with 1% (v/v) L-glutamine, 1% (v/v) antibiotic/antifungal solution (all reagents from Euroclone, Milan, IT) and 10% (v/v) fetal bovine serum (FBS) (Carlo Erba, Milan, IT). THP1 monocytes are differentiated into macrophages by 48 h incubation with 10 ng/ml phorbol 12-myristate 13-acetate (PMA) (Sigma, St. Louis, MO, USA) at 37 °C in 5% CO_2, as described by Kurihara et al (Kurihara and Furue 2013).

HepG2 and HuH7 human hepatocellular cell lines, kindly gifted by Dr. Elisabetta Rovida, were maintained in Dulbecco's modified Eagle's minimal medium supplemented with 1% (v/v) L-glutamine, 1% (v/v) nonessential amino acids, 1% (v/v) sodium pyruvate, 1% (v/v) antibiotic/antifungal solution (all from Euroclone, Milan, IT) and 10% (v/v) FBS (Carlo Erba, Milan, IT).

3.2 ISOLATION AND CULTURE OF HUMAN HEPATIC STELLATE CELLS

Human HSCs were isolated from normal liver tissue unsuitable for transplantation as described Casini et al (Casini et al. 1993). After washing in Hank's balanced salt solution (HBSS) (Euroclone, Milan, IT) at 37 °C, liver specimens were finely minced by using a sterile razor blade, placed in a sterile flask containing 0.5% pronase (Sigma, St. Louis, MO, USA), 0.05% type IV collagenase (Sigma, St. Louis, MO, USA) and 5 µg/mL of deoxyribonuclease (DNase) (bovine pancreas; Sigma, St. Louis, MO, USA) in 100 mL of HBSS and agitated for 30 minutes at 37 °C. The resulting cell suspension was filtered through a 100 µm nylon wire mesh and the undigested material was further digested with 0.05% pronase, 0.05% type IV collagenase and 5 µg/mL DNase, filtered again and pooled with the remainder of cell suspension. The digested material was washed 3-5 times by centrifugation at 450 x g for 5 minutes in HBSS containing 5 µg/mL of DNase and the resulting pellet was resuspended in 25 ml of the same solution. HSCs were separated from other non-parenchymal liver cells by density gradient centrifugation on 50 % and 35 % (v/v) Percoll (Sigma, St. Louis, MO, USA), at 1,200 RPM for 30 min at 4 °C. HSCs were recovered from the interface between the medium and the 35 % gradient. Cells were plated in uncoated flasks at an approximate density of 1 X 10^6 cells/ml and cultured in Iscove's modified Dulbecco's medium supplemented with 1% (v/v) L-glutamine, 1% (v/v) nonessential amino acids, 1% (v/v) sodium pyruvate, 1% (v/v) antibiotic/antifungal solution (all from Euroclone, Milan, IT) and 20% (v/v) FBS (Carlo Erba, Milan, IT) at 37 °C in

5% CO_2. Medium was replaced 24 hours after plating and every 72 hours thereafter. Primary cultures were grown up to confluency and then subcultured by trypsinization.

3.3 MONOCYTE ISOLATION FROM BUFFY COATS

Human monocytes were isolated from buffy coats of healthy subjects that have signed informed consent. A two step procedure was employed, as described by De Almeida et al. (de Almeida et al. 2000), using Lympholyte-H (Cedarlane; Burlington, CA) followed by slight hyperosmolar Percoll (density: 1.131 g/ml) (GE Healthcare Life Sciences, Sigma, St. Louis, MO, USA). Lympholyte-H, a density gradient separation medium designed to isolate lymphocytes/monocytes from human peripheral blood, allows to remove erythrocytes and dead cells as well as the majority of granulocytes, leading to a high and non-selective recovery of viable lymphocytes and monocytes. Percoll gradient centrifugation allows to obtain highly pure monocyte preparation (more than 90%).

Specifically, the protocol executed, includes the following steps:

- Each buffy coat should be diluted 1: 1 with sterile 1 mM PBS-EDTA (Euroclone, Milan, IT).
- For each diluted buffy coat fill three 50 ml tubes with 15 ml Lympholyte-H.
- Layer 30-35 ml of the buffy coat blood on top of the Lympholyte-H for the first density gradient.
- Centrifuge at 400 x g without brake for 30 min at room temperature.
- For each gradient collect the white ring of peripheral blood mononuclear cells (PBMCs) which is located between the two phases, pipette and transfer to a new tube (Figure 3.1).

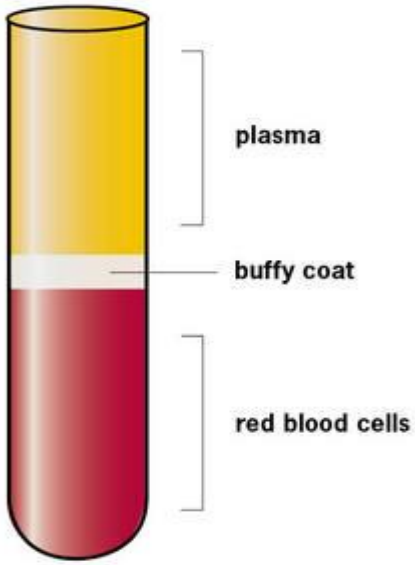

(Garcia 2016)

Figure 3.1. Illustration of layers obtained after Ficoll gradient centrifugation.

- Fill each tube with 1 mM PBS-EDTA up to 40 ml in total.
- Centrifuge at 300 x g for 10 min without brake at room temperature.
- Aspirate supernatant and wash pellet again with 40 ml sterile 1 mM PBS-EDTA.
- For each donor pool the pellets in 20 ml 1 mM PBS-EDTA.
- Prepare the iso-osmotic Percoll solution for the second density gradient: For two donors mix 23.13 ml Percoll solution with 1.87 ml 10-fold PBS.
- Then transfer 23 ml of this solution and add 27 ml complete RPMI-1640 to obtain a 46% iso-osmotic Percoll solution.
- For each donor transfer 25 ml of the prepared Percoll solution and layer the PBMC solution prepared on top of the Percoll solution.

- Centrifuge at 550 x g without brake for 30 min at room temperature.
- For each gradient collect the white ring of monocytes which is located between the two phases.
- Fill each tube with 1 mM PBS-EDTA up to 50 ml in total.
- Centrifuge at 400 x g for 10 min without brake at room temperature.
- Aspirate the supernatant and resuspend the pellets in 20 ml complete RPMI-1640 medium.

3.3.1 Differentiation of Monocytes to Macrophages

About 50 x 10^6 cells were seeded in 60 mm Petri dish and incubated for 2 hours at 37 °C in 5% CO_2 in complete RPMI 1640 medium.

The medium was removed and cells were carefully washed with 1 mM PBS-EDTA.

The medium was replaced with complete RPMI 1640 medium supplemented with Macrophage colony-stimulating factor (M-CSF) (50 ng/ml) (Peprotech, London, UK). M-CSF (50 ng/ml), IL-10 (50 ng/ml) (Peprotech, London, UK) and TGF-β (20 ng/ml) (Peprotech, London, UK) were added on the fifth day to differentiate the monocytes to M2C macrophages as described by Zizzo et al (Zizzo et al. 2012). After 3 days of incubation at 37 °C in 5% CO_2, terminally differentiated macrophages were obtained.

3.3.2 Analysis of cell-surface molecules by FACS

Flow cytometry analysis was performed in freshly isolated and in cultured cells after washing in cell staining buffer containing: PBS (without Ca^{2+} or Mg^{2+}) with 0.2 % (w/v) Bovine Serum Albumin and 0.1% (w/v) sodium azide, pH 7.4 (0.2 μm-pore filtered).

The following mouse mAbs were used:

anti-CD163(APC), CD163 expression was evaluated using appropriate APC-labeled isotype control, anti-CD206 (APC-Cy7), CD206 expression was evaluated using appropriate APC-Cy7-labeled isotype control, anti-CD209 (FITC), CD209 expression was evaluated using appropriate FITC-labeled isotype control (all reagents from Biolegend, San Diego, USA) and anti-MerTK (PE) (clone # 125518; R&D Systems, Minneapolis, MN), MerTK expression was evaluated using appropriate PE-labeled isotype control (clone # 133303; R&D Systems, Minneapolis, MN).

Appropriately conjugated fluorescent antibodies were added at predetermined optimum concentrations according to the manufacturer's recommendations and incubated in ice for 15-20 minutes in the dark.

Two washes were performed in cell staining buffer by centrifugation at 350 x g for 5 minutes. Cell pellet was resuspended in 0.5 ml of cell staining buffer and then 5 μl (0.25μg)/million cells of 7-AAD Viability Staining Solution (BioLegend, San Diego, USA) were added to exclude dead cells. After 3-5 minutes incubation on ice in the dark, samples were analyzed using Flow

Cytometer FACSCanto (BD Biosciences, Franklin Lakes, NJ, USA) and ModFit software.

3.4 TRANSFECTION OF THP1 CELLS

The protocol used provides a method for reliably and efficiently transfecting human THP1 macrophages and monocytes with high cell vitality, high transfection efficiency and minimal effects on cell behaviour. This approach is based on Nucleofection and the protocol has been optimized to maintain maximum capability for cell activation after transfection, as described by Schnoor et al (Schnoor et al. 2009).

The protocol includes the following phases:

Pre-differentiation of THP-1 Macrophages:

Seed 1.0-1.5 x 10^7 cells into a 75 cm² tissue culture flask in complete RPMI-1640 medium supplemented with 10 ng/ml phorbol 12-myristate 13-acetate (PMA) (Sigma, St. Louis, MO, USA) and incubate for 48 hours at 37 °C in 5% CO_2.

Preparation of Nucleofection:

1. Incubate cells with Accutase I (Euroclone, Milan, IT) for 30 min at 37 °C for full detachment of cells.
2. During Accutase I treatment, prepare the cultivation medium: complete RPMI-1640 medium supplemented with 2.5 ng/ml PMA.

3. Transfer cell suspension to a tube and centrifuge cell suspension for 5 min at 300 x g at room temperature.
4. Count cells to determine cell number. For each transfection sample prepare aliquots in centrifuge tubes containing 2.0-2.5 x 10^6 cells.

Nucleofection of THP-1 Macrophages:

1. Prepare one Nucleofector cuvette with 1 µg of siRNA for each transfection. Smart Pool siRNA specific for human MERTK (sequence accession no. # NM_006343) or non-targeting (Dharmacon, Lafayette, USA) were employed.
2. Resuspend cells in Nucleofector Solution V (Amaxa, Cologne).
3. Transfect cells by using program Y-001 in Nucleofector 2b device (Amaxa, Cologne).
4. Incubate transfected cells in complete RPMI-1640 medium for 4 hours at 37 ° C in 5% CO_2

Post-Nucleofection Care:

1. Carefully aspirate complete medium and replace with equal amount of cultivation medium.
2. Incubate cells for required period for maximal effect of siRNA (72 hours).

3.5 FOR CONDITIONED MEDIUM STUDIES

After gene silencing, THP1-derived macrophages were incubated for 24 hours in serum-free medium and then stimulated with 200 ng/ml Gas-6 (R&D Systems, Minneapolis, MN) for 8 hours.

To perform the treatment with UNC569, both THP1-derived and circulating monocytes-derived macrophages were incubated in serum-free medium for 24 hours and then exposed to UNC569 5 μM (Calbioche, Milan, IT) before stimulation with Gas-6 200 ng/ml for 8 hours.

All macrophages were then rinsed three times with PBS and further incubated overnight in serum-free medium. Finally, Conditioned Medium (C.M.) of macrophages in various conditions was collected, centrifuged at 2000 x g for 10 minutes and stored at -80 °C.

3.6 CELL MIGRATION ASSAY

Sub-confluent cells were serum-starved for 48 hours and then washed, trypsinized and resuspended in serum-free medium at a concentration of 2.5 x 10^5 cells/ml. Chemotaxis was measured in modified Boyden chambers equipped with 8 μm pore filters (Millipore Corp, MA, USA) coated with rat tail collagen (20 μg/ml) (Collaborative Biomedical Products, Bedford, USA), as described in detail elsewhere (Bonacchi et al. 2001). Cells were seeded in upper compartment, while the chemoattractants were placed in lower compartment (Figure 3.2).

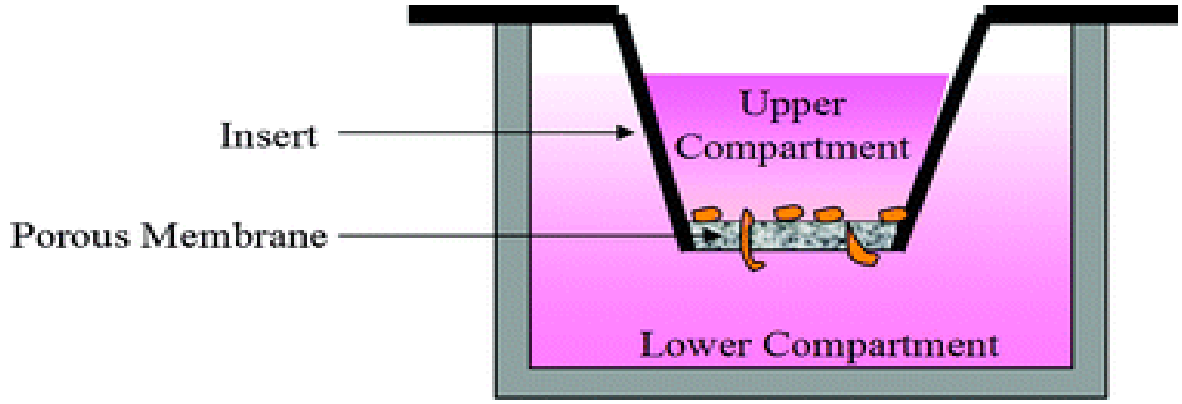

(Toetsch at al. 2009)

Figure 3.2. Illustration of migration assay using a Boyden chamber.

After the incubation period (six hours) at 37 °C, the cells migrated to the underside of the filters were fixed, stained with Giemsa, mounted and counted at 40X magnification. Data represent the average of cell counts obtained in ten randomly chosen high-power fields (HPF).

3.7 CELL PROLIFERATION ASSAY

HSC proliferation was evaluated by using a colorimetric immunoassay, based on the measurement of BrdU incorporation during DNA synthesis, (Roche Applied Science, Penzberg) according to the manufacturer's recommendations.

3.8 CELL VIABILITY ASSAY

The tetrazolium MTT (3-(4,5-dimethylthiazolyl-2)-2,5-diphenyltetrazolium bromide) (Sigma, St. Louis, MO, USA) was used to examine cell survival. The yellow tetrazolium is reduced by dehydrogenase of metabolically active cells to insoluble purple formazan, which can be solubilized and quantified by spectrophotometer (Thermo Fisher Scientific, Waltham, MA, USA).

3.9 TOTAL RNA EXTRACTION

Total RNA was isolated from HSCs using the NucleoSpin RNA II kit (Mackerey-Nagel, Dürer), according to the manufacturer's instructions.

3.9.1 Trizol RNA extraction

The isolation of total RNA from macrophages was performed by trizol reagent (Invitrogen, Waltham, MA, USA) according to the manufacturer's instructions.

3.10 RNA QUANTIFICATION

Concentration and quality of total RNA were measured using the NanoDrop 1000 Spectrophotometer (Thermo Fisher Scientific, Waltham, MA, USA).

260/280 is ratio of absorbance at 260 and 280 nm and it was used to assess the purity of RNA. Total RNA with a ratio of ~2.0 is generally accepted as "pure". If the ratio is appreciably lower, it may indicate the presence of protein, phenol or other contaminants that absorb strongly at or near 280 nm.

260/230 is ratio of sample absorbance at 260 and 230 nm. This was a secondary measure used to assess of RNA purity. It is commonly in the range of 1.8-2.2. If the ratio is appreciably lower, this may indicate the presence of co-purified contaminants.

3.11 cDNA SYNTHESIS

To amplify by qPCR transcripts encoding the protein of interest, 1 µg of mRNA was retrotranscribed into cDNA as indicated below.

COMPONENT	VOLUME PER REACTION (µl)
5x iScript Advanced Reaction Mix (dNTPs, oligo (dT) and random primers) (Bio Rad, Hercules, CA, USA)	4
iScript Advanced Revense Transcriptase (RNase H+ Moloney murine leukemia virus (MMLV) reverse transcriptase and RNase inhibitor) (Bio Rad, Hercules, CA, USA)	1
RNA template	Variable
Nuclease-free water	To 20
Total volume	20

The complete reaction mix was incubated according manufacturer's recommendation using a thermal cycler.

Reverse transcription	20 min at 46 °C
RT inactivation	1 min at 95 °C

3.12 GENE EXPRESSION ANALYSIS

The Real-Time PCR Analysis allows real time detection of PCR products as they accumulate during PCR cycles and create an amplification plot, which is the plot of fluorescence signal versus cycle number. In the initial cycles of PCR, there is little change in fluorescence signal. This defines the baseline for the amplification plot. An increase in fluorescence above the baseline indicates the detection of accumulated PCR products. A fixed fluorescence threshold can be set above the baseline. The parameter Ct (threshold cycle) is defined as the fractional cycle number at which the fluorescence passes the fixed threshold.

Quantitative Real-time PCR was performed using Assays-on-Demand gene Expression products (Applied Biosystem, Foster City, CA, USA) or the SYBR Green chemistry (Bio Rad, Hercules, CA, USA).

Assays-on-Demand gene expression products are a comprehensive collection of pre-designed primer and probe sets. Each pre-formulated assay contains two unlabelled PCR primers and a FAM dye-labeled gene specific TaqMan MGB probe. SYBR green is a fluorescent dye that intercalates into double-stranded DNA and produces a fluorescent signal.

3.12.1 TaqMan Universal PCR Master Mix and thermal cycling parameters

TaqMan Universal PCR Master Mix prepared by adding all required components, according to the following manufacturer's recommendation:

COMPONENT	VOLUME PER 20 µl REACTION
TaqMan Universal PCR Master Mix (2x) (Applied Biosystem, Foster City, CA, USA)	10 µl
Assay-on-demand specific (20x)	1.25 µl
Actin forward and reverse primers	0.3 µl
Fluorogenic probe	0.2 µl
DNA template	5 µl
H_2O	5.45 µl
Total reaction mix volume	25 µl

Thermal cycling parameters used are the following:

Parameter	**Polymerase activation**	**PCR (40 cycles)**	
	Hold	**Denature**	**Anneal/extend**
Temperature	95 ° C	95 ° C	60 °C
Time (mm:ss)	10:00	00:15	01:00

3.12.2 iTaq Universal SYBR Green supermix and thermal cycling parameters

iTaq Universal SYBR Green supermix prepared by adding all required components, according to the following manufacturer's recommendation:

COMPONENT	VOLUME PER 20 µl REACTION
iTaq Universal SYBR Green supermix (2x) (Bio Rad, Hercules, CA, USA)	12,5 µl
forward and reverse primers	1 µl
DNA template	5 µl
H_2O	5.5 µl
Total reaction mix volume	20 µl

Thermal cycling parameters used are the following:

Parameter	**Polymerase Activation and DNA denaturation**	**PCR (40 cycles)**	
	Hold	**Denature**	**Anneal/extend**
Temperature	50 ° C	95 ° C	60 °C
Time (mm:ss)	00:30	00:05	00:30

All amplification reactions were performed using Corbett/Qiagen Rotor-Gene 6600 Real Time analyzer (Thermo Fisher Scientific, Waltham, MA, USA).

3.12.3 Data analysis for quantification of gene expression

The different amount of target was given by: $2^{-\Delta\Delta Ct.}$

Where: ΔΔCt = ΔCt sample – ΔCt reference control.

β-actin was used as internal gene reference in quantitative real-time PCR performed using Assays-on-Demand and glyceraldehyde 3-phosphate dehydrogenase (GAPDH) was used as internal gene reference in real-time PCR performed using SYBR Green.

3.13 WESTERN BLOTTING ANALYSIS

3.13.1 Protein extraction

Cells were lysed for 30 minutes at 4 °C with lysis buffer (20 mM Tris–HCl pH 7.5, 2 mM EDTA, 2 mM EGTA, 2 mM dithiothreitol, 10 µl/mL protease inhibitor cocktail complete (Roche, Penzberg HR), 10 mM NaF, 1 µM okadaic acid, 1 mM Na vanadate 0.5% (v/v) Triton X-10, 150 mmol/L NaCl, 25 mM β-glycerol-phosphate and 2 mmol/L PMSF. After, cellular extracts were centrifuged 10 min at 12,000 x g and the supernatant was used for Western blotting.

3.13.2 Protein quantification

The estimation of protein concentration was carried out using BCA Protein Assay (Euroclone, Milan, IT). BCA Protein Assay is a formulation based on bicinchoninic acid (BCA) for the colorimetric detection and quantitation of total

protein. This method combines the reduction of Cu^{+2} to Cu^{+1} by proteins in an alkaline medium (the biuret reaction) with the highly sensitive and selective colorimetric detection of the cuprous cation (Cu^{+1}), using a unique reagent containing bicinchoninic acid (Smith et al. 1985).

Protein concentration of cell lysates is determined by using bovine serum albumin (BSA) as standard. A series of dilutions of BSA are prepared and assayed together with the unknown samples, adding BCA solution and incubating tubes at 60 °C for 30 minutes. The chelation of two molecules of BCA with one cuprous ion gives rise to a purple-colored reaction product. This water-soluble complex exhibits a strong absorbance at 562nm, detected by spectrophotometer (ThermoFisher Scientific, Waltham, MA, USA).

3.13.3 SDS-PAGE polyacrylamide Gel

Equal amounts of proteins were separated by SDS–PAGE polyacrylamide gel. The protein samples were boiled for 5 minutes and centrifuged briefly before loading into the gel. The run was performed in in 1x Running buffer (Bio Rad, Hercules, CA, USA) at 300V and 16 mA.

Gel and polyvinylidene difluoride membrane were equilibrated in Transfer Buffer: (1x Tris-Glycine (Bio Rad, Hercules, CA, USA) and 20% methanol). Proteins were electroporetically transferred from the gel to the membrane (Millipore Bedford, MA) at 100 V and 300 mA for 1 hour and 15 minutes. In order to confirm protein transfer, the membrane was stained with 1x Red Ponceau (Sigma-Aldrich St. Louis, MO, USA). The staining was reversed by distilled water.

3.13.4 Blocking of the membrane

To minimize any unspecific interaction of the antibody with the membrane, it was incubated in blocking solution 3% (w/v) BSA in 1x DPBS at room temperature.

3.13.5 Incubation with Antibodies

The membrane was incubated overnight at 4°C with the primary antibody in 1x PBS, containing 1% (w/v) BSA.

Antibodies were used for Western blotting analysis according to the manufacturer's recommendations.

Rabbit monoclonal anti-MerTK (ab52968 Abcam Cambridge, MA, USA), rabbit polyclonal anti-MerTK (phospho Y749 + Y753 + Y754) (ab14921 Abcam Cambridge, MA, USA), mouse monoclonal anti-Phospho-Akt (Ser473) (#4051 Cell Signaling Technology, Danvers, MA, USA), rabbit polyclonal anti-Akt (#9272 Cell Signaling Technology, Danvers, MA, USA), rabbit polyclonal anti-Phospho-Stat3 (Tyr705) (#9131 Cell Signaling Technology, Danvers, MA, USA), rabbit monoclonal anti-Stat3 (#4904 Cell Signaling Technology, Danvers, MA, USA) antibodies were used.

Monoclonal Anti-β-Actin antibody produced in mouse (A5441 Sigma-Aldrich St. Louis, MO, USA) was used as internal control (1:1,000) in 1% (w/v) BSA in 1x DPBS. Afterwards, the membrane was washed 3 times with 1x PBS at room temperature and incubated for 1 hour with anti-rabbit or anti-mouse secondary antibody (Cell Signaling Technology, Danvers, MA, USA) (1:4,000)

in 1x DPBS containing 1% (w/v) BSA and then again washed 3 times with 1x DPBS at room temperature.

3.13.6 Detection

Immunoreaction was revealed by Luminata (Merk Millipore, Darmstadt). The secondary antibodies are directly coupled to horseradish peroxidase. These antibodies permit direct detection of antigen-antibody complex on the membrane by chemiluminescence detection on Image Quant Las4000 (GE Healthcare Life Sciences, Little Chalfont, UK).

3.14 STATISTICAL ANALYSIS

Statistical significance among different cell treatments was assessed by Student's paired *t*-test and defined as $p<0.05$.

4. RESULTS

4.1 MerTK expression increased in THP1 cells during differentiation from monocytes to macrophages

To elucidate the role of MerTK in the pathogenesis of liver fibrosis, the first part of our study was conducted in THP1 cells.

We first investigated the MerTK expression in macrophages derived from THP1 cells, an immortalized monocytic line obtained from the peripheral blood of a childhood case of acute monocytic leukemia.

In accordance with previous reports (Kurihara and Furue 2013) THP1 monocytes exposed to Phorbol 12-myristate 13-acetate, at the dose of 10 ng/ml, differentiated to macrophages (THP1 macrophages) (Figure 4.1).

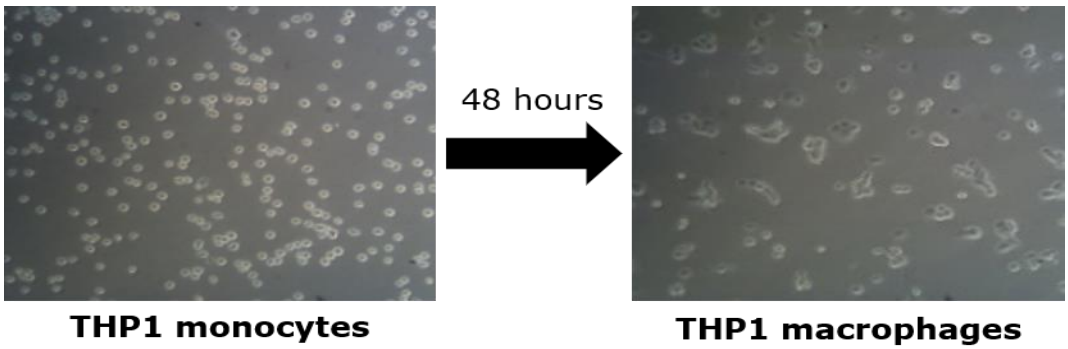

Figure 4.1. Differentiation of immortalized monocytic line THP1 towards the macrophage phenotype.

THP1 monocytes were differentiated into THP1 macrophages through the treatment with phorbol 12-myristate 13-acetate (PMA) (10 ng/ml) for 48 hours.

It has been recently shown that THP1 monocytes express low levels of all 3 TAM receptors and that in PMA differentiated THP1 macrophages the expression of MerTK, but not of Axl and Tyro3, results substantially increased (Liao et al. 2009). Accordingly, we found that MerTK expression, both at mRNA and protein level, was significantly higher in THP1 cells after treatment with PMA (Figure 4.2 - 4.3).

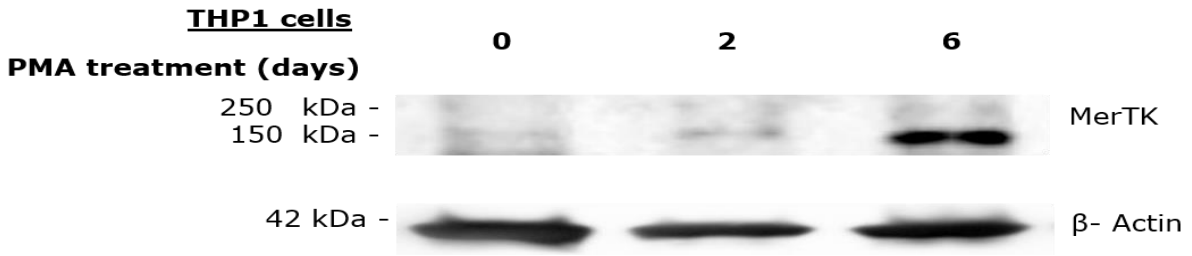

Figure 4.2. Protein expression of MerTK in differentiated PMA-treated THP1 cells compared to THP1 monocytic cells.

20 µg of cell lysates from serum-deprived THP1 cells untreated (day 0) or after 2-6 days of treatment with PMA, were analyzed by western blotting, by using an anti-MerTK antibody; β-Actin was used as loading control.

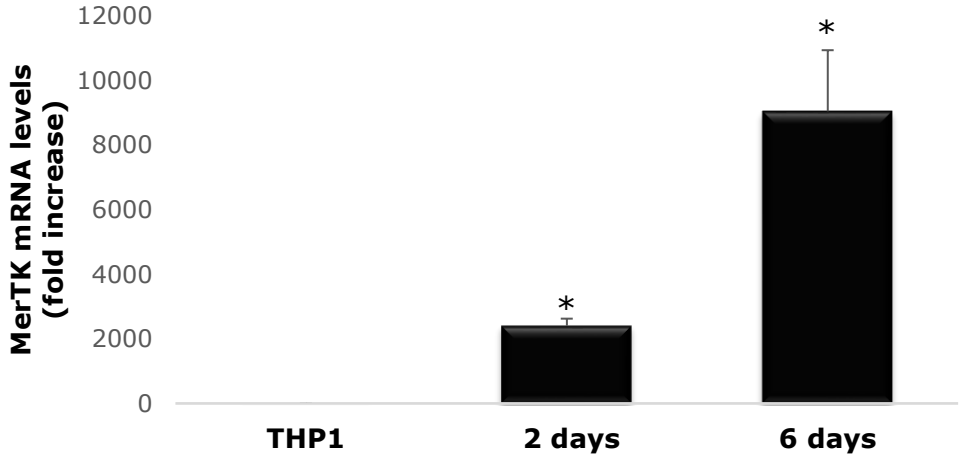

Figure 4.3. Gene expression of MerTK in differentiated PMA-treated THP1 cells compared to THP1 monocytic cells.

Total RNA was isolated from serum-deprived THP1 cells. In untreated THP1 or after 2-6 days of treatment with PMA, MerTK mRNA expression was analyzed by Real-Time PCR and normalized for the expression of the 'housekeeping' Actin gene. Data are expressed as fold increase over control. *(n=3 * p <0.05 vs undifferentiated)*

4.2 Gas-6 induced MerTK phosphorylation and downstream signaling in THP1 macrophages

In order to evaluate the effect of Gas-6 on MerTK activity in THP1 derived macrophages, cells were stimulated with 200 ng/ml Gas-6 for the indicated time periods. Gas-6 induced a time-dependent phosphorylation of MerTK and the activation of downstream molecules, such as AKT, a serine/threonine protein kinase, that plays a key role in multiple cellular processes, as glucose metabolism, cell proliferation and migration (Figure 4.4).

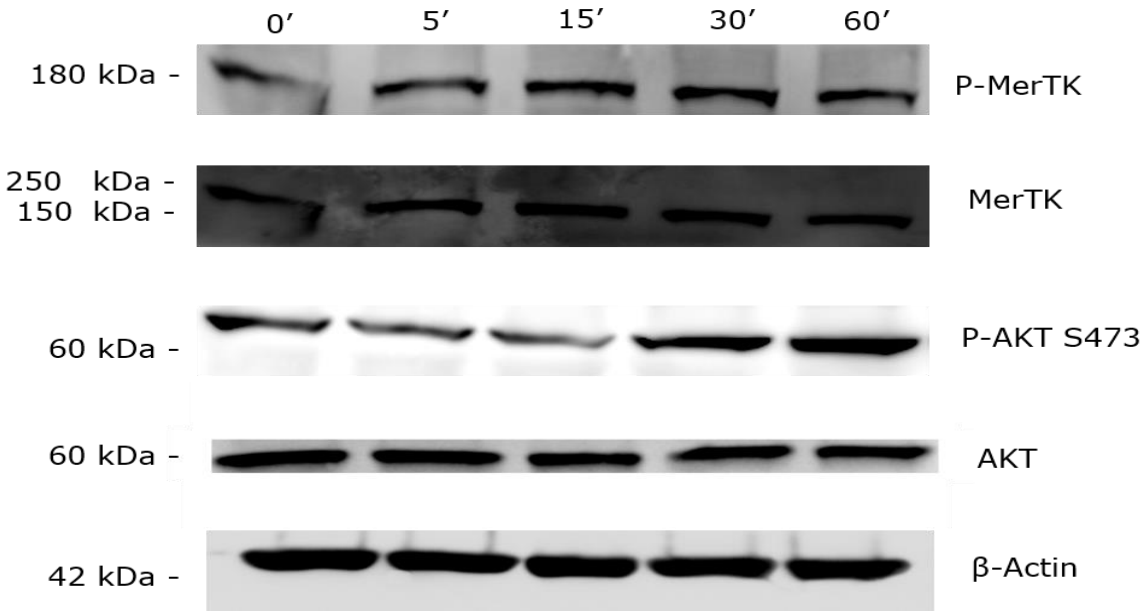

Figure 4.4. Gas-6 induced MerTK phosphorylation and downstream signaling in THP1 macrophages.

THP1 macrophages were serum deprived for 24 hours and stimulated with Gas-6 (200 ng/ml) for the indicated times. 20 μg of total cell lysate were analyzed by western blotting with the indicated antibodies; β-Actin was used as loading control.

4.3 Inhibition of MerTK in THP1 macrophages

To determine whether MerTK plays a critical role in regulating the biological features of differentiated THP1 macrophages, we used two different approaches: a pharmacological inhibition, aimed to block MerTK activity and a gene silencing technique, to reduce MerTK expression. To inhibit MerTK-induced signaling pathways, we employed a MerTK-selective small molecule inhibitor (Mer TKI), UNC569, a pyrazolopyrimidine with potent activity (Mer IC50 = 2.9 nM, Axl IC50=37 nM, Tyro3 IC50 = 48 nM) (Christoph et al. 2013). Downregulation of MerTK expression was achieved by gene silencing, using MerTK specific small interfering RNA (siRNA).

As expected (Figure 4.5), we found that Gas-6-induced MerTK phosphorylation was inhibited by pretreatment of THP1 macrophages with UNC569.

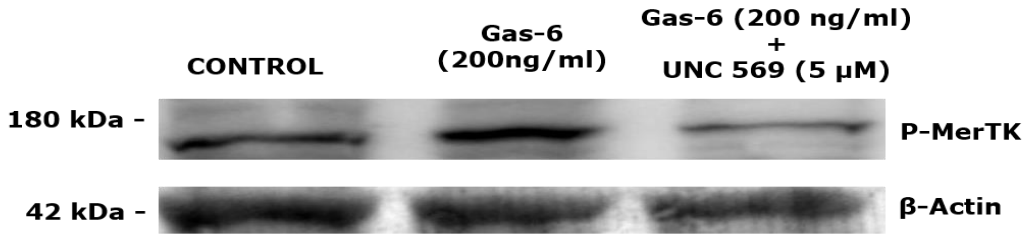

Figure 4.5. Gas-6-stimulated MerTK phosphorylation in THP1 macrophages was inhibited by UNC 569.

20 µg of total cell lysate from serum-deprived THP1 macrophages were analyzed by western blotting using anti-P-MerTK antibody; β-Actin was used as loading control.

To rule out that the effects of UNC569 were due to non-specific inhibition, THP1 macrophages were treated with specific MERTK siRNAs and efficiency was evaluated by Real Time PCR. As shown in Figure 4.6, we observed a significant reduction in MERTK gene expression.

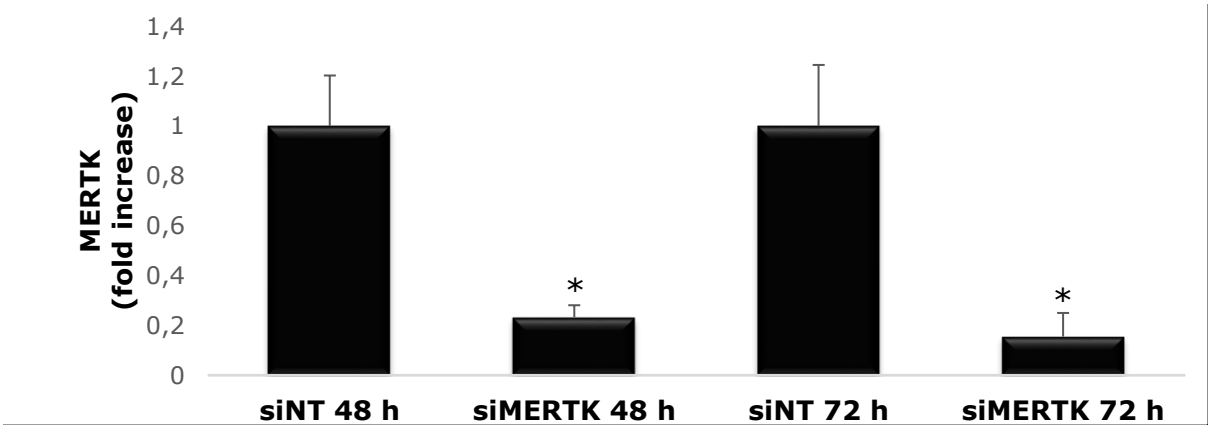

Figure 4.6. Gene expression of MERTK was significantly downregulated following gene silencing.

Total RNA from THP1 macrophages was isolated 48 and 72h after transfection. *MERTK* mRNA expression was analyzed by Real-Time PCR and normalized for the expression of the 'housekeeping' Actin gene. *(n=3 *p <0.05 vs (siNT) non-targeting siRNA)*

4.4 MerTK expression is restricted to M2c macrophages

It has been recently shown by Zizzo et al. (Zizzo et al. 2012) that MerTK expression was enhanced under M2c polarization, demonstrating that MerTK is highly expressed in macrophage subsets positive for CD206 and CD163. In line with these findings, our study focused on the M2c population. Monocytes from healthy subjects (blood donors) were isolated from buffy coats and

induced to differentiate towards M2c macrophages. After isolation monocytes were incubated (day 0) with M-CSF to promote differentiation towards M2 macrophage, after 5 days M-CSF, IL-10 and TGF-β were added to obtain M2c phenotype and cells were grown until day 8 (Figure 4.7).

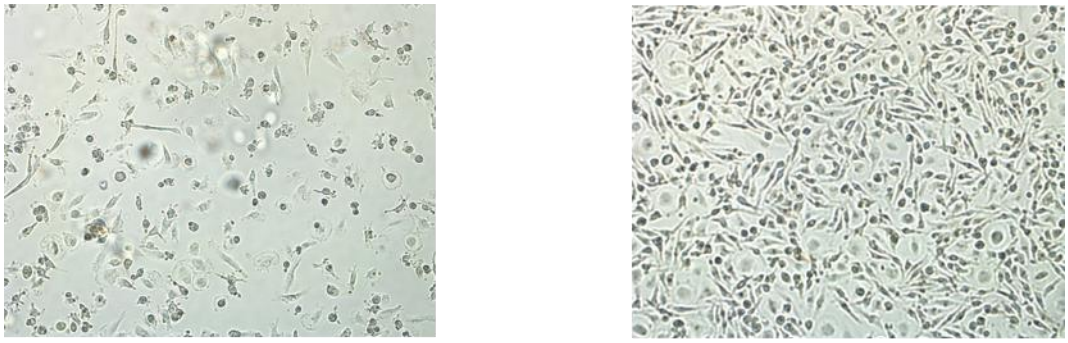

Day 5 **Day 8**

Figure 4.7. Polarization of peripheral monocytes towards M2c macrophages.

Monocytes were cultured for 8 days in complete medium, containing M-CSF (50 ng/ml); on day 5, medium was replaced and M-CSF (50 ng/ml), IL-10 (50 ng/ml) and TGF-β (20 ng/ml) were added.

To confirm that MerTK gradually increased during differentiation, we examined MerTK expression along with several M2 surface receptors, in particular: CD206, CD209 and CD163, in terminally differentiated macrophages.

CD206, known as mannose receptor and C-type lectin (Suzuki et al. 2018) was among the first identified markers for alternatively activated macrophages. CD209 (earlier known as DC-SIGN) is considered a specific marker of M2a polarization (Zizzo et al. 2012), whereas CD163 (hemoglobin-

haptoglobin scavenger receptor), according to a recent report (Ambarus et al. 2012), is a specific marker for M2c cells.

The macrophage population obtained after 8 days of differentiation was analyzed by flow cytometry. In agreement with previous reports, these cells expressed high levels of CD206, CD163 and low levels of CD209. Remarkably, although MerTK was expressed in the entire $CD206^{+}$/ $CD163^{+}$ population, we found the highest expression of MerTK in the CD206+ CD163+CD209- phenotype (Figure 4.8).

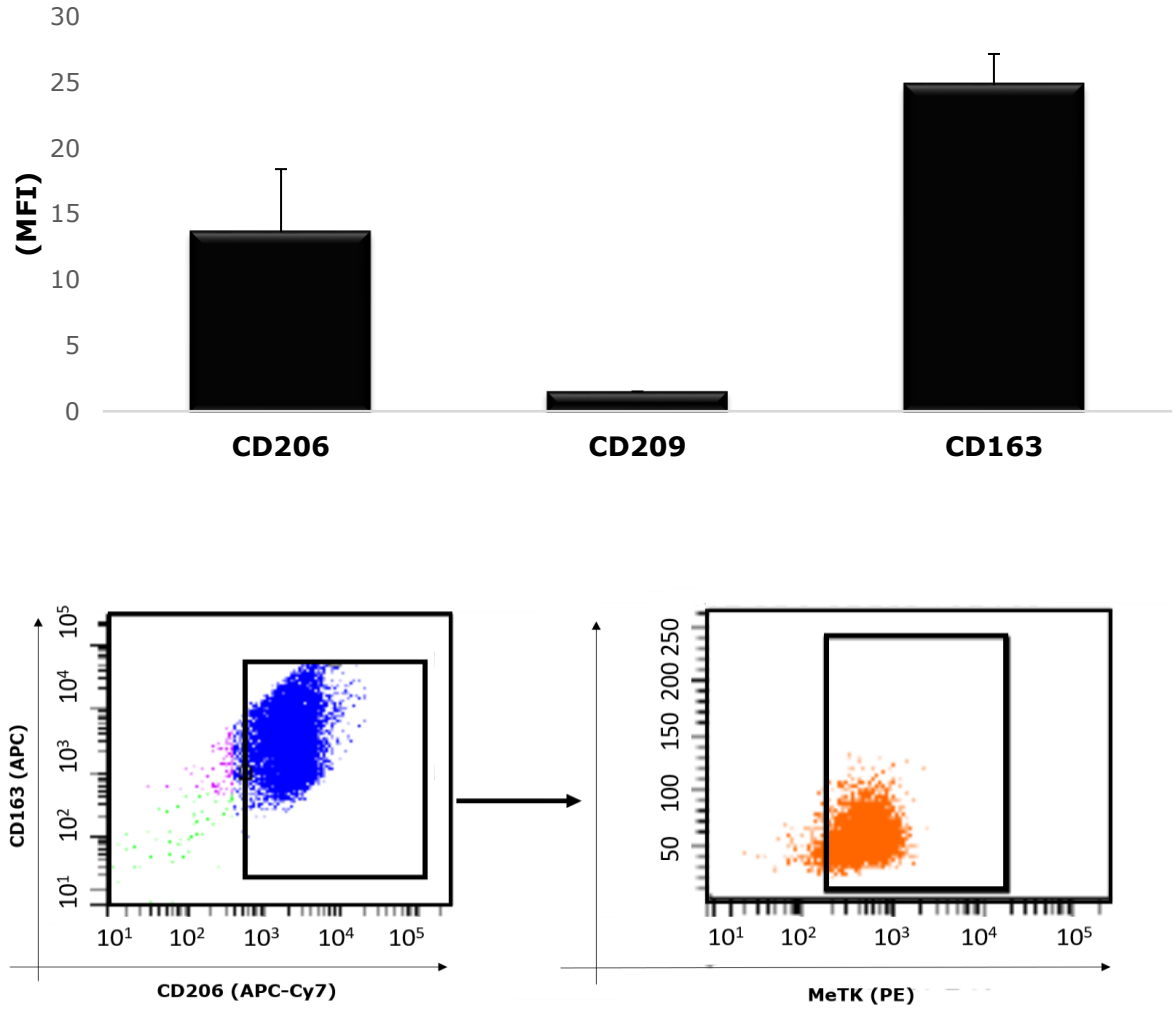

Figure 4.8. M- CSF, IL-10 and TGF-β induce M2C differentiation.

Peripheral monocytes differentiated to macrophages after growth for 8 days in complete medium, in the presence of M-CSF (50 ng/ml) and starting from day 5, IL-10 (50 ng/ml) and TGF-β (20 ng/ml) were added for 3 days. Cells were stained for CD206, CD163, CD209 and MerTK and analyzed by flow cytometry. Histograms show MFI (mean fluorescence intensity). Data shown are representative of 3 independent experiments.

Moreover, expression of CD206 and CD163 was assessed by Real-Time PCR at day 0 and after 5 and 8 days of culture. Real-Time PCR showed that CD206 significantly increased on the fifth day following treatment with M-CSF, while the M2c polarization induced in the last 3 days was confirmed by a significant increase in CD163 gene expression (Figure 4.9).

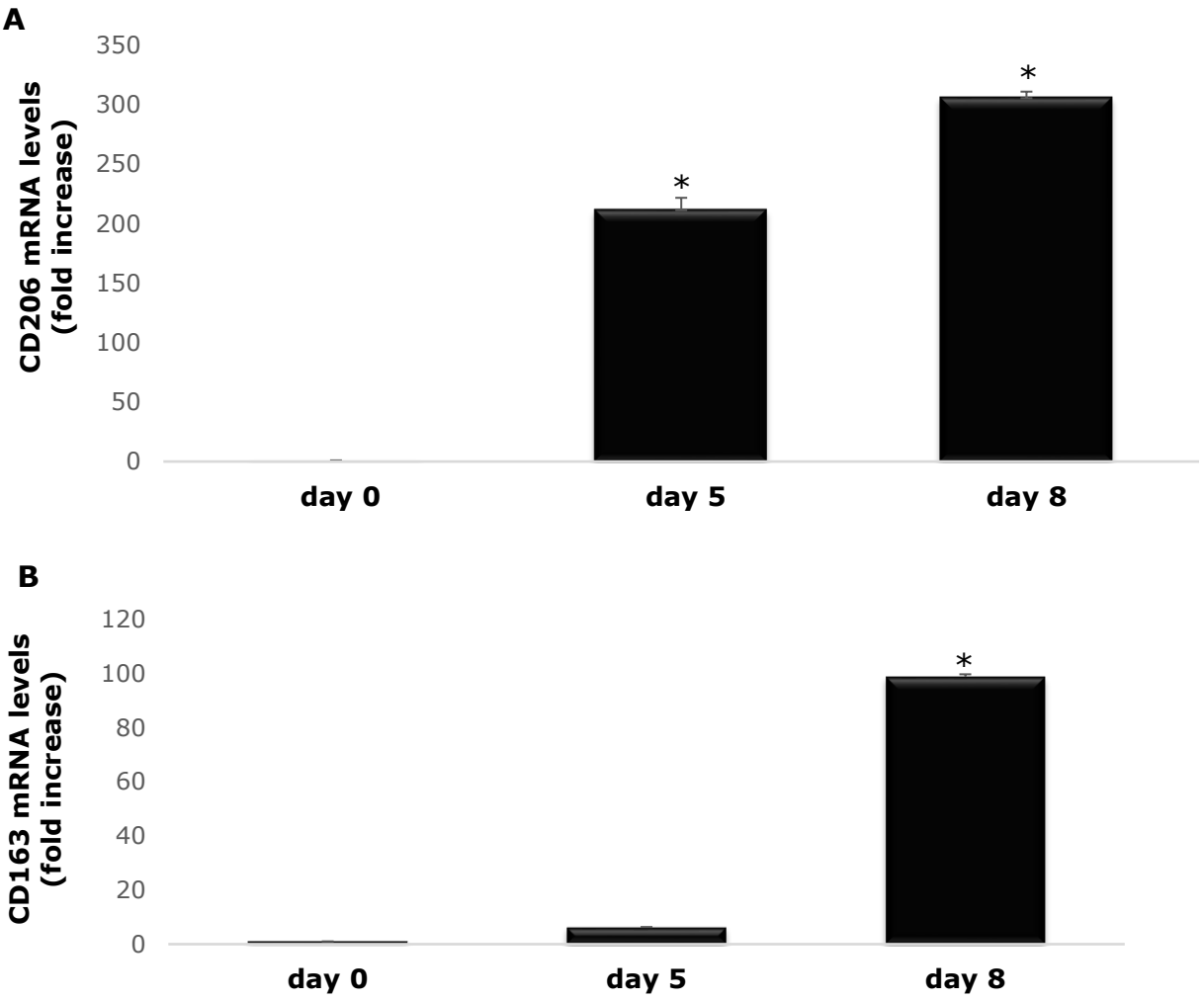

Figure 4.9. Gene expression of CD206 and CD163 during macrophage polarizzation.

Monocytes were isolated from buffy coats of blood donors and allow to differentiate towards the M2c phenotype*. CD206* (**A**) and *CD163* (**B**) mRNA expression was analyzed by Real-Time PCR at day 0 and after 5 and 8 days of culture. Gene expression was normalized for expression of the 'housekeeping' GAPDH gene. Data are expressed as increase over control. *(n=3 * p <0.05 vs undifferentiated)*

Furthermore, we observed by Real-Time PCR that the expression of CD68, a marker for human macrophages and of MERTK was gradually acquired during monocyte to macrophage differentiation and become more evident in terminally differentiated macrophages (Figure 4.10).

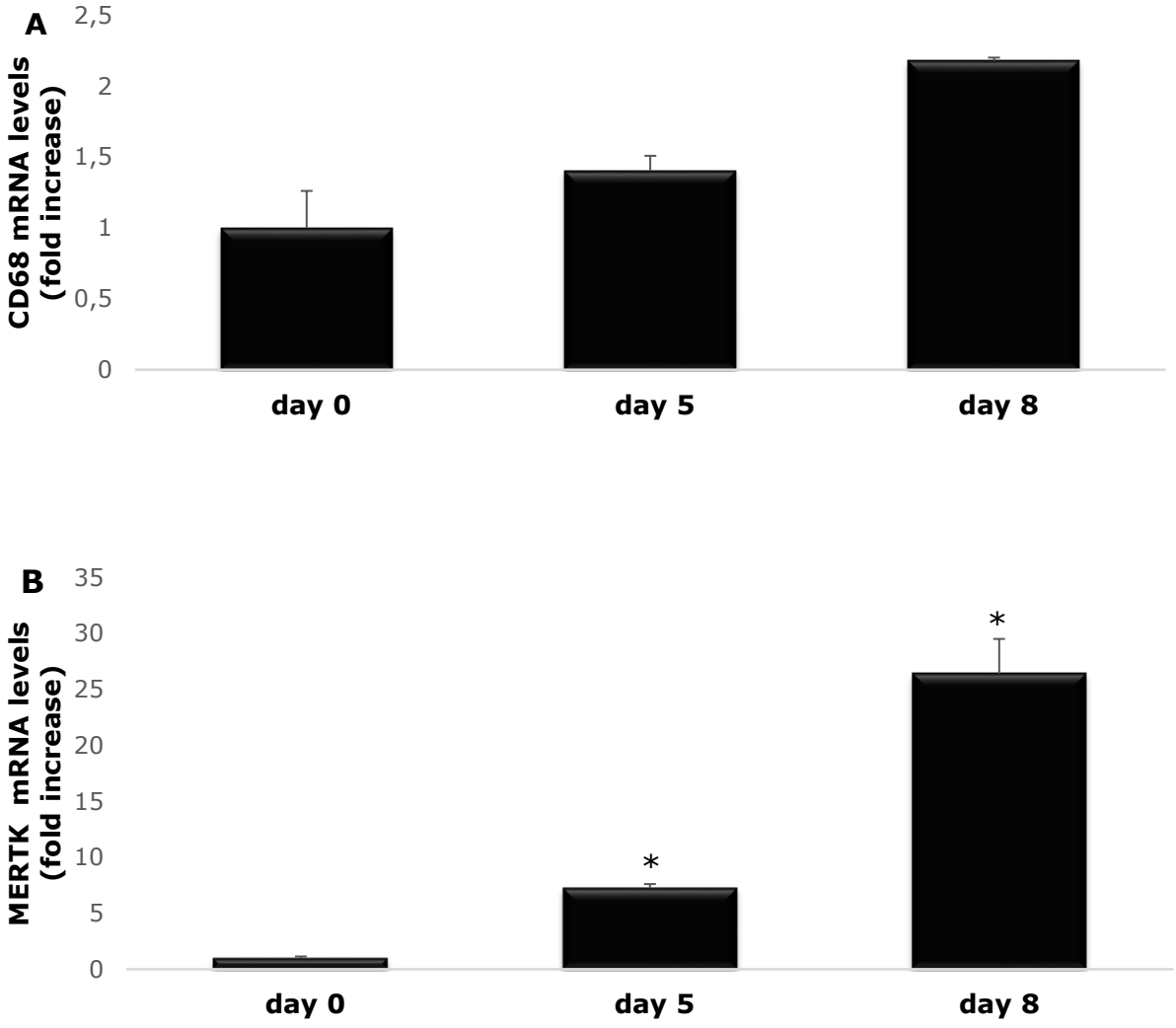

Figure 4.10. Gene expression of CD68 and MERTK during macrophage polarizzation.

Monocytes were isolated from buffy coats of blood donors and allow to differentiate towards the M2c phenotype. *CD68* (**A**) and *MERTK* (**B**) mRNA expression were analyzed by Real-Time PCR at day 0 and after 5 and 8 days of culture. MERTK expression was normalized for the expression of the 'housekeeping' Actin gene and CD68 expression normalized for the expression of the 'housekeeping' GAPDH gene. Data are expressed as increase over control. *(n=3 * p <0.05 vs undifferentiated).*

4.5 MerTK phosphorylation and downstream signaling activation in M2c macrophages

To determine the functional significance of MerTK in M2 macrophages we analyzed the activation of MerTK pathway by western blotting. Following M2c polarization, we observed an increase in the phosphorylation of MerTK and the activation of AKT and STAT3, two downstream pathways promoting proliferation, migration and reduction of apoptosis (Figure 4.11).

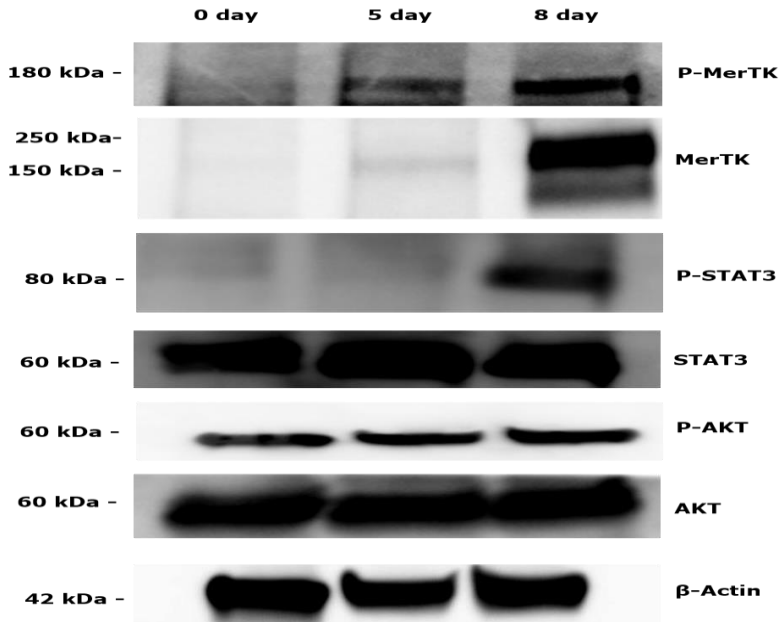

Figure 4.11. MerTK phosphorylation and downstream signaling in M2c macrophages.

M2c macrophages were deprived of serum and lysed at the indicated times. 20 μg of total cell lysate were analyzed by western blotting with the indicated antibodies; β-Actin was used as loading control.

4.6 Inhibition of MerTK in M2c macrophages

Exposure of M2c macrophages to Gas-6 further increased the phosphorylation of MerTK, that was reverted by pretreatment with UNC569 (Figure 4.12).

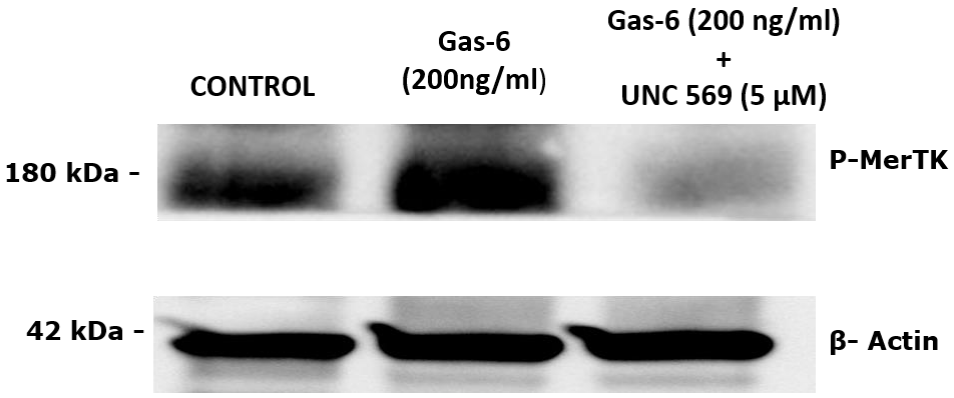

Figure 4.12. MerTK phosphorylation in M2c macrophages was decreased after treatment with UNC 569.
20 µg of total cell lysate from serum-deprived M2c macrophages were analyzed by western blotting using the anti-P-MerTK antibody, β-Actin was used as loading control.

4.7 Effect of THP1 macrophage Conditioned Medium (C.M.) on profibrogenic phenotype of HSCs

THP1 monocytes and THP1 derived macrophages represent valuable tools to investigate monocyte/macrophage functions within the innate immune system, where they act as major regulators of tissue development, homeostasis, repair and disease. To examine the involvement of MerTK signaling in the cross-talk between macrophages and HSCs, we evaluated the

effect of Conditioned Medium obtained from THP1 macrophages on HSC biological features.

4.7.1 Effect of THP1 macrophage C.M on HSC migration

We first evaluated the effect of THP1 macrophage C.M. on HSC chemotaxis. HSCs exposed to C.M. of THP1 macrophages showed a significant increase in migration and this effect was boosted in response to C.M. of macrophages treated to Gas-6 (200 ng/ml) compared to C.M. of untreated macrophages (Figure 4.13).

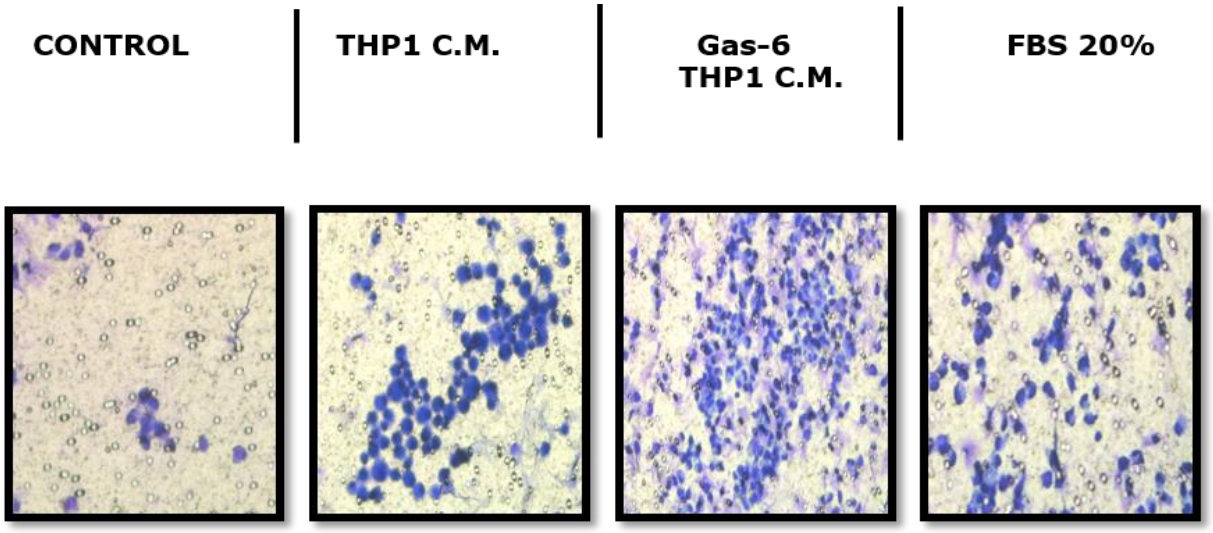

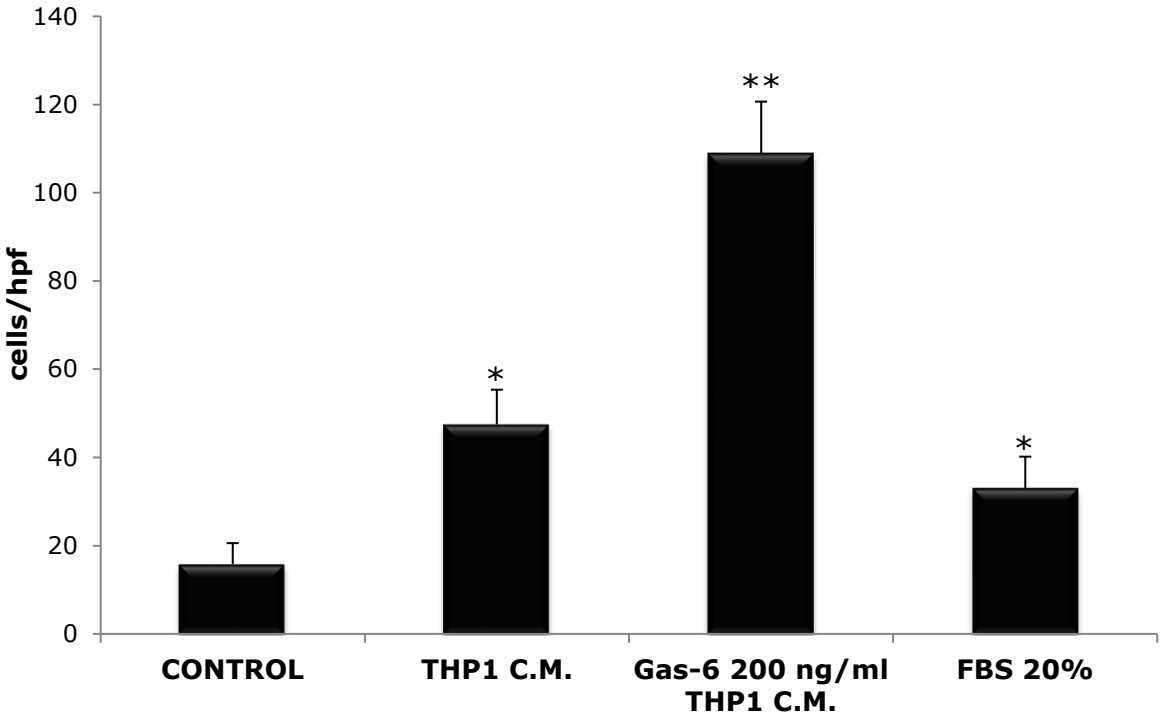

Figure 4.13. HSC migration in response to C.M. of THP1 macrophages. Migration of HSCs was measured using modified Boyden chamber. 20% fetal bovine serum was used as positive control. *(n=3 *p <0.05 vs control; **P<0.05 vs C.M. of unstimulated THP1 macrophages)*

To evaluate whether the effects of macrophage C.M. on HSC migration were mediated by Gas-6-induced MerTK activity in THP1 macrophages, C.M. of macrophages subjected to pharmacological or genetic inhibition of MerTK was employed.

We observed that the increased migration of HSCs in response to the C.M. of Gas-6-stimulated macrophages, was significantly reduced by pre-treatment of macrophages with UNC569 (5 μM) (Figure 4.14).

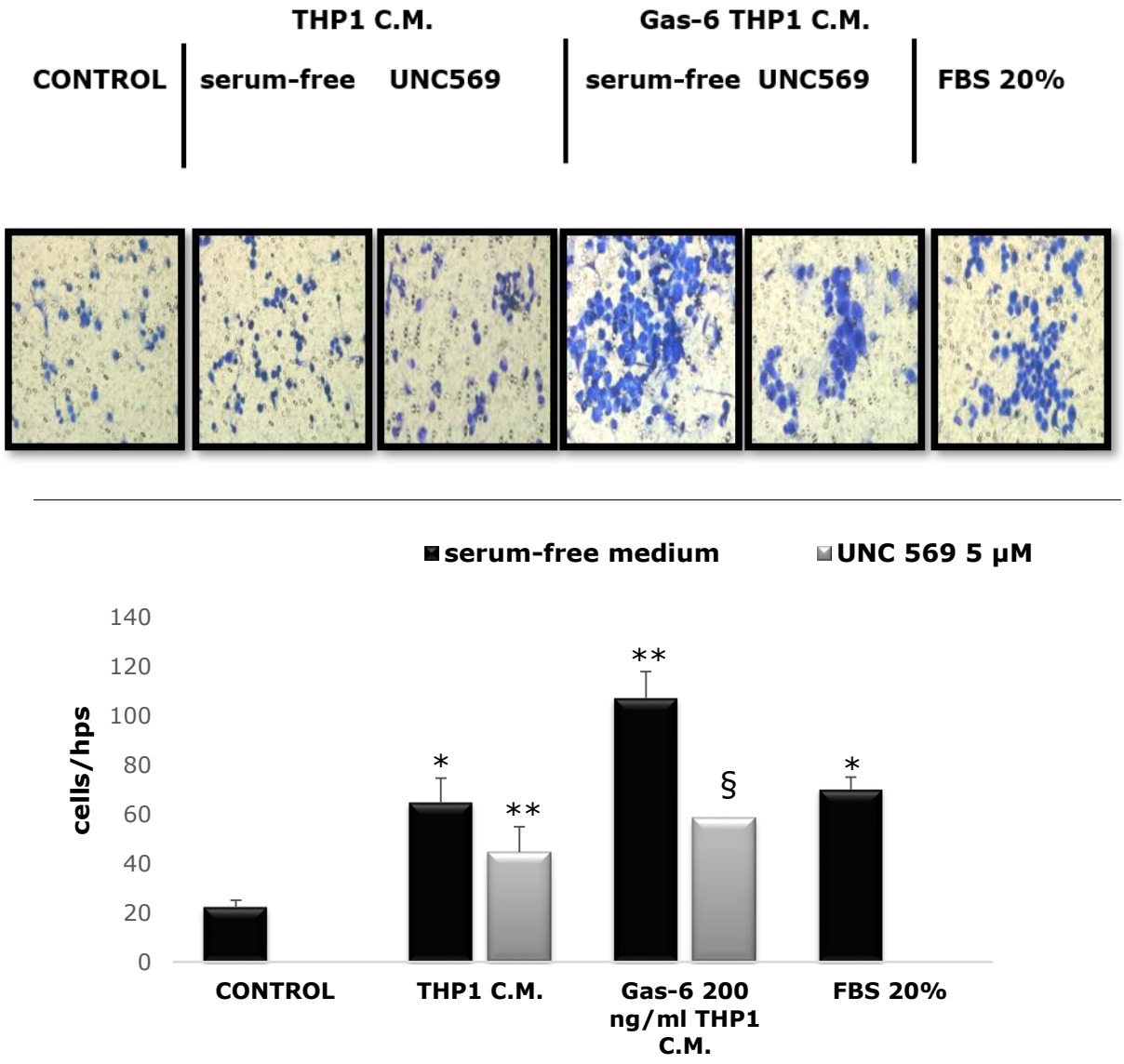

Figure 4.14. HSC migration in response to C.M. of THP1 macrophages pretreated with UNC 569 under stimulation of Gas-6.

Migration of HSCs was measured using modified Boyden chamber. 20% fetal bovine serum was used as positive control. *(n=3 *p <0.05 vs control; **p <0.05 vs C.M. of unstimulated THP1 macrophages; § p <0.05 vs C.M. of THP1 macrophage stimulated with Gas-6 (200 ng/ml) without inhibition for MerTK)*

Similar effects were obtained when HSC were exposed to the C.M. of THP1 macrophages with MERTK knockdown achieved by specific siRNA (Figure 4.15).

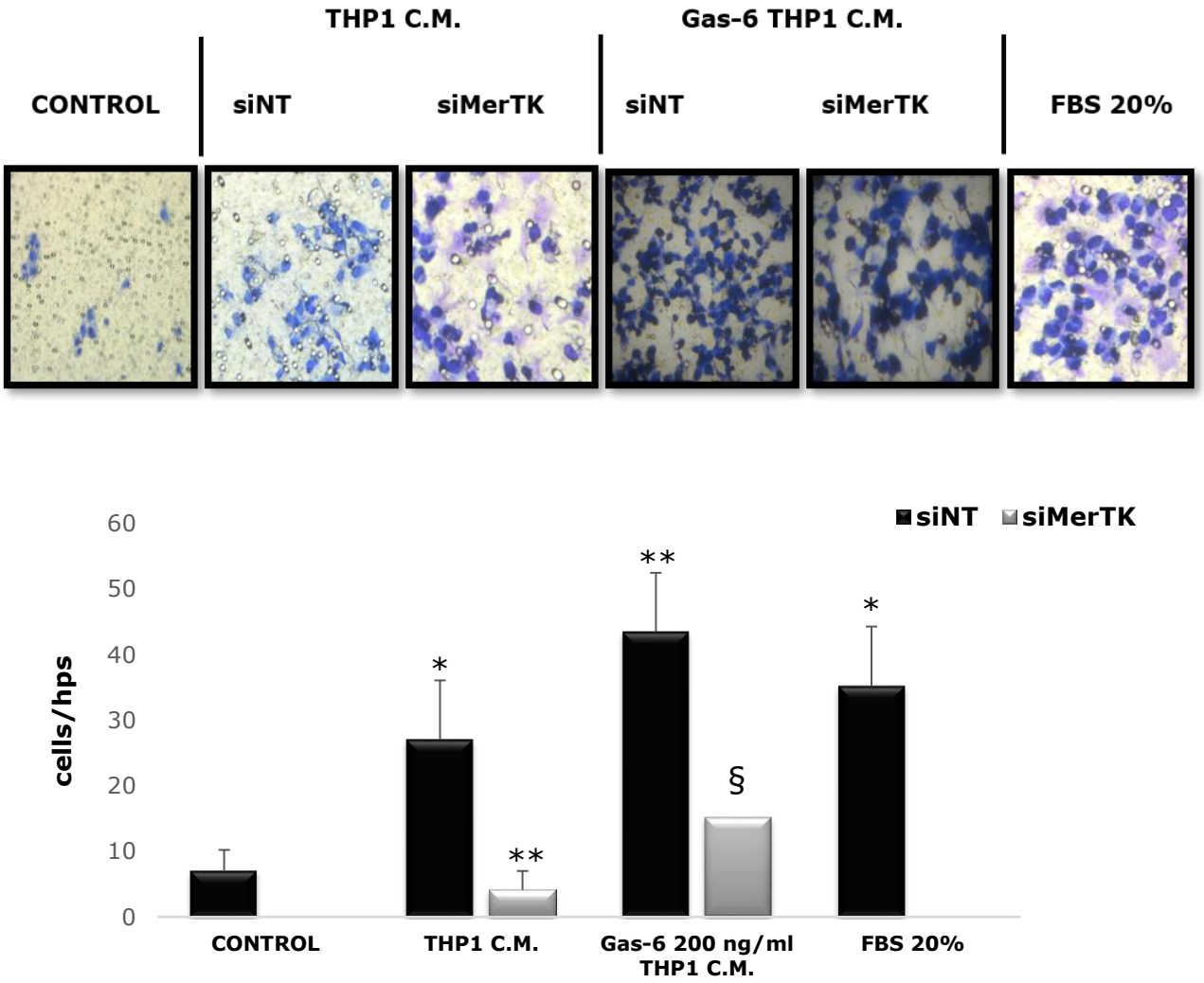

Figure 4.15. HSC migration in response to C.M. of THP1 transfected with MerTK-specific siRNA under stimulation of Gas-6.

Migration of HSCs was measured using modified Boyden chamber. 20% fetal bovine serum was used as positive control. *(n=3 *p <0.05 vs control; **p <0.05 vs C.M. of unstimulated THP1 macrophages; § p <0.05 vs C.M. of THP1 macrophage stimulated with Gas-6 (200 ng/ml) without inhibition for MerTK)*

4.7.2 Effect of THP1 macrophage C.M. on HSC viability

We examined the effects of C.M. of THP1 macrophages on HSC viability. Exposure of HSCs to C.M. of Gas-6-stimulated macrophages determined a significant increase in cell survival and this effect was reduced following pre-treatment of macrophages with UNC569 (5 μM) (Figure 4.16).

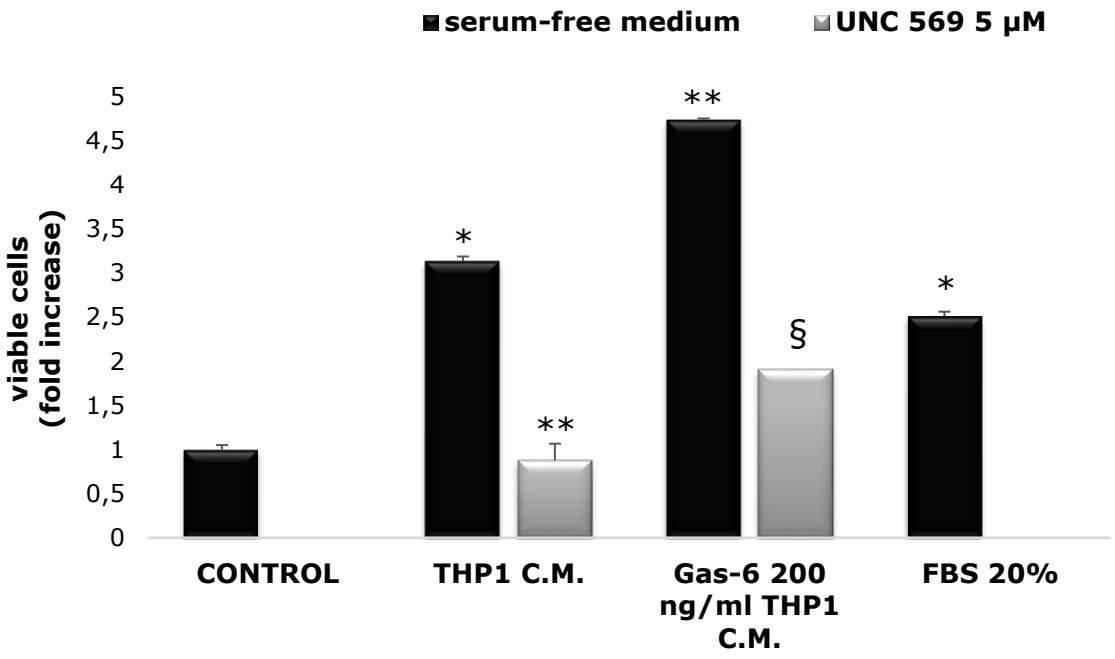

Figure 4.16. HSC survival in response to C.M. of THP1 macrophages treated with UNC 569 under stimulation of Gas-6.

Survival of HSCs was measured by MTT assay after 48 hours of treatment. 20% fetal bovine serum was used as positive control. Data are expressed as fold increase over control (serum-deprived medium). *(n=3 *p <0.05 vs control; **p <0.05 vs C.M. of unstimulated THP1 macrophages; § p <0.05 vs C.M. of THP1 macrophage stimulated with Gas-6 (200 ng/ml) without inhibition for MerTK)*

A similar effect on cell survival was observed in HSC exposed to C.M. of MERTK knockdown THP1 macrophages (Figure 4.17).

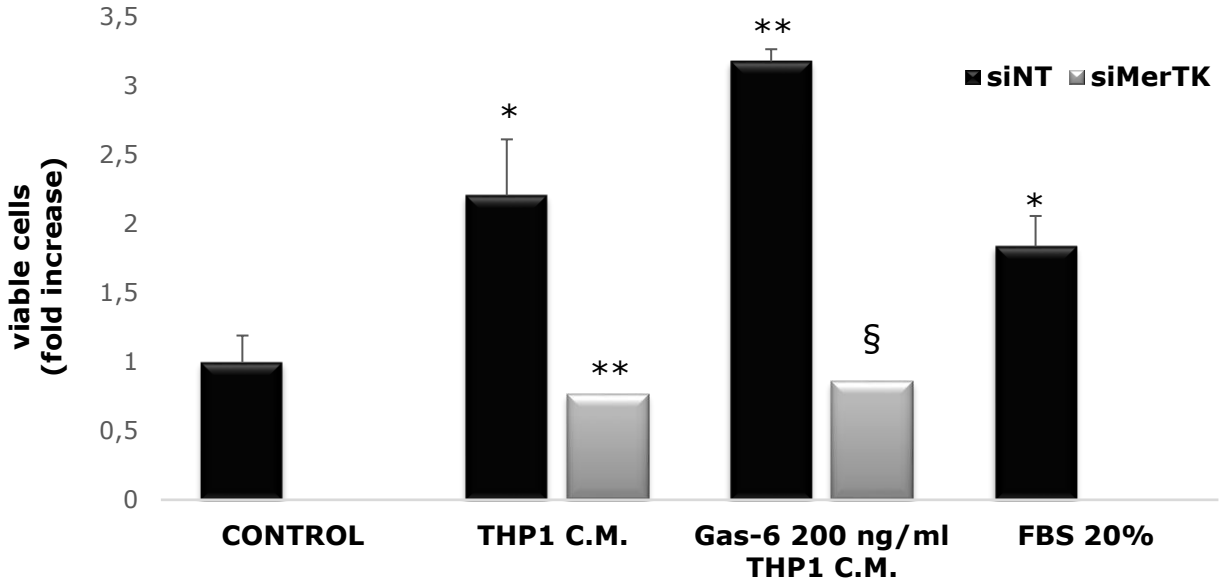

Figure 4.17. HSC survival in response to C.M. of THP1 macrophages transfected with MerTK-specific siRNA under stimulation of Gas-6.
Survival of HSCs was measured by MTT assay after 48 hours of treatment. 20% fetal bovine serum was used as positive control. Data are expressed as fold increase over control (serum-deprived medium). *(n=3 *p <0.05 vs control; **p <0.05 vs C.M. of unstimulated THP1 macrophages; § p <0.05 vs C.M. of THP1 macrophage stimulated with Gas-6 (200 ng/ml) without inhibition for MerTK)*

4.7.3 Gene expression analysis in response to C.M. of the THP1 macrophages

To better elucidate the role of MerTK macrophages' activity in modulating the profibrogenic properties of HSCs, we analysed the mRNA expression of genes upregulated under HSC activation, in response to C.M. of THP1 macrophages. Real-Time PCR analysis showed that in HSCs treated with C.M. from Gas-6-stimulated macrophages, mRNA expression of *TIMP1, TGF-β1*, *IL-8* and *VEGF-A* was significantly increased compared to HSCs treated with C.M. of untreated

macrophages. These effects were blunted by macrophage pre-treatment with UNC569, indicating that Gas-6 actions are mediated by MerTK (Figure 4.18).

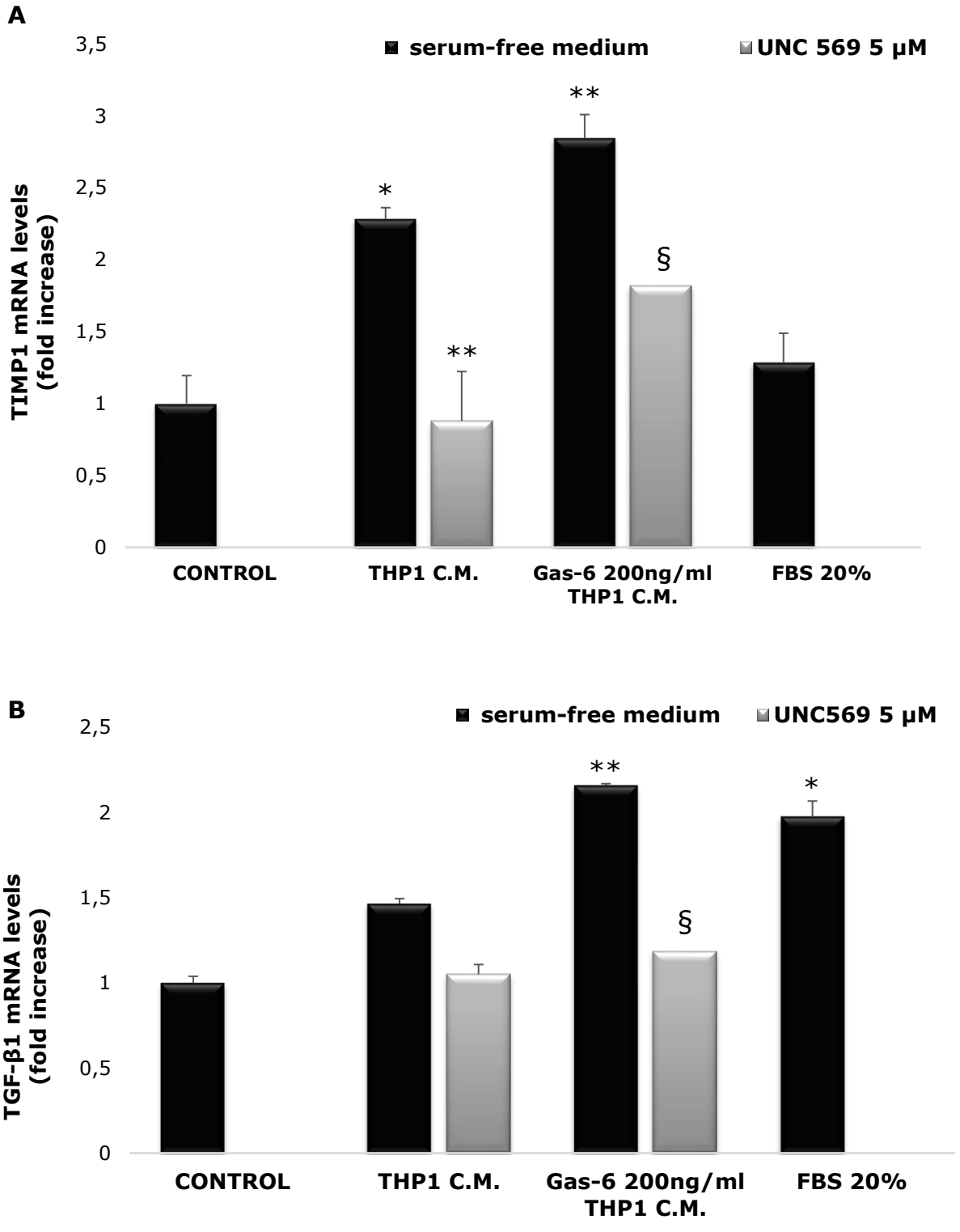

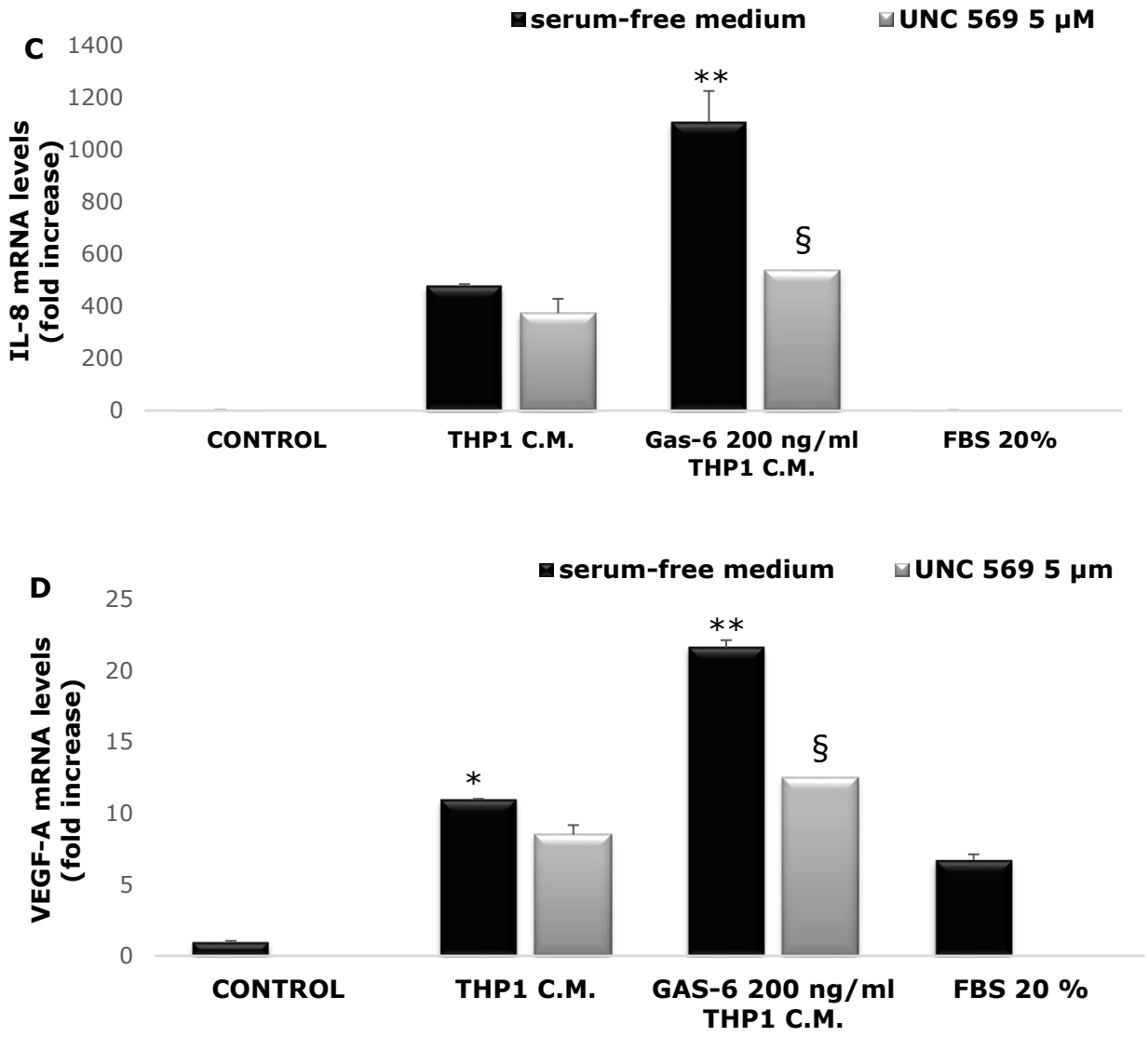

Figure 4. 18. *TIMP1, TGF-β1, IL-8* and *VEGF-A* gene expression in response to C.M. of the THP1 macrophages treated with UNC 569 under stimulation of Gas-6.

Total RNA was isolated from the THP1 macrophages and *TIMP1* (**A**)*, TGF-β1* (**B**), *IL-8* (**C**) and *VEGF-A* (**D**) mRNA expression were analyzed by Real-Time PCR and normalized for expression of the 'housekeeping' Actin gene. Data are expressed as fold increase over control (serum-deprived medium). *(n=3 *p <0.05 vs control; **p <0.05 vs C.M. of unstimulated THP1 macrophages; § p <0.05 vs C.M. of THP1 macrophage stimulated with Gas-6 (200 ng/ml) without inhibition for MerTK)*

To rule out that the effects of UNC569 were due to non-specific inhibition, we stimulated HSC with C.M. of MERTK knockdown THP1 macrophages treated or untreated with Gas-6. As shown in Figure 4.19, C.M. of MerTK knockdown macrophages showed a reduced capability to induce fibrogenic genes in HSCs. Taken together, these data suggest a pro-fibrogenic role of MerTK expressed by differentiated PMA-treated THP1 cells on HSCs.

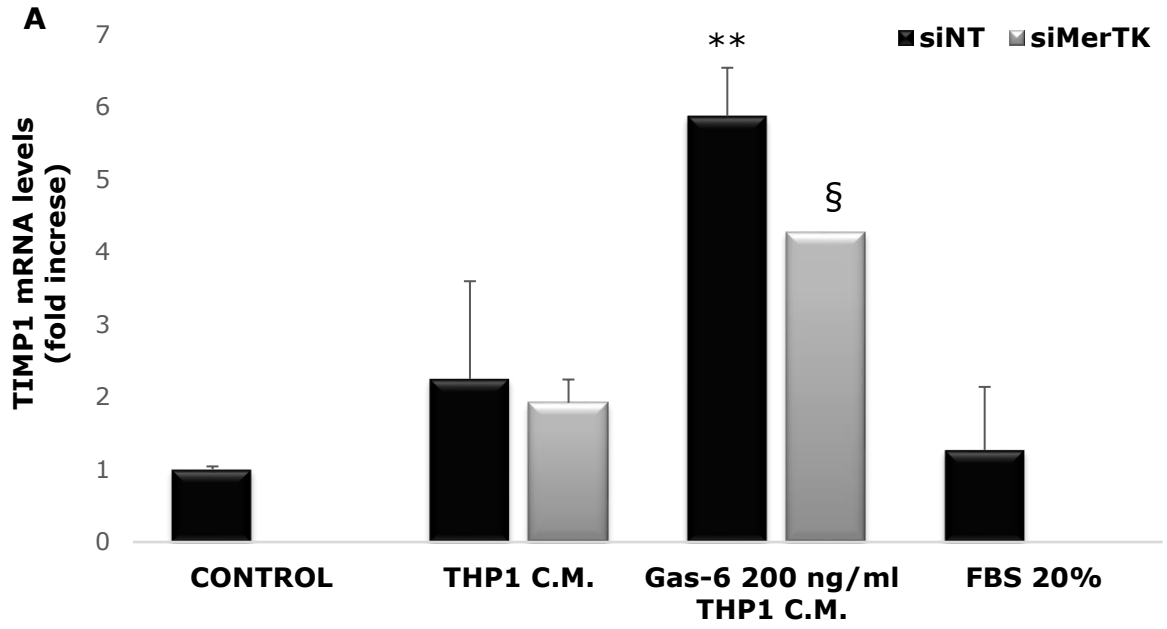

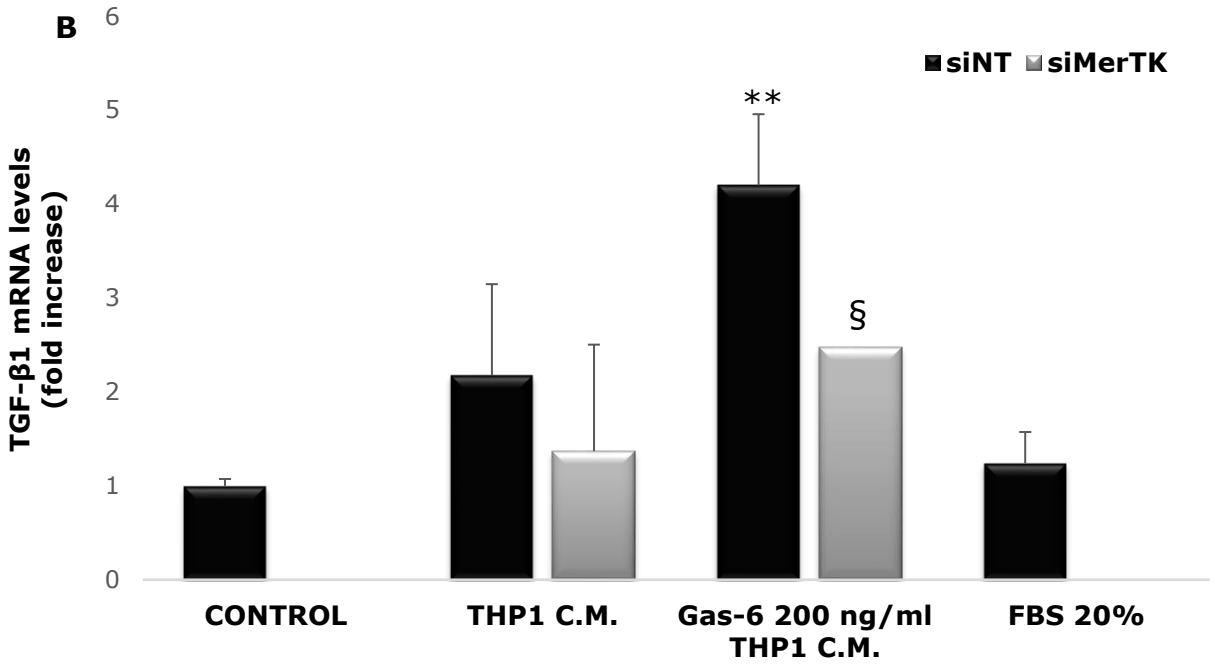
B
siNT
siMerTK
TGF-β1 mRNA levels (fold increase)
0
1
2
3
4
5
6
**
§
CONTROL
THP1 C.M.
Gas-6 200 ng/ml THP1 C.M.
FBS 20%

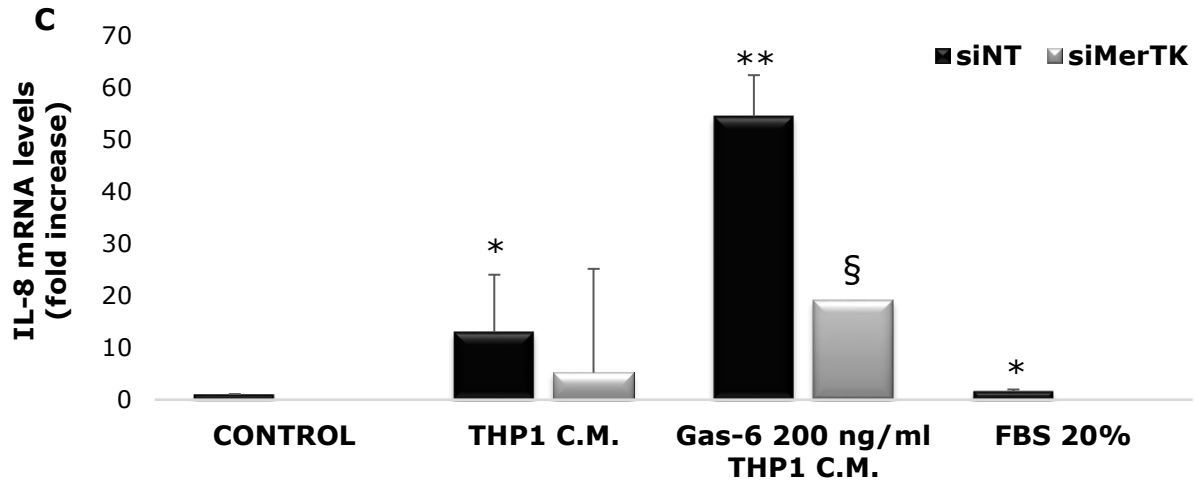
C
siNT
siMerTK
IL-8 mRNA levels (fold increase)
0
10
20
30
40
50
60
70
*
**
§
*
CONTROL
THP1 C.M.
Gas-6 200 ng/ml THP1 C.M.
FBS 20%

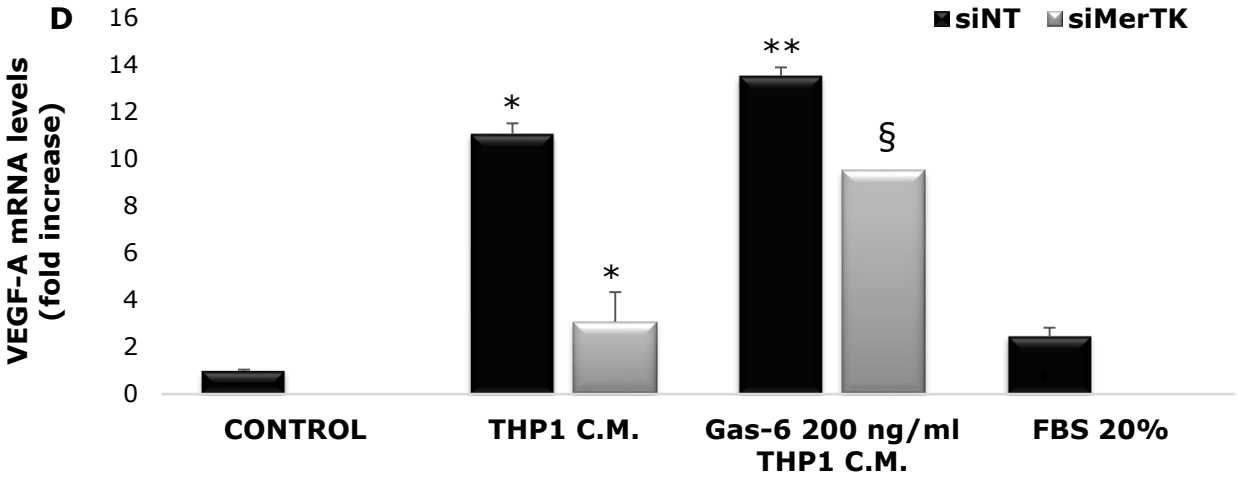

Figure 4.19. *TIMP1, TGF-β1, IL-8* and *VEGF-A* gene expression in response to C.M. of the MERTK knockdown THP1 macrophages under stimulation of Gas-6.

Total RNA was isolated from the THP1 macrophages and *TIMP1* (**A**)*, TGF-β1* (**B**), *IL-8* (**C**) and *VEGF-A* (**D**) mRNA expression were analyzed by Real-Time PCR and normalized for expression of the 'housekeeping' Actin gene. Data are expressed as fold increase over control (serum-deprived medium). *(n=3 *p <0.05 vs control; **p <0.05 vs C.M. of unstimulated THP1 macrophages; § p <0.05 vs C.M. of THP1 macrophage stimulated with Gas-6 (200 ng/ml) without inhibition for MerTK)*

4.8 Effect of M2c macrophage C.M. on profibrogenic phenotype of HSCs

4.8.1 Effect of M2c macrophage C.M. on HSC migration

To evaluate the involvement of MerTK signaling in the cross-talk between macrophages and HSCs we repeated the experiments using C. M. of M2c macrophages. We examined the effect of C.M. of M2c macrophages on HSC migration observing a significant increase in HSC chemotaxis in response to C.M. of M2c macrophages. This effect was further increased by Gas-6 and

markedly reduced by macrophages pre-treatment with UNC569 (5 μM) (Figure 4.20).

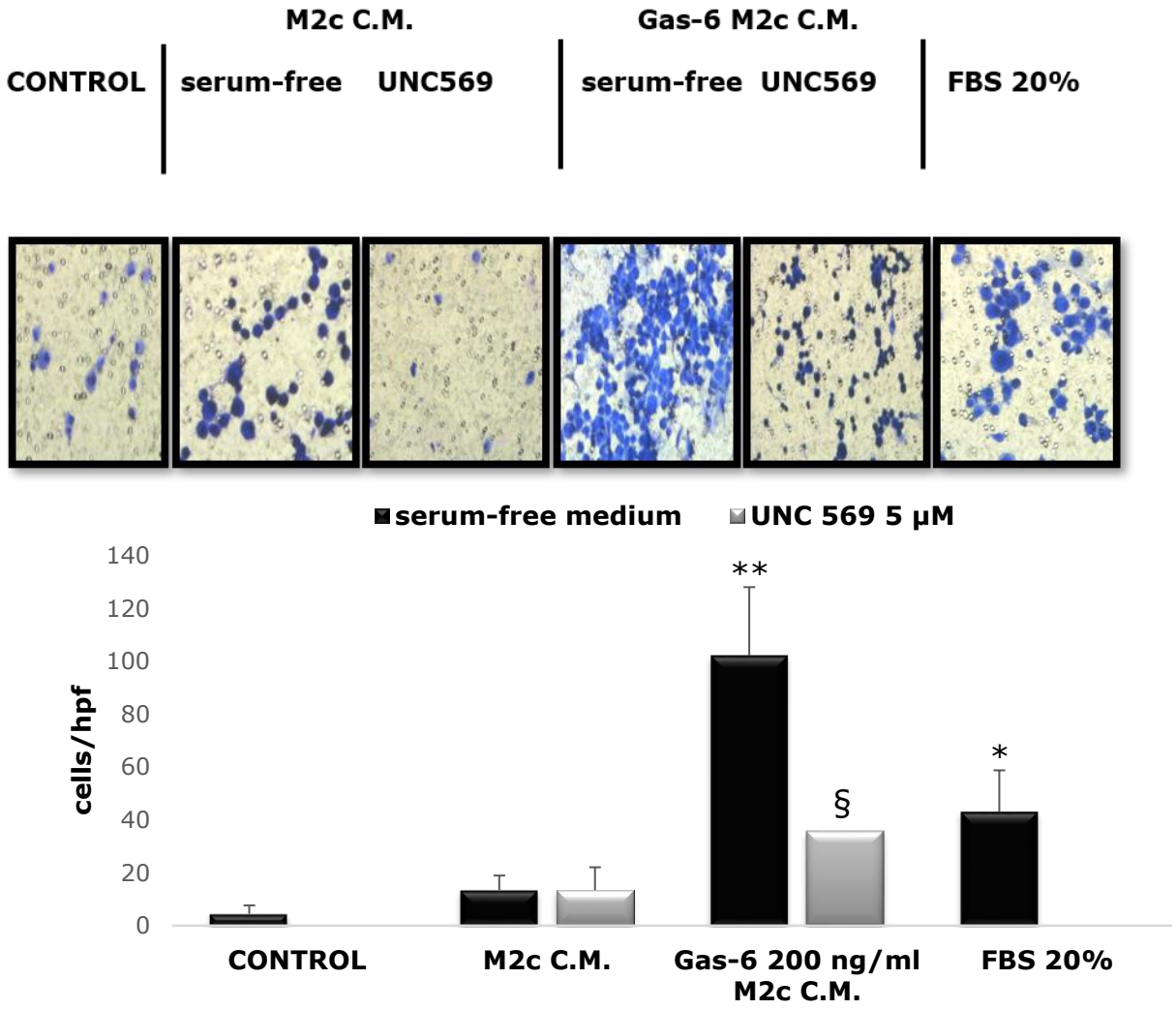

Figure 4.20. HSC migration in response to C.M. of M2c macrophages treated with UNC 569 under stimulation of Gas-6.

Migration of HSCs was measured using modified Boyden chamber. 20% fetal bovine serum was used as positive control. *(n=3 *p <0.05 vs control; **p <0.05 vs C.M. of unstimulated M2c macrophages; § p <0.05 vs C.M. of M2c macrophage stimulated with Gas-6 (200 ng/ml) without inhibition for MerTK)*

4.8.2 Effect of M2c macrophage C.M. on HSC proliferation

Similarly, exposure of HSCs to C.M. of Gas-6-stimulated M2c macrophages determined a significant increase in cell proliferation and this effect was reduced by pre-treatment with UNC569 (5 μM) (Figure 4.21).

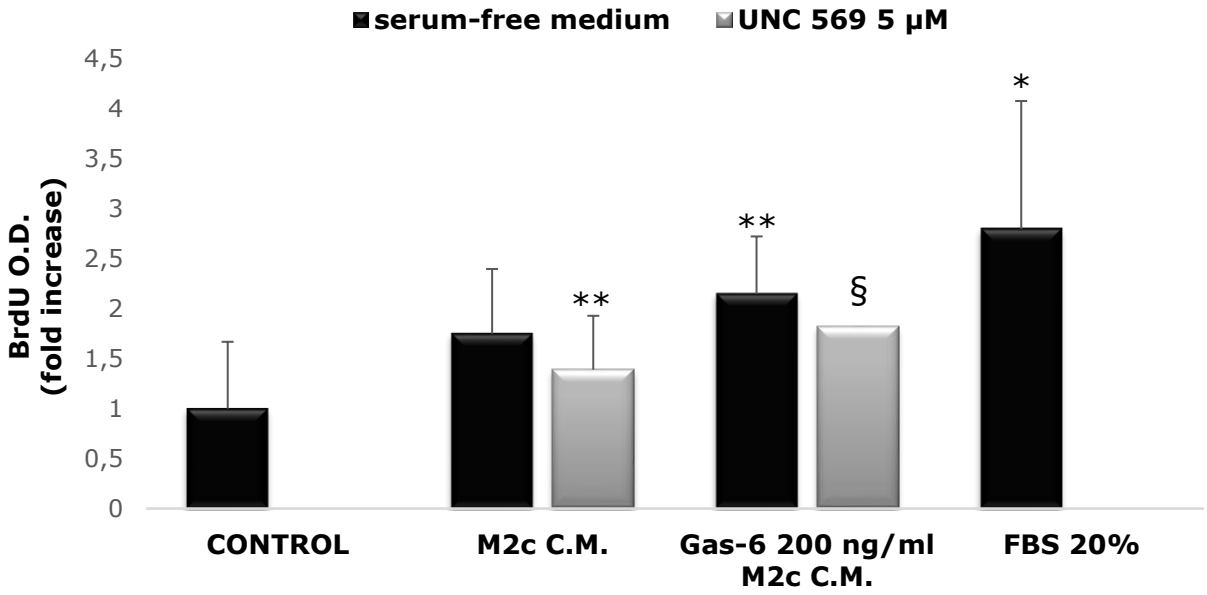

Figure 4.21. HSC proliferation in response to C.M. of M2c macrophages treated with UNC 569 under stimulation of Gas-6.

Proliferation of HSCs was measured by BrDU Cell Proliferation ELISA Kit. 20% fetal bovine serum was used as positive control. Data are expressed as fold increase over control (serum-deprived medium). *(n=3 *p <0.05 vs control; **p <0.05 vs C.M. of unstimulated M2c macrophages; § p <0.05 vs C.M. of M2c macrophage stimulated with Gas-6 (200 ng/ml) without inhibition for MerTK)*

4.8.3 Effect of M2c macrophage C.M. on HSC viability

As shown in Figure 4.22, similar results were obtained, when HSC viability evaluated by MTT assay.

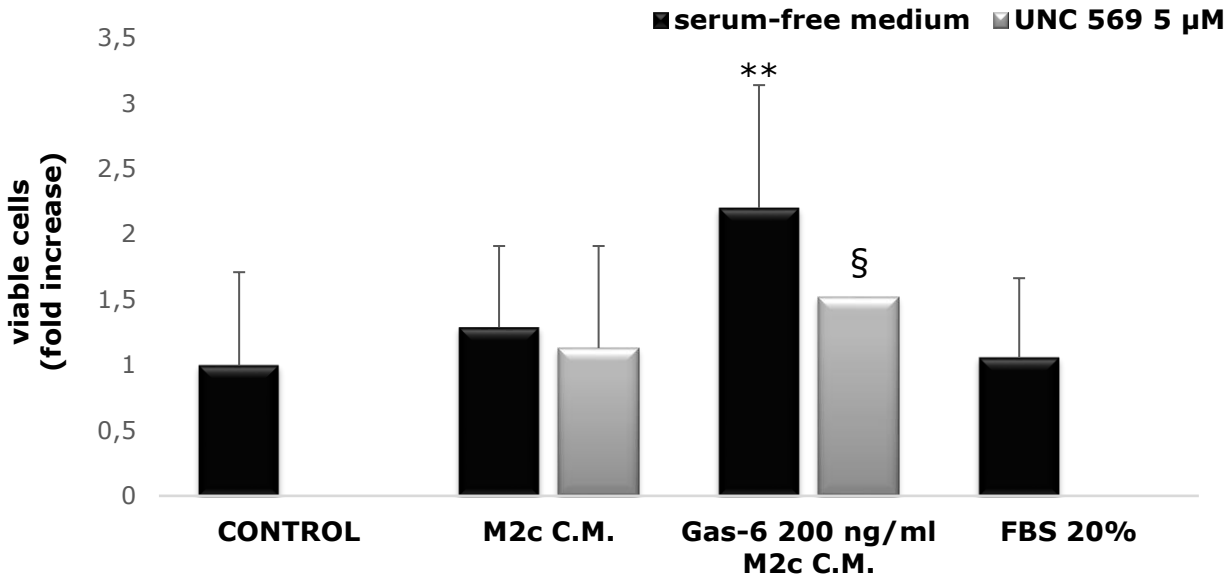

Figure 4.22. HSC viability in response to C.M. of M2c macrophages treated with UNC 569 under stimulation of Gas-6.

Survival of HSCs was measured by MTT assay at the end of treatment. 20% fetal bovine serum was used as positive control. Data are expressed as fold increase over control (serum-deprived medium). *(n=3 *p <0.05 vs control; **p <0.05 vs C.M. of unstimulated M2c macrophages; § p <0.05 vs C.M. of M2c macrophage stimulated with Gas-6 (200 ng/ml) without inhibition for MerTK)*

4.8.4 Gene expression analysis in response to C.M. of the M2c macrophages

To identify changes in gene expression of HSC profibrogenic factors in response to C.M. of M2c macrophages, we performed RT PCR analysis.

In HSCs treated with C.M. from Gas-6-stimulated M2c macrophages, *TIMP1, TGF-β1*, *IL-8* and *VEGF-A* expression was increased compared to HSCs

treated with C.M. of unstimulated macrophages. These effects were significantly reduced when macrophages were pre-treated with UNC569, indicating that they are specifically mediated by MerTK (Figure 4.23).

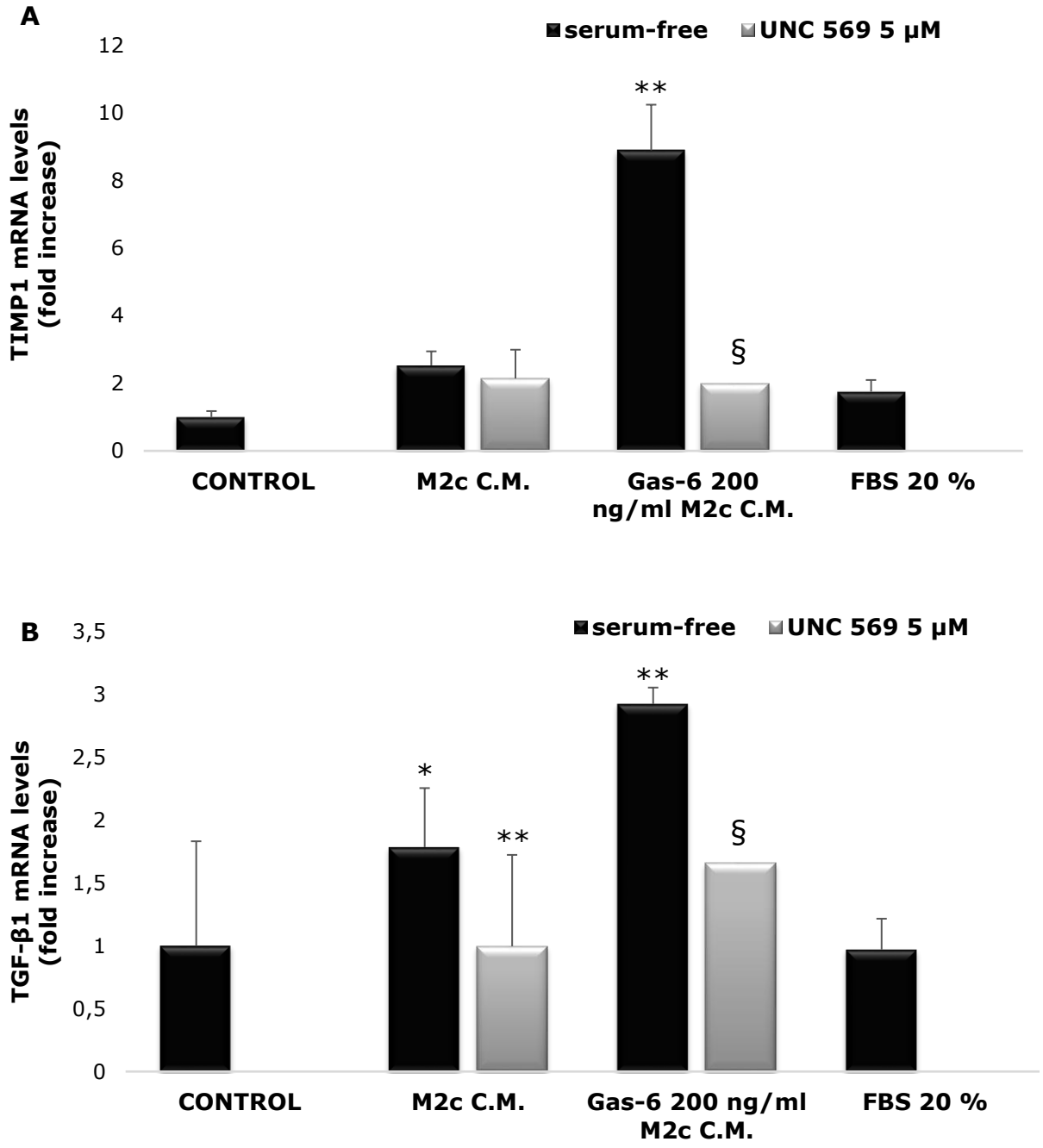

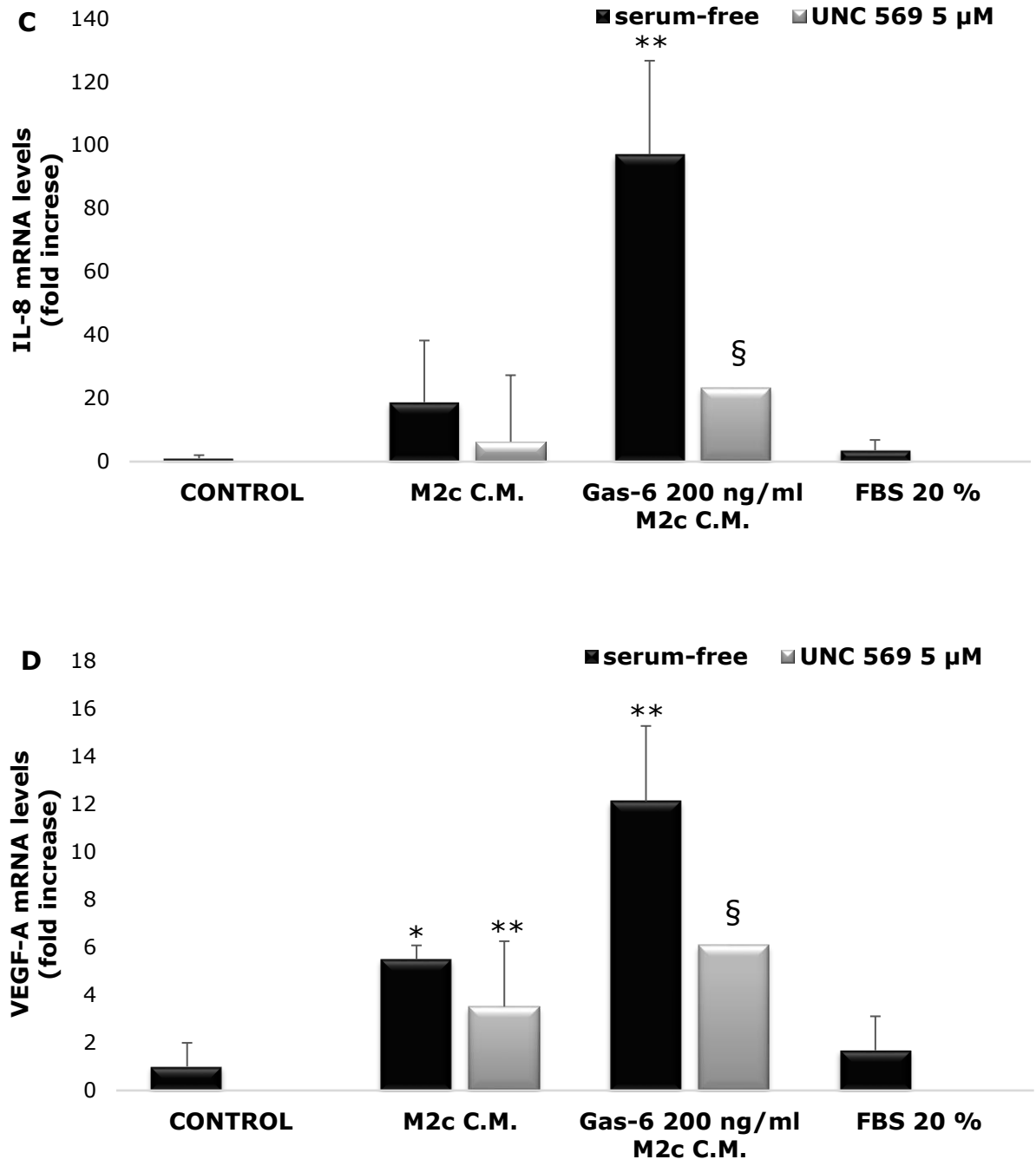

Figure 4.23. *TIMP1, TGF-β1, IL-8* and *VEGF-A* gene expression in response to C.M. of the M2c macrophages treated with UNC 569 under stimulation of Gas-6.

Total RNA was isolated from the M2c macrophages and *TIMP1* (**A**)*, TGF-β1*(**B**), *IL-8* (**C**) and *VEGF-A* (**D**) mRNA expression were analyzed by Real-Time PCR and normalized for expression of the 'housekeeping' Actin gene. Data are expressed as fold increase over control (serum-deprived medium). *(n=3 *p <0.05 vs control; **p <0.05 vs C.M. of unstimulated M2c macrophages; § p <0.05 vs C.M. of M2c macrophage stimulated with Gas-6 (200 ng/ml) without inhibition for MerTK)*

These data indicate that alternatively activated macrophages (M2c) significantly contribute to migration, proliferation, survival and increase of profibrogenic factors in HSCs; these actions are mediated by MerTK, as demonstrated by the inhibition experiments.

4.9 MerTK expression in HCC cell lines

Expression of MerTK has been correlated with poor prognosis or chemoresistance in several human tumors (Linger et al. 2008). Recent studies showed that MerTK activation initiates signaling cascades that are essential for tumor progression (Graham et al. 2014). However, only limited information is available on the relevance of MerTK in the biology of liver cells and no studies have been conducted to evaluate the role of MerTK in the pathogenesis of HCC.

In the second session of this study, the protein expression of MerTK in HCC cell lines was analyzed by western blotting.

MerTK was expressed by HuH7 and in HepG2 (Figure 4.24).

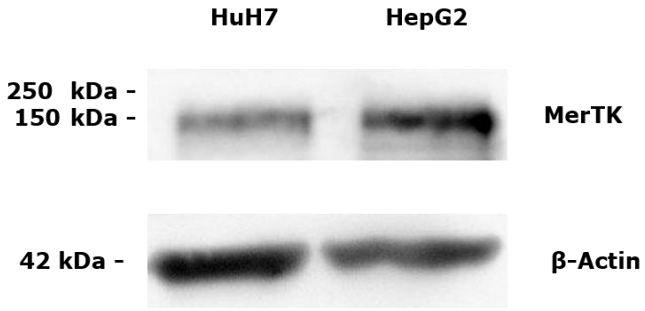

Figure 4.24. MerTK expression in HCC cells.

25 µg of total cell lysate from HuH7 and HepG2 were analyzed by western blotting using anti-MerTK antibody, β-Actin was used as loading control.

4.10 Effects of Gas-6 on MerTK activation in HCC cell lines

We further examined the effects of Gas-6 on MerTK activation in the HCC cell lines. The phosphorylation of MerTK was assessed by western blotting with anti-phosphorylation antibody. We found that Gas-6 induces a time-dependent phosphorylation of MerTK both in Huh7 (Figure 4.25) and in HepG2 (Figure 4.26).

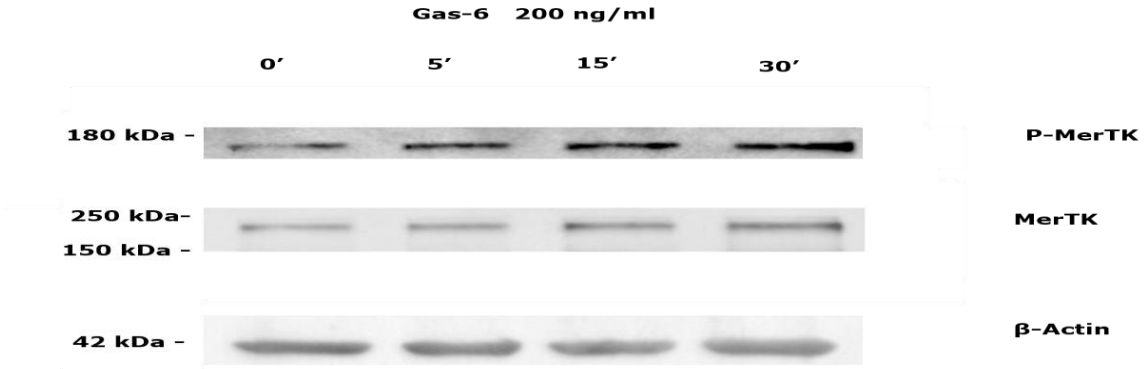

Figure 4.25. Gas-6 induced MerTK phosphorylation in HuH7.
HuH7 were deprived of serum for 24 hours and then stimulated with Gas-6 (200 ng/ml). At the indicated times, 20 µg of total cells were lysed and analyzed by western blotting with the indicated antibodies, β-Actin was used as loading control.

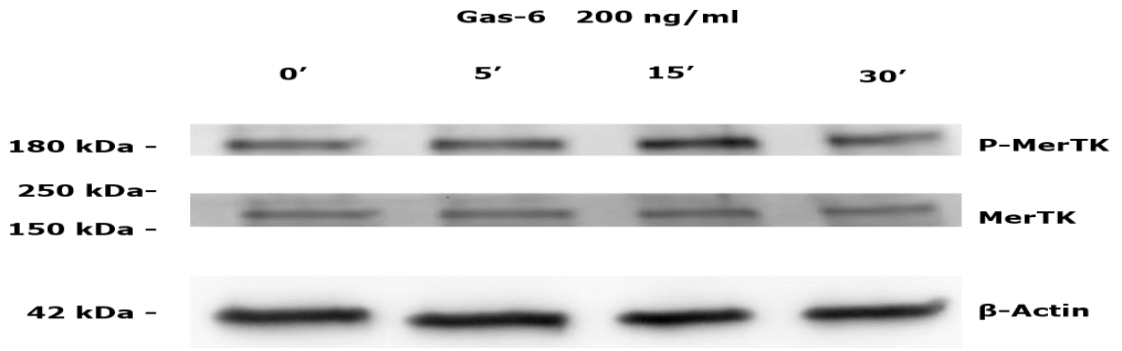

Figure 4.26. Gas-6 induced MerTK phosphorylation in HepG2.
HepG2 were deprived of serum for 24 hours and then stimulated with Gas-6 (200 ng/m). At the indicated times, 20 µg of total cell lysate were analyzed by western blotting with the indicated antibodies, β-Actin was used as loading control.

Subsequently, we evaluated the effect of Gas-6 on migration of HuH7 and HepG2. In both cell lines, Gas-6 exposure resulted in a significant increase in cell migration that was reverted by pre-treatment with UNC569 (Figure 4.27-4.28). Collectively, these data indicate that HCC cell lines express functional MerTK.

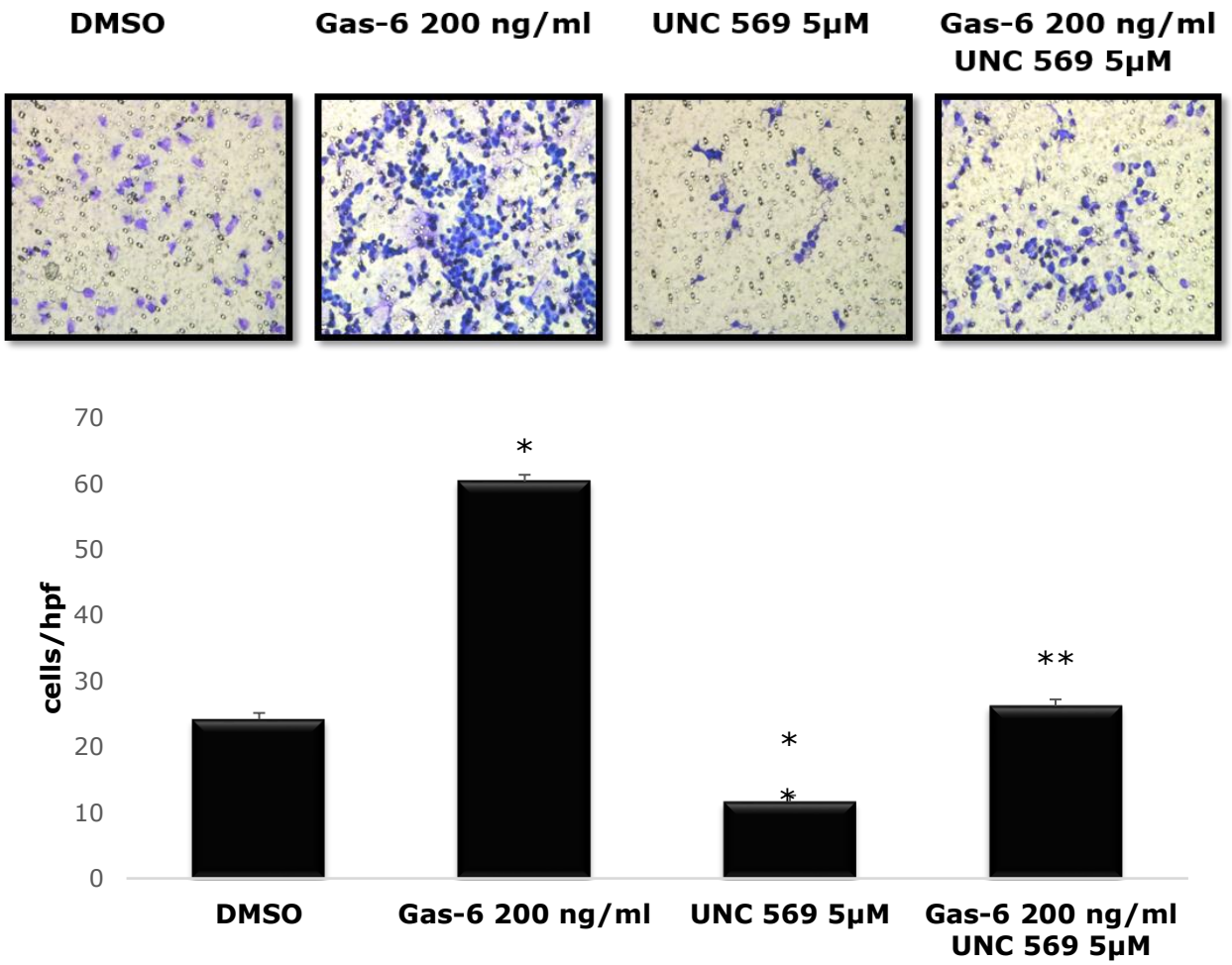

Figure 4.27. HuH7 migration in response to Gas-6 with or without pre-treatment with UNC 569.
Migration of HuH7 was measured using modified Boyden chamber. *(n=3 *p <0.05 vs vehicle (DMSO); **p <0.05 vs HuH7 stimulated with Gas-6 (200 ng/ml) without inhibition for MerTK)*

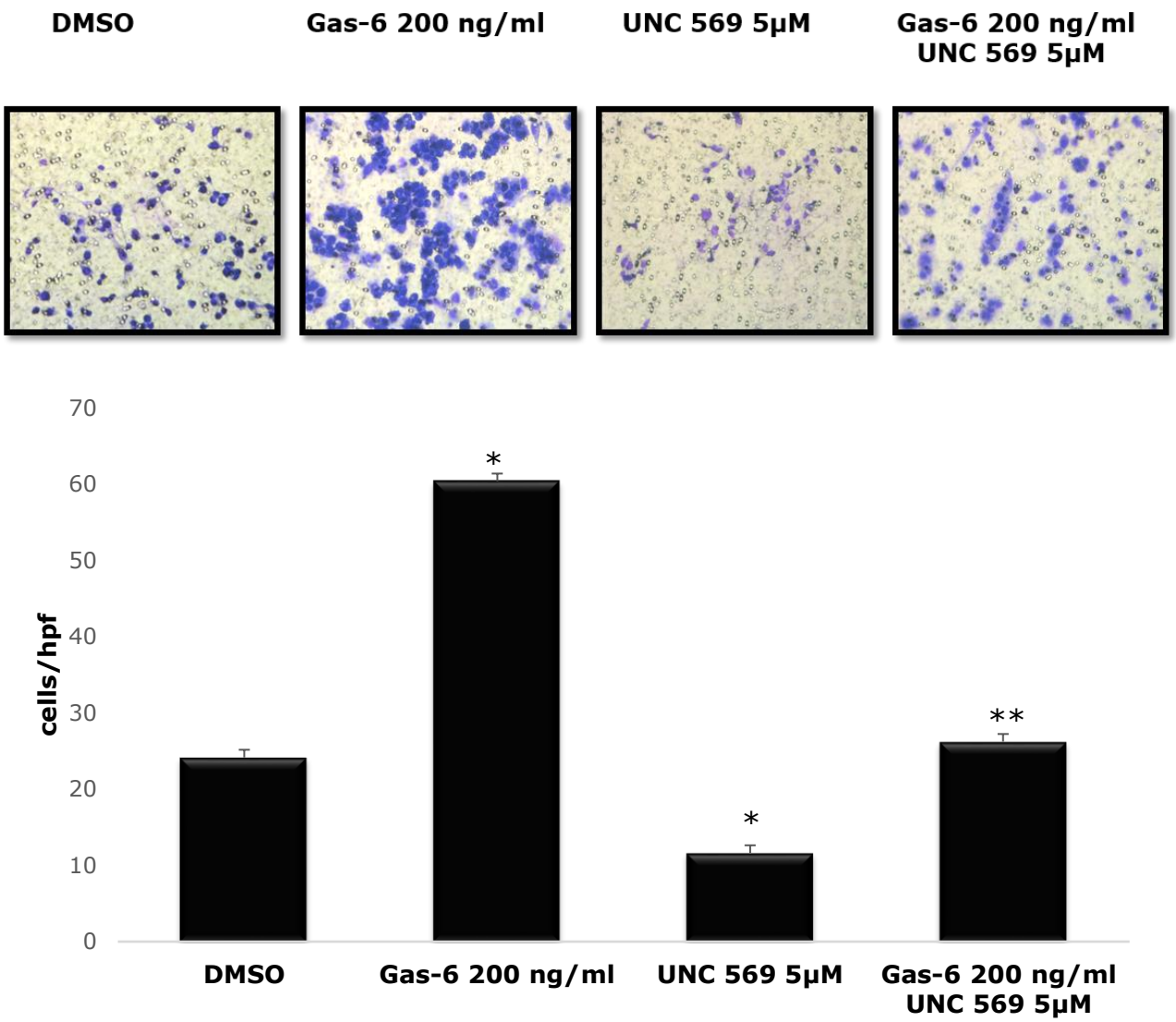

Figure 4.28. HepG2 migration in response to Gas-6 with or without pre-treatment with UNC 569.

Migration of HepG2 was measured using modified Boyden chamber. *(n=3 *p <0.05 vs vehicle (DMSO); **p <0.05 vs HepG2 stimulated with Gas-6 (200 ng/ml) without inhibition for MerTK)*

5. DISCUSSION

Although there is a clear association between the causes and the development of liver fibrosis, the underlying mechanisms are only summarily delineated.

The hepatocellular damage due to liver injury leads to the release of proinflammatory and profibrotic factors from infiltrating inflammatory cells, especially macrophages, that resulted in the activation of liver fibrogenic cells including HSCs. HSCs, widely recognized as the principal effector of hepatic fibrogenesis, undergo an activation process acquiring a myofibroblast-like phenotype characterized by morphological and functional changes. Macrophages localize in close proximity to the activated HSCs, playing a key role in the progression of liver injury from inflammation to fibrosis and eventually cirrhosis and HCC.

Hepatic macrophages arise either from circulating bone-marrow derived monocytes recruited to the injured liver or from proliferating resident macrophages (Kupffer cells). The cross-talk between HSCs and macrophages is crucial for fibrosis development, but many facets of this interaction need to be explored. The identification of new targets that modulate macrophages-HSCs interplay could represent a promising approach to treat fibrotic diseases.

MerTK, a tyrosine kinase receptor has been under intense study over the last years for its involvement in the resolution of inflammation, autoimmunity, cancer progression and tumor immunology. It has also been associated with

liver diseases. Petta et al. observed high hepatic expression of MERTK in NAFLD patients with severe fibrosis; the analysis of liver specimens from these patients revealed that MerTK was mainly expressed in macrophages and HSCs loosely aggregated within inflammatory foci (Petta et al. 2016). Moreover, Dr. Antoniades' group found that MerTK expression in circulating monocytes impaired antimicrobial defense in patients with acute-on-chronic liver failure (ACLF), contributing to adverse prognosis (Bernsmeier et al. 2015).

Based on these data, the aim of this study was to investigate the implication of MerTK expressed in macrophages in the development of hepatic fibrosis and the potential role of this kinase in HCC.

It was previously shown that MerTK is highly expressed both in THP1 -derived macrophages and in M2c macrophages. The THP1 cell line is often used as a model for primary monocytes, however there are important differences between these immortalized cells and their physiological counterparts, i.e. human peripheral blood monocytes. The use of cultured THP1 cells as a model for primary human monocytes exemplifies the basic concept of translational research. The approximation that characterizes this type of translational research, i.e., the use of cultured, immortalized cells as a proxy for primary cells, often receives marginal or no consideration in the discussion section of research reports. For this reason, we decided to use also the C.M. of M2c macrophages to evaluate the involvement of MerTK signaling in the cross-talk between macrophages and HSCs.

In our study we confirmed that MerTK is expressed in these cell types and showed that MerTK induces the activation of AKT and STAT3, two recently identified downstream effectors of MerTK, promoting survival in leukemia and in several solid tumors.

To evaluate the cross-talk between macrophages and HSCs, we employed macrophage Conditioned Medium (C.M.). It is well known that C.M. obtained by macrophages contains soluble factors (as cytokines and growth factors), exosomes and microparticles that can influence HSC phenotype (Friedman and Arthur 1989).

An intriguing finding of this study is that the interplay between macrophages and HSCs is regulated by MerTK signaling pathway. The C.M. of both Gas-6-stimulated THP1 macrophages and Gas-6-stimulated M2c macrophages induced an increase in HSC migration, viability and proliferation, suggesting a paracrine effect mediated by macrophage MerTK activation. The specificity of MerTK activation was assessed with two different approaches: using the UNC569 inhibitor or by gene silencing technique. We observed that the increase in migration, viability and proliferation of HSCs in response to M.C. of Gas-6-stimulated macrophages results significantly reduced by MerTK inhibition in macrophages, providing evidences that the effects of C.M. are mediated by MerTK. In addition, we showed that macrophage MerTK pathways positively modulated fibrogenic genes in HSCs. In particular, we observed that *TIMP1, TGF-β1, IL-8* and *VEGF-A* gene expression increased in HSCs treated with C.M. of Gas-6-stimulated macrophages. The increase of profibrogenic factors in HSCs was blunted following inhibition of macrophage

MerTK, confirming the regulatory actions of MerTK pathway on macrophage-driven HSCs activation.

In the second session of this study we analyzed the potential role of MerTK in the development of HCC.

MerTK is overexpressed and activated in a wide variety of cancers, as leukaemia, glioblastoma, astrocytoma and prostate cancer where it promotes tumor development. MerTK activates a complex network of pro-oncogenic pathways which mediate survival, proliferation, and migration of cancer cells. Moreover, recent studies conducted in preclinical models indicated that MERTK inhibition is a possible strategy for decreasing tumor burden (Cummings et al. 2013). However, no studies have been performed to investigate the role of MerTK in the pathogenesis of HCC. We showed that MerTK is expressed in two HCC cell lines, HuH7 and HepG2 and that MerTK activation induced by Gas-6 promotes a significant increase in cell migration, which is markedly reduced under pre-treatment with UNC569. These data suggest the potential involvement of MerTK in HCC development, even if further investigations are warranted to identify the pathways downstream MerTK that may contribute to HCC progression. In conclusion, our study suggests that inhibition of MerTK could represent a novel strategy to dampen fibrogenic progression in NAFLD and neoplastic transformation.

6. REFERENCES

Ambarus, C. A., S. Krausz, M. van Eijk, J. Hamann, T. R. Radstake, K. A. Reedquist, P. P. Tak, and D. L. Baeten. 2012. "Systematic validation of specific phenotypic markers for in vitro polarized human macrophages." *J Immunol Methods* 375 (1-2):196-206. doi: 10.1016/j.jim.2011.10.013.

Anania, F. A., L. Womack, M. Jiang, and N. K. Saxena. 2001. "Aldehydes potentiate alpha(2)(I) collagen gene activity by JNK in hepatic stellate cells." *Free Radic Biol Med* 30 (8):846-57.

Anderson, H. A., C. A. Maylock, J. A. Williams, C. P. Paweletz, H. Shu, and E. Shacter. 2003. "Serum-derived protein S binds to phosphatidylserine and stimulates the phagocytosis of apoptotic cells." *Nat Immunol* 4 (1):87-91. doi: 10.1038/ni871.

Angelillo-Scherrer, A., P. de Frutos, C. Aparicio, E. Melis, P. Savi, F. Lupu, J. Arnout, M. Dewerchin, M. Hoylaerts, J. Herbert, D. Collen, B. Dahlbäck, and P. Carmeliet. 2001. "Deficiency or inhibition of Gas6 causes platelet dysfunction and protects mice against thrombosis." *Nat Med* 7 (2):215-21. doi: 10.1038/84667.

Angulo, P. 2010. "Long-term mortality in nonalcoholic fatty liver disease: is liver histology of any prognostic significance?" *Hepatology* 51 (2):373-5. doi: 10.1002/hep.23521.

Arthur, M. J. 2000. "Fibrogenesis II. Metalloproteinases and their inhibitors in liver fibrosis." *Am J Physiol Gastrointest Liver Physiol* 279 (2):G245-9. doi: 10.1152/ajpgi.2000.279.2.G245.

Asaoka, Y., S. Terai, I. Sakaida, and H. Nishina. 2013. "The expanding role of fish models in understanding non-alcoholic fatty liver disease." *Dis Model Mech* 6 (4):905-14. doi: 10.1242/dmm.011981.

Aterman, K. 1986. "The parasinusoidal cells of the liver: a historical account." *Histochem J* 18 (6):279-305.

Bachem, M. G., D. Meyer, R. Melchior, K. M. Sell, and A. M. Gressner. 1992. "Activation of rat liver perisinusoidal lipocytes by transforming growth factors derived from myofibroblastlike cells. A potential mechanism of self perpetuation in liver fibrogenesis." *J Clin Invest* 89 (1):19-27. doi: 10.1172/JCI115561.

Balogh, I., S. Hafizi, J. Stenhoff, K. Hansson, and B. Dahlbäck. 2005. "Analysis of Gas6 in human platelets and plasma." *Arterioscler Thromb Vasc Biol* 25 (6):1280-6. doi: 10.1161/01.ATV.0000163845.07146.48.

Bataller, R., and D. A. Brenner. 2005. "Liver fibrosis." *J Clin Invest* 115 (2):209-18. doi: 10.1172/JCI24282.

Behrens, E. M., P. Gadue, S. Y. Gong, S. Garrett, P. L. Stein, and P. L. Cohen. 2003. "The mer receptor tyrosine kinase: expression and function suggest a role in innate immunity." *Eur J Immunol* 33 (8):2160-7. doi: 10.1002/eji.200324076.

Bernsmeier, C., O. T. Pop, A. Singanayagam, E. Triantafyllou, V. C. Patel, C. J. Weston, S. Curbishley, F. Sadiq, N. Vergis, W. Khamri, W. Bernal, G. Auzinger, M. Heneghan, Y. Ma, W. Jassem, N. D. Heaton, D. H. Adams, A. Quaglia, M. R. Thursz, J. Wendon, and C. G. Antoniades. 2015. "Patients with acute-on-chronic liver failure have increased numbers of regulatory immune cells expressing the receptor tyrosine kinase MERTK." *Gastroenterology* 148 (3):603-615.e14. doi: 10.1053/j.gastro.2014.11.045.

Bilzer, M., F. Roggel, and A. L. Gerbes. 2006. "Role of Kupffer cells in host defense and liver disease." *Liver Int* 26 (10):1175-86. doi: 10.1111/j.1478-3231.2006.01342.x.

Blomhoff, R., M. H. Green, T. Berg, and K. R. Norum. 1990. "Transport and storage of vitamin A." *Science* 250 (4979):399-404.

Bonacchi, A., P. Romagnani, R. G. Romanelli, E. Efsen, F. Annunziato, L. Lasagni, M. Francalanci, M. Serio, G. Laffi, M. Pinzani, P. Gentilini, and F. Marra. 2001. "Signal transduction by the chemokine receptor CXCR3: activation of Ras/ERK, Src, and phosphatidylinositol 3-kinase/Akt controls cell migration and

proliferation in human vascular pericytes." *J Biol Chem* 276 (13):9945-54. doi: 10.1074/jbc.M010303200.

Borkham-Kamphorst, E., C. R. van Roeyen, T. Ostendorf, J. Floege, A. M. Gressner, and R. Weiskirchen. 2007. "Pro-fibrogenic potential of PDGF-D in liver fibrosis." *J Hepatol* 46 (6):1064-74. doi: 10.1016/j.jhep.2007.01.029.

Brandao, L. N., A. Winges, S. Christoph, S. Sather, J. Migdall-Wilson, J. Schlegel, A. McGranahan, D. Gao, X. Liang, D. Deryckere, and D. K. Graham. 2013. "Inhibition of MerTK increases chemosensitivity and decreases oncogenic potential in T-cell acute lymphoblastic leukemia." *Blood Cancer J* 3:e101. doi: 10.1038/bcj.2012.46.

Bronfenmajer, S., F. Schaffner, and H. Popper. 1966. "Fat-storing cells (lipocytes) in human liver." *Arch Pathol* 82 (5):447-53.

Buzzetti, E., M. Pinzani, and E. A. Tsochatzis. 2016. "The multiple-hit pathogenesis of non-alcoholic fatty liver disease (NAFLD)." *Metabolism* 65 (8):1038-48. doi: 10.1016/j.metabol.2015.12.012.

Böttcher, K., and M. Pinzani. 2017. "Pathophysiology of liver fibrosis and the methodological barriers to the development of anti-fibrogenic agents." *Adv Drug Deliv Rev* 121:3-8. doi: 10.1016/j.addr.2017.05.016.

Caligiuri, A., A. Gentilini, and F. Marra. 2016. "Molecular Pathogenesis of NASH." *Int J Mol Sci* 17 (9). doi: 10.3390/ijms17091575.

Canbay, A., S. Friedman, and G. J. Gores. 2004. "Apoptosis: the nexus of liver injury and fibrosis." *Hepatology* 39 (2):273-8. doi: 10.1002/hep.20051.

Carloni, V., T. V. Luong, and K. Rombouts. 2014. "Hepatic stellate cells and extracellular matrix in hepatocellular carcinoma: more complicated than ever." *Liver Int* 34 (6):834-43. doi: 10.1111/liv.12465.

Casini, A., M. Pinzani, S. Milani, C. Grappone, G. Galli, A. M. Jezequel, D. Schuppan, C. M. Rotella, and C. Surrenti. 1993. "Regulation of extracellular matrix synthesis by transforming growth factor beta 1 in human fat-storing cells." *Gastroenterology* 105 (1):245-53.

Christoph, S., D. Deryckere, J. Schlegel, J. K. Frazer, L. A. Batchelor, A. Y. Trakhimets, S. Sather, D. M. Hunter, C. T. Cummings, J. Liu, C. Yang, D. Kireev, C. Simpson, J. Norris-Drouin, E. A. Hull-Ryde, W. P. Janzen, G. L. Johnson, X. Wang, S. V. Frye, H. S. Earp, and D. K. Graham. 2013. "UNC569, a novel small-molecule mer inhibitor with efficacy against acute lymphoblastic leukemia in vitro and in vivo." *Mol Cancer Ther* 12 (11):2367-77. doi: 10.1158/1535-7163.MCT-13-0040.

Cui, J., Y. Chen, H. Y. Wang, and R. F. Wang. 2014. "Mechanisms and pathways of innate immune activation and regulation in health and cancer." *Hum Vaccin Immunother* 10 (11):3270-85. doi: 10.4161/21645515.2014.979640.

Cummings, C. T., D. Deryckere, H. S. Earp, and D. K. Graham. 2013. "Molecular pathways: MERTK signaling in cancer." *Clin Cancer Res* 19 (19):5275-80. doi: 10.1158/1078-0432.CCR-12-1451.

Cummings, C. T., R. M. Linger, R. A. Cohen, S. Sather, G. D. Kirkpatrick, K. D. Davies, D. DeRyckere, H. S. Earp, and D. K. Graham. 2014. "Mer590, a novel monoclonal antibody targeting MER receptor tyrosine kinase, decreases colony formation and increases chemosensitivity in non-small cell lung cancer." *Oncotarget* 5 (21):10434-45. doi: 10.18632/oncotarget.2142.

Dal-Secco, D., J. Wang, Z. Zeng, E. Kolaczkowska, C. H. Wong, B. Petri, R. M. Ransohoff, I. F. Charo, C. N. Jenne, and P. Kubes. 2015. "A dynamic spectrum of monocytes arising from the in situ reprogramming of CCR2+ monocytes at a site of sterile injury." *J Exp Med* 212 (4):447-56. doi: 10.1084/jem.20141539.

Danobeitia, J. S., A. Djamali, and L. A. Fernandez. 2014. "The role of complement in the pathogenesis of renal ischemia-reperfusion injury and fibrosis." *Fibrogenesis Tissue Repair* 7:16. doi: 10.1186/1755-1536-7-16.

de Almeida, M. C., A. C. Silva, A. Barral, and M. Barral Netto. 2000. "A simple method for human peripheral blood monocyte isolation." *Mem Inst Oswaldo Cruz* 95 (2):221-3.

Del Campo, J. A., R. Gallego-Durán, P. Gallego, and L. Grande. 2018. "Genetic and Epigenetic Regulation in Nonalcoholic Fatty Liver Disease (NAFLD)." *Int J Mol Sci* 19 (3). doi: 10.3390/ijms19030911.

Ekman, C., A. Linder, P. Akesson, and B. Dahlbäck. 2010. "Plasma concentrations of Gas6 (growth arrest specific protein 6) and its soluble tyrosine kinase receptor sAxl in sepsis and systemic inflammatory response syndromes." *Crit Care* 14 (4):R158. doi: 10.1186/cc9233.

Finn, R. S. 2013. "Emerging targeted strategies in advanced hepatocellular carcinoma." *Semin Liver Dis* 33 Suppl 1:S11-9. doi: 10.1055/s-0033-1333632.

Friedman, S. L. 2008. "Hepatic stellate cells: protean, multifunctional, and enigmatic cells of the liver." *Physiol Rev* 88 (1):125-72. doi: 10.1152/physrev.00013.2007.

Friedman, S. L., and M. J. Arthur. 1989. "Activation of cultured rat hepatic lipocytes by Kupffer cell conditioned medium. Direct enhancement of matrix synthesis and stimulation of cell proliferation via induction of platelet-derived growth factor receptors." *J Clin Invest* 84 (6):1780-5. doi: 10.1172/JCI114362.

Gabbiani, G., E. Schmid, S. Winter, C. Chaponnier, C. de Ckhastonay, J. Vandekerckhove, K. Weber, and W. W. Franke. 1981. "Vascular smooth muscle cells differ from other smooth muscle cells: predominance of vimentin filaments and a specific alpha-type actin." *Proc Natl Acad Sci U S A* 78 (1):298-302.

Gaça, M. D., X. Zhou, R. Issa, K. Kiriella, J. P. Iredale, and R. C. Benyon. 2003. "Basement membrane-like matrix inhibits proliferation and collagen synthesis by activated rat hepatic stellate cells: evidence for matrix-dependent deactivation of stellate cells." *Matrix Biol* 22 (3):229-39.

Gentilini, A., A. Caligiuri, A. Provenzano, and F. Marra. 2016. "Novel Aspects in the Pathogenesis of Nonalcoholic Steatohepatitis." *Curr Mol Med* 16 (8):710-720.

Giampieri, M. P., A. M. Jezequel, and F. Orlandi. 1981. "The lipocytes in normal human liver. A quantitative study." *Digestion* 22 (4):165-9. doi: 10.1159/000198640.

Golpon, H. A., V. A. Fadok, L. Taraseviciene-Stewart, R. Scerbavicius, C. Sauer, T. Welte, P. M. Henson, and N. F. Voelkel. 2004. "Life after corpse engulfment: phagocytosis of apoptotic cells leads to VEGF secretion and cell growth." *FASEB J* 18 (14):1716-8. doi: 10.1096/fj.04-1853fje.

Gordon, S., and P. R. Taylor. 2005. "Monocyte and macrophage heterogeneity." *Nat Rev Immunol* 5 (12):953-64. doi: 10.1038/nri1733.

Graham, D. K., D. DeRyckere, K. D. Davies, and H. S. Earp. 2014. "The TAM family: phosphatidylserine sensing receptor tyrosine kinases gone awry in cancer." *Nat Rev Cancer* 14 (12):769-85. doi: 10.1038/nrc3847.

Graham, D. K., D. B. Salzberg, J. Kurtzberg, S. Sather, G. K. Matsushima, A. K. Keating, X. Liang, M. A. Lovell, S. A. Williams, T. L. Dawson, M. J. Schell, A. A. Anwar, H. R. Snodgrass, and H. S. Earp. 2006. "Ectopic expression of the proto-oncogene Mer in pediatric T-cell acute lymphoblastic leukemia." *Clin Cancer Res* 12 (9):2662-9. doi: 10.1158/1078-0432.CCR-05-2208.

Han, Y. P., C. Yan, L. Zhou, L. Qin, and H. Tsukamoto. 2007. "A matrix metalloproteinase-9 activation cascade by hepatic stellate cells in trans-differentiation in the three-dimensional extracellular matrix." *J Biol Chem* 282 (17):12928-39. doi: 10.1074/jbc.M700554200.

Hartmann, P., M. Haimerl, M. Mazagova, D. A. Brenner, and B. Schnabl. 2012. "Toll-like receptor 2-mediated intestinal injury and enteric tumor necrosis factor receptor I contribute to liver fibrosis in mice." *Gastroenterology* 143 (5):1330-1340.e1. doi: 10.1053/j.gastro.2012.07.099.

He, G., and M. Karin. 2011. "NF-κB and STAT3 - key players in liver inflammation and cancer." *Cell Res* 21 (1):159-68. doi: 10.1038/cr.2010.183.

Heeb, M. J. 2008. "Role of the PROS1 gene in thrombosis: lessons and controversies." *Expert Rev Hematol* 1 (1):9-12. doi: 10.1586/17474086.1.1.9.

Hernandez-Gea, V., and S. L. Friedman. 2011. "Pathogenesis of liver fibrosis." *Annu Rev Pathol* 6:425-56. doi: 10.1146/annurev-pathol-011110-130246.

Huang, M., A. C. Rigby, X. Morelli, M. A. Grant, G. Huang, B. Furie, B. Seaton, and B. C. Furie. 2003. "Structural basis of membrane binding by Gla domains of vitamin K-dependent proteins." *Nat Struct Biol* 10 (9):751-6. doi: 10.1038/nsb971.

Hunter, T. 1998. "The role of tyrosine phosphorylation in cell growth and disease." *Harvey Lect* 94:81-119.

Inagaki, Y., and I. Okazaki. 2007. "Emerging insights into Transforming growth factor beta Smad signal in hepatic fibrogenesis." *Gut* 56 (2):284-92. doi: 10.1136/gut.2005.088690.

Iredale, J. P. 2007. "Models of liver fibrosis: exploring the dynamic nature of inflammation and repair in a solid organ." *J Clin Invest* 117 (3):539-48. doi: 10.1172/JCI30542.

Issa, R., E. Williams, N. Trim, T. Kendall, M. J. Arthur, J. Reichen, R. C. Benyon, and J. P. Iredale. 2001. "Apoptosis of hepatic stellate cells: involvement in resolution of biliary fibrosis and regulation by soluble growth factors." *Gut* 48 (4):548-57.

Jemal, A., F. Bray, M. M. Center, J. Ferlay, E. Ward, and D. Forman. 2011. "Global cancer statistics." *CA Cancer J Clin* 61 (2):69-90. doi: 10.3322/caac.20107.

Kinnman, N., R. Hultcrantz, V. Barbu, C. Rey, D. Wendum, R. Poupon, and C. Housset. 2000. "PDGF-mediated chemoattraction of hepatic stellate cells by bile duct segments in cholestatic liver injury." *Lab Invest* 80 (5):697-707.

Kurihara, Y., and M. Furue. 2013. "Interferon-γ enhances phorbol myristate acetate-induced cell attachment and tumor necrosis factor production via the NF-κB pathway in THP-1 human monocytic cells." *Mol Med Rep* 7 (6):1739-44. doi: 10.3892/mmr.2013.1419.

Laleman, W., L. Van Landeghem, T. Severi, I. Vander Elst, M. Zeegers, R. Bisschops, J. Van Pelt, T. Roskams, D. Cassiman, J. Fevery, and F. Nevens. 2007. "Both Ca2+ -dependent and -independent pathways are involved in rat hepatic stellate cell contraction and intrahepatic hyperresponsiveness to methoxamine." *Am J Physiol Gastrointest Liver Physiol* 292 (2):G556-64. doi: 10.1152/ajpgi.00196.2006.

Lechuga, C. G., Z. H. Hernández-Nazara, E. Hernández, M. Bustamante, G. Desierto, A. Cotty, N. Dharker, M. Choe, and M. Rojkind. 2006. "PI3K is involved in PDGF-beta receptor upregulation post-PDGF-BB treatment in mouse HSC." *Am J Physiol Gastrointest Liver Physiol* 291 (6):G1051-61. doi: 10.1152/ajpgi.00058.2005.

Lee, Y. J., S. H. Lee, Y. S. Youn, J. Y. Choi, K. S. Song, M. S. Cho, and J. L. Kang. 2012. "Preventing cleavage of Mer promotes efferocytosis and suppresses acute lung injury in bleomycin treated mice." *Toxicol Appl Pharmacol* 263 (1):61-72. doi: 10.1016/j.taap.2012.05.024.

Lee-Sherick, A. B., W. Zhang, K. K. Menachof, A. A. Hill, S. Rinella, G. Kirkpatrick, L. S. Page, M. A. Stashko, C. T. Jordan, Q. Wei, J. Liu, D. Zhang, D. DeRyckere, X. Wang, S. Frye, H. S. Earp, and D. K. Graham. 2015. "Efficacy of a Mer and Flt3 tyrosine kinase small molecule inhibitor, UNC1666, in acute myeloid leukemia." *Oncotarget* 6 (9):6722-36. doi: 10.18632/oncotarget.3156.

Lemke, G. 2013. "Biology of the TAM receptors." *Cold Spring Harb Perspect Biol* 5 (11):a009076. doi: 10.1101/cshperspect.a009076.

Lemke, G., and Q. Lu. 2003. "Macrophage regulation by Tyro 3 family receptors." *Curr Opin Immunol* 15 (1):31-6.

Lemke, G., and C. V. Rothlin. 2008. "Immunobiology of the TAM receptors." *Nat Rev Immunol* 8 (5):327-36. doi: 10.1038/nri2303.

Lemmon, M. A., and J. Schlessinger. 2010. "Cell signaling by receptor tyrosine kinases." *Cell* 141 (7):1117-34. doi: 10.1016/j.cell.2010.06.011.

Lewis, P. M., K. E. Crosier, C. R. Wood, and P. S. Crosier. 1996. "Analysis of the murine Dtk gene identifies conservation of genomic structure within a new receptor tyrosine kinase subfamily." *Genomics* 31 (1):13-9. doi: 10.1006/geno.1996.0003.

Li, B., C. Zhang, and Y. T. Zhan. 2018. "Nonalcoholic Fatty Liver Disease Cirrhosis: A Review of Its Epidemiology, Risk Factors, Clinical Presentation, Diagnosis, Management, and Prognosis." *Can J Gastroenterol Hepatol* 2018:2784537. doi: 10.1155/2018/2784537.

Li, Y. W., S. J. Qiu, J. Fan, Q. Gao, J. Zhou, Y. S. Xiao, Y. Xu, X. Y. Wang, J. Sun, and X. W. Huang. 2009. "Tumor-infiltrating macrophages can predict favorable prognosis in hepatocellular carcinoma after resection." *J Cancer Res Clin Oncol* 135 (3):439-49. doi: 10.1007/s00432-008-0469-0.

Liao, D., X. Wang, M. Li, P. H. Lin, Q. Yao, and C. Chen. 2009. "Human protein S inhibits the uptake of AcLDL and expression of SR-A through Mer receptor tyrosine kinase in human macrophages." *Blood* 113 (1):165-74. doi: 10.1182/blood-2008-05-158048.

Linger, R. M., A. K. Keating, H. S. Earp, and D. K. Graham. 2008. "TAM receptor tyrosine kinases: biologic functions, signaling, and potential therapeutic targeting in human cancer." *Adv Cancer Res* 100:35-83. doi: 10.1016/S0065-230X(08)00002-X.

Linger, R. M., A. B. Lee-Sherick, D. DeRyckere, R. A. Cohen, K. M. Jacobsen, A. McGranahan, L. N. Brandão, A. Winges, K. K. Sawczyn, X. Liang, A. K. Keating, A. C. Tan, H. S. Earp, and D. K. Graham. 2013. "Mer receptor tyrosine kinase is a therapeutic target in pre-B-cell acute lymphoblastic leukemia." *Blood* 122 (9):1599-609. doi: 10.1182/blood-2013-01-478156.

Lu, Q., M. Gore, Q. Zhang, T. Camenisch, S. Boast, F. Casagranda, C. Lai, M. K. Skinner, R. Klein, G. K. Matsushima, H. S. Earp, S. P. Goff, and G. Lemke. 1999. "Tyro-3 family receptors are essential regulators of mammalian spermatogenesis." *Nature* 398 (6729):723-8. doi: 10.1038/19554.

Lu, Q., and G. Lemke. 2001. "Homeostatic regulation of the immune system by receptor tyrosine kinases of the Tyro 3 family." *Science* 293 (5528):306-11. doi: 10.1126/science.1061663.

Ludwig, J., T. R. Viggiano, D. B. McGill, and B. J. Oh. 1980. "Nonalcoholic steatohepatitis: Mayo Clinic experiences with a hitherto unnamed disease." *Mayo Clin Proc* 55 (7):434-8.

Malhi, H., M. E. Guicciardi, and G. J. Gores. 2010. "Hepatocyte death: a clear and present danger." *Physiol Rev* 90 (3):1165-94. doi: 10.1152/physrev.00061.2009.

Mantovani, A., P. Allavena, A. Sica, and F. Balkwill. 2008. "Cancer-related inflammation." *Nature* 454 (7203):436-44. doi: 10.1038/nature07205.

Mao, S. A., J. M. Glorioso, and S. L. Nyberg. 2014. "Liver regeneration." *Transl Res* 163 (4):352-62. doi: 10.1016/j.trsl.2014.01.005.

Mark, M. R., J. Chen, R. G. Hammonds, M. Sadick, and P. J. Godowsk. 1996. "Characterization of Gas6, a member of the superfamily of G domain-containing proteins, as a ligand for Rse and Axl." *J Biol Chem* 271 (16):9785-9.

Marra, F., R. DeFranco, C. Grappone, S. Milani, M. Pinzani, G. Pellegrini, G. Laffi, and P. Gentilini. 1998. "Expression of the thrombin receptor in human liver: up-regulation during acute and chronic injury." *Hepatology* 27 (2):462-71. doi: 10.1002/hep.510270221.

Marra, F., A. Gastaldelli, G. Svegliati Baroni, G. Tell, and C. Tiribelli. 2008. "Molecular basis and mechanisms of progression of non-alcoholic steatohepatitis." *Trends Mol Med* 14 (2):72-81. doi: 10.1016/j.molmed.2007.12.003.

Marra, F., R. G. Romanelli, C. Giannini, P. Failli, S. Pastacaldi, M. C. Arrighi, M. Pinzani, G. Laffi, P. Montalto, and P. Gentilini. 1999. "Monocyte chemotactic protein-1 as a chemoattractant for human hepatic stellate cells." *Hepatology* 29 (1):140-8. doi: 10.1002/hep.510290107.

Melton, A. C., and H. F. Yee. 2007. "Hepatic stellate cell protrusions couple platelet-derived growth factor-BB to chemotaxis." *Hepatology* 45 (6):1446-53. doi: 10.1002/hep.21606.

Milani, S., H. Herbst, D. Schuppan, C. Grappone, G. Pellegrini, M. Pinzani, A. Casini, A. Calabró, G. Ciancio, and F. Stefanini. 1994. "Differential expression of matrix-metalloproteinase-1 and -2 genes in normal and fibrotic human liver." *Am J Pathol* 144 (3):528-37.

Minato, Y., Y. Hasumura, and J. Takeuchi. 1983. "The role of fat-storing cells in Disse space fibrogenesis in alcoholic liver disease." *Hepatology* 3 (4):559-66.

Morimoto, K., H. Amano, F. Sonoda, M. Baba, M. Senba, H. Yoshimine, H. Yamamoto, T. Ii, K. Oishi, and T. Nagatake. 2001. "Alveolar macrophages that phagocytose apoptotic neutrophils produce hepatocyte growth factor during bacterial pneumonia in mice." *Am J Respir Cell Mol Biol* 24 (5):608-15. doi: 10.1165/ajrcmb.24.5.4292.

Murray, P. J., and T. A. Wynn. 2011. "Protective and pathogenic functions of macrophage subsets." *Nat Rev Immunol* 11 (11):723-37. doi: 10.1038/nri3073.

Novo, E., F. Marra, E. Zamara, L. Valfrè di Bonzo, A. Caligiuri, S. Cannito, C. Antonaci, S. Colombatto, M. Pinzani, and M. Parola. 2006. "Dose dependent and divergent effects of superoxide anion on cell death, proliferation, and migration of activated human hepatic stellate cells." *Gut* 55 (1):90-7. doi: 10.1136/gut.2005.069633.

Ofosu, A., D. Ramai, and M. Reddy. 2018. "Non-alcoholic fatty liver disease: controlling an emerging epidemic, challenges, and future directions." *Ann Gastroenterol* 31 (3):288-295. doi: 10.20524/aog.2018.0240.

Pakshir, P., and B. Hinz. 2018. "The big five in fibrosis: Macrophages, myofibroblasts, matrix, mechanics, and miscommunication." *Matrix Biol* 68-69:81-93. doi: 10.1016/j.matbio.2018.01.019.

Parola, M., and M. Pinzani. 2018. "Liver fibrosis: Pathophysiology, pathogenetic targets and clinical issues." *Mol Aspects Med*. doi: 10.1016/j.mam.2018.09.002.

Pawson, T. 2004. "Specificity in signal transduction: from phosphotyrosine-SH2 domain interactions to complex cellular systems." *Cell* 116 (2):191-203.

Petta, S., L. Valenti, F. Marra, S. Grimaudo, C. Tripodo, E. Bugianesi, C. Cammà, A. Cappon, V. Di Marco, G. Di Maira, P. Dongiovanni, R. Rametta, A. Gulino, E. Mozzi, E. Orlando, M. Maggioni, R. M. Pipitone, S. Fargion, and A. Craxì. 2016. "MERTK rs4374383 polymorphism affects the severity of fibrosis in non-alcoholic fatty liver disease." *J Hepatol* 64 (3):682-90. doi: 10.1016/j.jhep.2015.10.016.

Pinzani, M., and F. Marra. 2001. "Cytokine receptors and signaling in hepatic stellate cells." *Semin Liver Dis* 21 (3):397-416. doi: 10.1055/s-2001-17554.

Pradere, J. P., J. Kluwe, S. De Minicis, J. J. Jiao, G. Y. Gwak, D. H. Dapito, M. K. Jang, N. D. Guenther, I. Mederacke, R. Friedman, A. C. Dragomir, C. Aloman, and R. F. Schwabe. 2013. "Hepatic macrophages but not dendritic cells contribute to liver fibrosis by promoting the survival of activated hepatic stellate cells in mice." *Hepatology* 58 (4):1461-73. doi: 10.1002/hep.26429.

Protzer, U., M. K. Maini, and P. A. Knolle. 2012. "Living in the liver: hepatic infections." *Nat Rev Immunol* 12 (3):201-13. doi: 10.1038/nri3169.

Rezende, S. M., R. E. Simmonds, and D. A. Lane. 2004. "Coagulation, inflammation, and apoptosis: different roles for protein S and the protein S-C4b binding protein complex." *Blood* 103 (4):1192-201. doi: 10.1182/blood-2003-05-1551.

Rockey, D. C., J. K. Boyles, G. Gabbiani, and S. L. Friedman. 1992. "Rat hepatic lipocytes express smooth muscle actin upon activation in vivo and in culture." *J Submicrosc Cytol Pathol* 24 (2):193-203.

Rogers, A. E., J. P. Le, S. Sather, B. M. Pernu, D. K. Graham, A. M. Pierce, and A. K. Keating. 2012. "Mer receptor tyrosine kinase inhibition impedes glioblastoma multiforme migration and alters cellular morphology." *Oncogene* 31 (38):4171-81. doi: 10.1038/onc.2011.588.

Rothlin, C. V., S. Ghosh, E. I. Zuniga, M. B. Oldstone, and G. Lemke. 2007. "TAM receptors are pleiotropic inhibitors of the innate immune response." *Cell* 131 (6):1124-36. doi: 10.1016/j.cell.2007.10.034.

Sasaki, T., P. G. Knyazev, Y. Cheburkin, W. Göhring, D. Tisi, A. Ullrich, R. Timpl, and E. Hohenester. 2002. "Crystal structure of a C-terminal fragment of growth arrest-specific protein Gas6. Receptor tyrosine kinase activation by laminin G-like domains." *J Biol Chem* 277 (46):44164-70. doi: 10.1074/jbc.M207340200.

Sasaki, T., P. G. Knyazev, N. J. Clout, Y. Cheburkin, W. Göhring, A. Ullrich, R. Timpl, and E. Hohenester. 2006. "Structural basis for Gas6-Axl signalling." *EMBO J* 25 (1):80-7. doi: 10.1038/sj.emboj.7600912.

Sather, S., K. D. Kenyon, J. B. Lefkowitz, X. Liang, B. C. Varnum, P. M. Henson, and D. K. Graham. 2007. "A soluble form of the Mer receptor tyrosine kinase inhibits macrophage clearance of apoptotic cells and platelet aggregation." *Blood* 109 (3):1026-33. doi: 10.1182/blood-2006-05-021634.

Schlegel, J., M. J. Sambade, S. Sather, S. J. Moschos, A. C. Tan, A. Winges, D. DeRyckere, C. C. Carson, D. G. Trembath, J. J. Tentler, S. G. Eckhardt, P. F. Kuan, R. L. Hamilton, L. M. Duncan, C. R. Miller, N. Nikolaishvili-Feinberg, B. R. Midkiff, J. Liu, W. Zhang, C. Yang, X. Wang, S. V. Frye, H. S. Earp, J. M. Shields, and D. K. Graham. 2013. "MERTK receptor tyrosine kinase is a therapeutic target in melanoma." *J Clin Invest* 123 (5):2257-67. doi: 10.1172/JCI67816.

Schlessinger, J. 2000. "Cell signaling by receptor tyrosine kinases." *Cell* 103 (2):211-25.

Schnoor, M., I. Buers, A. Sietmann, M. F. Brodde, O. Hofnagel, H. Robenek, and S. Lorkowski. 2009. "Efficient non-viral transfection of THP-1 cells." *J Immunol Methods* 344 (2):109-15. doi: 10.1016/j.jim.2009.03.014.

Shafit-Zagardo, B., R. C. Gruber, and J. C. DuBois. 2018. "The role of TAM family receptors and ligands in the nervous system: From development to pathobiology." *Pharmacol Ther* 188:97-117. doi: 10.1016/j.pharmthera.2018.03.002.

Si-Tayeb, K., F. P. Lemaigre, and S. A. Duncan. 2010. "Organogenesis and development of the liver." *Dev Cell* 18 (2):175-89. doi: 10.1016/j.devcel.2010.01.011.

Singal, A. G., and H. B. El-Serag. 2015. "Hepatocellular Carcinoma From Epidemiology to Prevention: Translating Knowledge into Practice." *Clin Gastroenterol Hepatol* 13 (12):2140-51. doi: 10.1016/j.cgh.2015.08.014.

Smith, P. K., R. I. Krohn, G. T. Hermanson, A. K. Mallia, F. H. Gartner, M. D. Provenzano, E. K. Fujimoto, N. M. Goeke, B. J. Olson, and D. C. Klenk. 1985. "Measurement of protein using bicinchoninic acid." *Anal Biochem* 150 (1):76-85.

Spiller, K. L., E. A. Wrona, S. Romero-Torres, I. Pallotta, P. L. Graney, C. E. Witherel, L. M. Panicker, R. A. Feldman, A. M. Urbanska, L. Santambrogio, G. Vunjak-Novakovic, and D. O. Freytes. 2016. "Differential gene expression in human, murine, and cell line-derived macrophages upon polarization." *Exp Cell Res* 347 (1):1-13. doi: 10.1016/j.yexcr.2015.10.017.

Stenhoff, J., B. Dahlbäck, and S. Hafizi. 2004. "Vitamin K-dependent Gas6 activates ERK kinase and stimulates growth of cardiac fibroblasts." *Biochem Biophys Res Commun* 319 (3):871-8. doi: 10.1016/j.bbrc.2004.05.070.

Sun, Y. Y., X. F. Li, X. M. Meng, C. Huang, L. Zhang, and J. Li. 2017. "Macrophage Phenotype in Liver Injury and Repair." *Scand J Immunol* 85 (3):166-174. doi: 10.1111/sji.12468.

Suzuki, Y., M. Shirai, K. Asada, H. Yasui, M. Karayama, H. Hozumi, K. Furuhashi, N. Enomoto, T. Fujisawa, Y. Nakamura, N. Inui, T. Shirai, H. Hayakawa, and T. Suda. 2018. "Macrophage mannose receptor, CD206, predict prognosis in patients with pulmonary tuberculosis." *Sci Rep* 8 (1):13129. doi: 10.1038/s41598-018-31565-5.

Svegliati Baroni, G., L. D'Ambrosio, G. Ferretti, A. Casini, A. Di Sario, R. Salzano, F. Ridolfi, S. Saccomanno, A. M. Jezequel, and A. Benedetti. 1998. "Fibrogenic effect of oxidative stress on rat hepatic stellate cells." *Hepatology* 27 (3):720-6. doi: 10.1002/hep.510270313.

Tacke, F., and C. Trautwein. 2015. "Mechanisms of liver fibrosis resolution." *J Hepatol* 63 (4):1038-9. doi: 10.1016/j.jhep.2015.03.039.

Théret, N., O. Musso, A. L'Helgoualc'h, and B. Clément. 1997. "Activation of matrix metalloproteinase-2 from hepatic stellate cells requires interactions with hepatocytes." *Am J Pathol* 150 (1):51-8.

Tibrewal, N., Y. Wu, V. D'mello, R. Akakura, T. C. George, B. Varnum, and R. B. Birge. 2008. "Autophosphorylation docking site Tyr-867 in Mer receptor tyrosine kinase allows for dissociation of multiple signaling pathways for phagocytosis of apoptotic cells and down-modulation of lipopolysaccharide-inducible NF-kappaB transcriptional activation." *J Biol Chem* 283 (6):3618-27. doi: 10.1074/jbc.M706906200.

Tilg, H., and A. M. Diehl. 2000. "Cytokines in alcoholic and nonalcoholic steatohepatitis." *N Engl J Med* 343 (20):1467-76. doi: 10.1056/NEJM200011163432007.

Vyas, S. K., H. Leyland, J. Gentry, and M. J. Arthur. 1995. "Rat hepatic lipocytes synthesize and secrete transin (stromelysin) in early primary culture." *Gastroenterology* 109 (3):889-98.

Wake, K. 1971. ""Sternzellen" in the liver: perisinusoidal cells with special reference to storage of vitamin A." *Am J Anat* 132 (4):429-62. doi: 10.1002/aja.1001320404.

Wake, K. 1989. "Three-dimensional structure of the sinusoidal wall in the liver: a Golgi study." *Prog Clin Biol Res* 295:257-62.

Wake, K. 1999. "Cell-cell organization and functions of 'sinusoids' in liver microcirculation system." *J Electron Microsc (Tokyo)* 48 (2):89-98.

Wan, J., M. Benkdane, F. Teixeira-Clerc, S. Bonnafous, A. Louvet, F. Lafdil, F. Pecker, A. Tran, P. Gual, A. Mallat, S. Lotersztajn, and C. Pavoine. 2014. "M2 Kupffer cells promote M1 Kupffer cell apoptosis: a protective mechanism against alcoholic and nonalcoholic fatty liver disease." *Hepatology* 59 (1):130-42. doi: 10.1002/hep.26607.

Weiskirchen, R., and F. Tacke. 2014. "Cellular and molecular functions of hepatic stellate cells in inflammatory responses and liver immunology." *Hepatobiliary Surg Nutr* 3 (6):344-63. doi: 10.3978/j.issn.2304-3881.2014.11.03.

Weiskirchen, R., S. Weiskirchen, and F. Tacke. 2018a. "Organ and tissue fibrosis: Molecular signals, cellular mechanisms and translational implications." *Mol Aspects Med*. doi: 10.1016/j.mam.2018.06.003.

Weiskirchen, R., S. Weiskirchen, and F. Tacke. 2018b. "Recent advances in understanding liver fibrosis: bridging basic science and individualized treatment concepts." *F1000Res* 7. doi: 10.12688/f1000research.14841.1.

Wong, L., G. Yamasaki, R. J. Johnson, and S. L. Friedman. 1994. "Induction of beta-platelet-derived growth factor receptor in rat hepatic lipocytes during cellular activation in vivo and in culture." *J Clin Invest* 94 (4):1563-9. doi: 10.1172/JCI117497.

Xu, H., Y. Zhou, C. Lu, J. Ping, and L. M. Xu. 2012. "Salvianolic acid B lowers portal pressure in cirrhotic rats and attenuates contraction of rat hepatic stellate cells by inhibiting RhoA signaling pathway." *Lab Invest* 92 (12):1738-48. doi: 10.1038/labinvest.2012.113.

Yamagata, M., J. R. Sanes, and J. A. Weiner. 2003. "Synaptic adhesion molecules." *Curr Opin Cell Biol* 15 (5):621-32.

Yang, J., L. E. Mowry, K. N. Nejak-Bowen, H. Okabe, C. R. Diegel, R. A. Lang, B. O. Williams, and S. P. Monga. 2014. "β-catenin signaling in murine liver zonation and regeneration: a Wnt-Wnt situation!" *Hepatology* 60 (3):964-76. doi: 10.1002/hep.27082.

Yoshiji, H., S. Kuriyama, J. Yoshii, Y. Ikenaka, R. Noguchi, D. J. Hicklin, Y. Wu, K. Yanase, T. Namisaki, M. Yamazaki, H. Tsujinoue, H. Imazu, T. Masaki, and H. Fukui. 2003. "Vascular endothelial growth factor and receptor interaction is a prerequisite for murine hepatic fibrogenesis." *Gut* 52 (9):1347-54.

Younossi, Z. M., A. B. Koenig, D. Abdelatif, Y. Fazel, L. Henry, and M. Wymer. 2016. "Global epidemiology of nonalcoholic fatty liver disease-Meta-analytic assessment of prevalence, incidence, and outcomes." *Hepatology* 64 (1):73-84. doi: 10.1002/hep.28431.

Yu, C., F. Wang, C. Jin, X. Huang, D. L. Miller, C. Basilico, and W. L. McKeehan. 2003. "Role of fibroblast growth factor type 1 and 2 in carbon tetrachloride-induced hepatic injury and fibrogenesis." *Am J Pathol* 163 (4):1653-62. doi: 10.1016/S0002-9440(10)63522-5.

Zhang, W., D. DeRyckere, D. Hunter, J. Liu, M. A. Stashko, K. A. Minson, C. T. Cummings, M. Lee, T. G. Glaros, D. L. Newton, S. Sather, D. Zhang, D. Kireev, W. P. Janzen, H. S. Earp, D. K. Graham, S. V. Frye, and X. Wang. 2014. "UNC2025, a potent and orally bioavailable MER/FLT3 dual inhibitor." *J Med Chem* 57 (16):7031-41. doi: 10.1021/jm500749d.

Zimmermann, H. W., C. Trautwein, and F. Tacke. 2012. "Functional role of monocytes and macrophages for the inflammatory response in acute liver injury." *Front Physiol* 3:56. doi: 10.3389/fphys.2012.00056.

Zizzo, G., B. A. Hilliard, M. Monestier, and P. L. Cohen. 2012. "Efficient clearance of early apoptotic cells by human macrophages requires M2c polarization and MerTK induction." *J Immunol* 189 (7):3508-20. doi: 10.4049/jimmunol.1200662.